HIGHWAY RESEARCH RECORD

Number 134

Bituminous Materials

6 Reports

Subject Classification

31 Bituminous Materials and Mixes
34 General Materials

HIGHWAY RESEARCH BOARD
DIVISION OF ENGINEERING NATIONAL RESEARCH COUNCIL
NATIONAL ACADEMY OF SCIENCES—NATIONAL ACADEMY OF ENGINEERING

Washington, D. C., 1966 Publication 1378

Department of Materials and Construction

R. L. Peyton, Chairman
Assistant State Highway Engineer
State Highway Commission of Kansas, Topeka

HIGHWAY RESEARCH BOARD STAFF

R. E. Bollen, Engineer of Materials and Construction
W. G. Gunderman, Assistant Engineer of Materials and Construction

BITUMINOUS DIVISION

William H. Goetz, Chairman
Joint Highway Research Project
Purdue University, Lafayette, Indiana

COMMITTEE ON CHARACTERISTICS OF BITUMINOUS MATERIALS
(As of December 31, 1965)

J. York Welborn, Chairman
U. S. Bureau of Public Roads
Washington, D. C.

Stephen H. Alexander, Research Center, Monsanto Chemical Company, St. Louis, Missouri
John H. Barton, Director, Chemical & Bituminous Laboratories, Missouri State Highway Department, Jefferson City
James V. Evans, Marketing Technical Service Department, American Oil Company, Chicago, Illinois
J. H. Goshorn, Managing Engineer, The Asphalt Institute, Columbus, Ohio
W. H. Gotolski, Associate Professor, Department of Civil Engineering, Pennsylvania State University, University Park
F. C. Gzemski, The Atlantic Refining Company, Research and Development Department, Philadelphia, Pennsylvania
W. J. Halstead, Chemical Engineer, Materials Research Division, U. S. Bureau of Roads, Washington, D. C.
James H. Havens, Director of Research, Kentucky Department of Highways, Lexington, Kentucky
Arnold J. Hoiberg, Assistant Director, The Flintkote Company, Whippany, New Jersey
John J. Lyons, Research and Materials Engineer, Massachusetts Department of Public Works, Wellesley Hills
Kamran Majidzadeh, Department of Civil Engineering, University of Florida, Gainesville
Robert E. Meskill, Standard Oil Company (New Jersey), New York, N. Y.
Vytautas P. Puzinauskas, Associate Research Engineer, The Asphalt Institute, University of Maryland, College Park
J. C. Reed, Division of Materials, New Jersey State Highway Department, Trenton
E. O. Rhodes, Pittsburgh, Pennsylvania
F. S. Rostler, Director of Research, Materials R and D Division, Woodward, Clyde, Sherard and Associates, Oakland, California

R. J. Schmidt, California Research Corporation, Richmond
H. E. Schweyer, Department of Chemical Engineering, University of Florida, Gainesville
E. G. Swanson, Staff Materials Engineer, Colorado Department of Highways, Denver
Edmund Thelen, Manager, Colloids and Polymers Laboratory, Franklin Institute, Philadelphia, Pennsylvania
R. N. Traxler, Texas Transportation Institute, Texas A and M University, College Station
W. B. Warden, President, Miller-Warden Associates, Raleigh, North Carolina
Frank M. Williams, Engineer of Tests, State Highway Testing Laboratory, Columbus, Ohio
L. E. Wood, Department of Civil Engineering, Purdue University, Lafayette, Indiana

Foreword

To provide a better understanding of the properties of component materials and bituminous paving mixtures and their effect on the durability and performance of pavements, more research emphasis is being placed on the fundamental properties of the asphalt binders. The papers published here include information on the development and application of fundamental physical and chemical techniques and knowledge to study the durability of pavements and the flow properties of asphalt.

The information should be of value to those material engineers and asphalt technologists who are interested in the development of improved paving mixture designs, and in the performance and durability of bituminous pavements.

The paper on inverse gas liquid chromatography (GLC) by Davis and Petersen describes a new technique that is being used to study the oxidation characteristics of asphalt. In this technique the asphalt serves as a liquid substrate in a gas liquid chromatographic column and is oxidized within the chromatograph. The changes due to oxidation are reflected in the retention behavior caused by interaction. Data are presented for air-blown roofing asphalts showing that inverse GLC oxidation techniques may be useful in studying the initial chemical composition of asphalt and in predicting asphalt durability as determined by an accelerated-weathering machine. The approach used appears to hold promise for use in predicting the durability of asphalt cements used for paving mixtures.

The paper by A. Please, et al., deals with the influence of source and type of asphalt on the durability and surface texture of asphalt pavements. The results of a full-scale experimental pavement indicated that for the majority of the asphalts the surfacing was very durable provided a sufficient quantity of binder was used. However, the surfacing on the various experimental sections varied in texture sufficiently to affect the skid resistance. For the types of mixtures studied the rough textured surfaces were those containing asphalts having a low resistance to weathering.

The difference in performance of the pavement surfaces was partially explained by the changes in constitution of asphalts in service. The authors also indicated that contamination of the pavement surface by oil drippings from vehicles was of importance in studying performance.

A knowledge of the fundamental flow properties of asphaltic materials is needed to provide a better understanding of the properties of asphalt-aggregate mixtures that can be applied to a more rational method of mixture design and to the selection of the most suitable asphalt for a specific loading and environmental condition.

The two papers by Moavenzadeh and Stander and by Shoor, et al., on the subject of flow of asphalt present methods and concepts for analyzing and expressing flow characteristics over a range of temperatures. Data are presented to show that different viscometers can be used to obtain shear data over a wide range of shear rates and shear stress and apply the principal of reduced variables to extend these ranges. One paper reports data for a penetrometric technique to determine glass transition temperature of asphalt cements. This confirms the hypothesis of other investigators that this is an important characteristic temperature for viscoelastic substances such as asphalt.

This record also contains an abridgment of a paper by Sisko and Brunstrum, "Asphalt Durability and Its Relation to Pavement Performance—Rheology, I."

Contents

Inverse GLC—An Extension of the Technique to The Study of Oxidation of Asphalts

T. C. DAVIS and J. C. PETERSEN
Respectively, Research Chemist, and Project Leader, Laramie Petroleum Research Center, Bureau of Mines, Laramie, Wyoming

An extension of the inverse GLC technique to the study of the oxidation of asphalts is reported. In the new approach, an asphalt, serving as the liquid substrate in a gas liquid chromatographic column, is oxidized directly within the chromatograph. The retention behavior of a group of selected test compounds possessing different functional groups is determined before and after oxidation. Because the retention behavior is dependent on interactions between the functional groups of the test compound and chemical functionalities in the asphalt, the changes occurring in the asphalt on oxidation are reflected as changes in retention behavior. Inverse GLC was found sensitive in detecting changes that take place on oxidation, and holds promise as a method of predicting asphalt durability.

•THE USE of inverse gas liquid chromatography (GLC) as a technique for studying petroleum asphalts has been previously outlined by Davis, Petersen, and Haines (1). The present paper presents an extension of this technique by which the oxidation of asphalts can be studied.

In the application, the retention behavior of carefully selected volatile test compounds of known chemical composition is determined on an asphalt stationary phase. The asphalt column is then oxidized in place within the GLC instrument, and the retention behavior of the test compounds is again determined. Retention behavior of the test compounds is largely determined by interactions between the test compounds and the chemical functionality of the asphalt; thus, changes in the behavior of the test compounds upon oxidation reflect changes in the chemical composition of the asphalt.

This report covers preliminary oxidation studies using the six asphalts from the original work by Davis et al. (1), plus six roofing asphalts previously characterized by Greenfeld and Wright (2). The latter group of asphalts forms the basis for correlations between changes in test compound retention behavior on asphalt oxidation and durability.

EXPERIMENTAL

Apparatus

GLC data were obtained on a Beckman GC-2* gas chromatograph that was modified to allow diverting the carrier gas and substituting compressed air during oxidation. The instrument was also modified to allow bypassing the column detector during the oxidation step.

*References to specific commercial materials or models of equipment in this report are made to facilitate understanding, and do not imply endorsement by the Bureau of Mines.

Paper sponsored by Committee on Characteristics of Bituminous Materials and presented at the 45th Annual Meeting.

Procedure

A ¼-in. by 13-ft GLC column was packed with one part of asphalt on 10 parts by weight of Fluoropak 80 and conditioned for a minimum of 6 hr under normal operating conditions using a helium inlet gage pressure of 15 psi and an instrument operating temperature of 130 C. Following conditioning, the test compounds were introduced as previously described (1). The asphalt was then oxidized within the column by replacing the helium carrier gas with filtered air at an inlet gage pressure of 15 psi (flow rate approximately 30 ml/min). The column temperature was maintained at 130 C for an oxidation period of 24 hr. (Other oxidation conditions were investigated and are discussed later.) Following oxidation, normal operating conditions were reestablished and the column conditioned for a minimum of 2 hr. Test compound retention data were then obtained on the oxidized column.

To quantify the test compound retention data, and thus provide for data comparison, the data were calculated as interaction coefficients (1). (The interaction coefficient, I_p, is 100 times the logarithm of the corrected retention volume of the test compound, minus 100 times the logarithm of the corrected retention volume of a hypothetical n-paraffin of equivalent molecular weight, both values determined on the asphalt.) The oxidation data are reported as the change on oxidation, or ΔI_p, which is equal to the I_p obtained on the oxidized asphalt minus the I_p obtained prior to oxidation.

DISCUSSION OF EXPERIMENTAL TECHNIQUES

Oxidation of asphalts in the GLC offers a technique for the examination of small samples, gives easy control over temperature and air flow rate, and eliminates the additional handling required for separately oxidized samples. In addition, oxidation of asphalt in a GLC column provides a method of exposing large surface areas.

During the oxidation of the asphalt, the concentration of the oxygen in the air may vary along the column length due to both its reaction with the asphalt and the normal pressure drop through the column. In order to minimize the change in concentration resulting from reaction of oxygen with the asphalt, it is necessary that the exit gas contain nearly the same concentration of oxygen as the inlet gas. Three different oxidation conditions were evaluated as shown in Figure 1, in which the percent of unreacted oxygen in the column exit stream is plotted as a function of time. These data were obtained by GLC analyses of the exit gases on a molecular sieve column. Of the oxidation conditions shown, only at 130 C and 30 ml/min air flow rate (corresponding to 15-psi inlet gage pressure) does the amount of unreacted oxygen in the column exit stream approach that in the air entering the column. At 200 C, a high percentage of the oxygen in the air passing through the column was consumed by the asphalt, thus contributing significantly to a nonuniform oxidation. This nonuniform oxidation was also evidenced by a darkening of the asphalt packing at the front end of the column, and by differences in benzene solubility along the column length. The actual pressure drop through the column at the 30 ml/min air-flow rate was measured to determine its effect in producing an oxygen concentration differential along the column. Although the absolute gas-inlet pressure of the instrument was 26.2 psia (15 psi instrument gage reading at Laramie, Wyoming, where atmospheric pressure averages 11.2 psia), the actual inlet and outlet pressures of the column averaged 17.5 psia and 13.5 psia, respectively. The additional pressure drops between the 26.2-psia inlet pressure and 11.2-psia atmospheric pressure are accounted for primarily by capillary restrictions inherent within the GLC instrument. The measured 4.0-psi pressure drop through the column thus produces a drop in oxygen concentration of 23 percent. The total combined drop in oxygen concentration along the column length due to both chemical reaction and pressure drop for a typical asphalt was thus estimated at 25-30 percent, when operating at 130 C and 30 ml/min air-flow rate.

Test compounds were run on asphalt columns (both unoxidized and oxidized) before and after 48-hr thermal treatments to determine the possibility of significant mechanical or chemical changes occurring in the columns at test temperatures due to heat alone. Results of these tests indicated 130 C to be a safe operating temperature to avoid significant thermal changes.

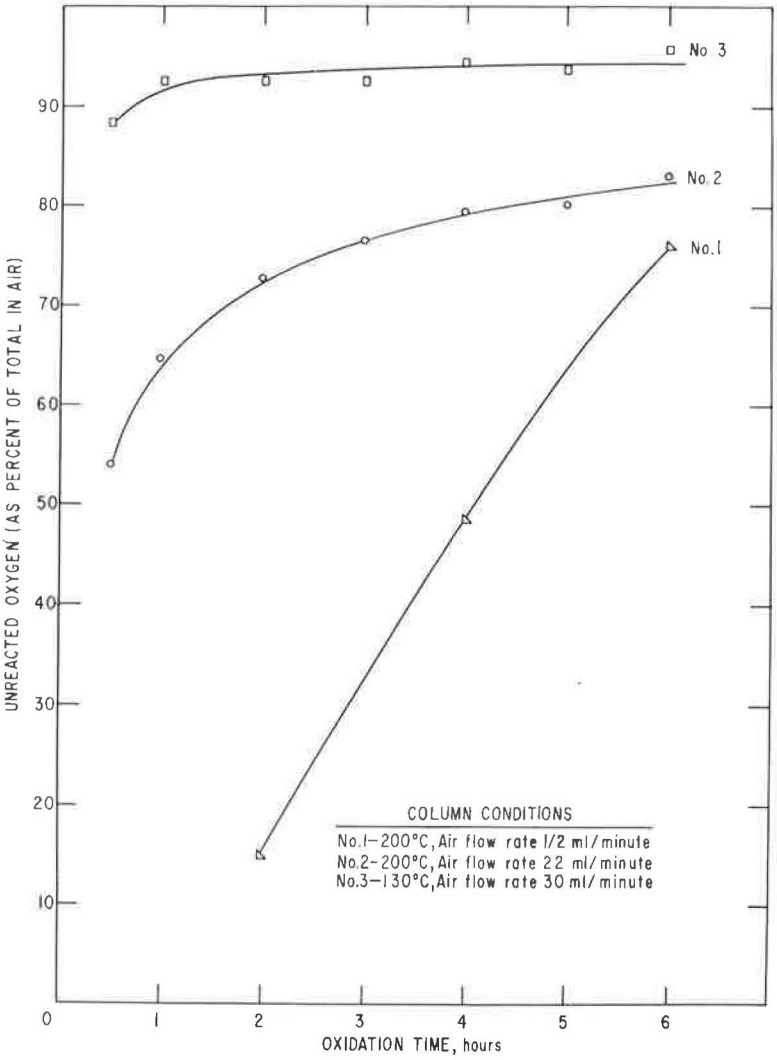

Figure 1. Oxygen in column exit gas during air oxidation.

To determine if test compounds reacted with the asphalts and thus altered the course of subsequent oxidation, asphalts were oxidized both before and after exposure to test compounds. Test compound retention data showed no significant differences.

RESULTS AND DISCUSSION

Types of Forces in Inverse GLC

In inverse GLC, the test compound retention behavior is governed to a large degree by intermolecular forces between the test compound and the asphalt. The forces to be considered in gas liquid chromatography can be grouped into four types (3).

1. London, or dispersion, forces. These are intermolecular forces between two nonpolar substances, and arise from synchronized variations in the instantaneous dipoles of the two interacting substances. They are present in all cases, and are the only attraction forces between two nonpolar substances.

2. Debye, or induced dipole forces. These forces result from the interactions of a permanent dipole with an induced dipole in a neighboring molecule. The size of such forces is usually small.

3. Keesom, or orientation, forces. These are orientation forces which arise from the interaction of two permanent dipoles. Among these is the "hydrogen bond."

4. Chemical bonding forces arising from the formation of loose chemical adducts.

An understanding of the interactions of the test compound with the asphalt in terms of the forces involved would be most useful in providing information about the chemical composition of asphalt and the products formed on oxidation.

In the method used for calculating inverse GLC data (1), test compound retention behavior is referenced to the behavior of normal paraffins on asphalt. Normal paraffins generally exhibit only London, or dispersion forces; therefore, these forces are not significantly reflected in the interaction coefficients reported. As a result, the interaction coefficients, and the changes in I_p on oxidation, are essentially a measure of the stronger forces resulting from induced and permanent dipoles and chemical bonding forces. Inverse GLC, therefore, is particularly adaptable to the study of functional groups (which are often strongly polar) initially present or produced in the asphalt on oxidation. The freedom to choose from a variety of test compounds adds versatility to the method and makes possible the collection of many bits of information about the composition of the asphalt without prior fractionation.

Changes in Asphalt on Oxidation as Indicated by Inverse GLC

Interaction coefficient data for 24-hr, 130 C oxidation studies are shown in Table 1 for the six asphalt samples used in the original work (1). The individual test compound data obtained on the unoxidized asphalts (I_p) and the change on oxidation (ΔI_p) are shown. The test compounds in Table 1 have been arranged in the order of increasing ΔI_p on asphalt No. 1. Examination of the data indicates that the relatively nonpolar and nonpolarizable compounds near the top of the table are nearly insensitive to oxidation changes in asphalt. Those compounds that would be expected to interact with oxygen containing groups produced in asphalt on oxidation show large changes in interaction coefficients. For example, butanol, propionic acid, and phenol have both oxygen and hydrogen which can share in hydrogen bonds with groups formed in the asphalt. These

TABLE 1

EFFECTS OF ASPHALT OXIDATION ON TEST COMPOUND RETENTION BEHAVIOR

Test Compound	Interaction Coefficient (I_p)[a]						Change on Oxidation (ΔI_p)[b]					
	Asphalt No.						Asphalt No.					
	1	2	3	4	5	6	1	2	3	4	5	6
Methylcyclohexane	24	23	24	24	23	29	-1	3	-1	-2	1	3
Toluene	47	47	51	48	43	69	0	5	0	2	5	9
2-Methyl-2-pentanethiol	4	2	6	3	1	22	0	3	0	2	4	6
2-Thiahexane	40	42	45	43	38	58	1	0	0	0	2	5
Allyl ether	5	3	8	7	2	30	1	4	3	0	3	3
1-Decane	4	2	3	2	2	8	2	-1	2	1	0	-1
Heptaldehyde	34	33	42	37	25	68	2	3	-1	0	4	2
Butyl acetate	-2	-3	5	0	-5	25	2	1	0	2	2	10
2-Methylpyridine	61	62	71	69	56	98	2	10	-1	0	0	2
Butanol	44	45	60	51	41	71	5	17	3	7	3	11
Propionic acid	73	83	128	99	63	75	9	19	10	3	12	25
Pyrrole	86	89	108	94	80	124	12	20	9	11	13	26
Formamide	127	132	164	149	118	179	14	34	17	15	22	50
Phenol	118	120	147	125	106	138	30	50	15	27	15	40
1-Methylpyrrolidine	36	37	42	50	36	61	113	167	79	143	88	27

[a]Before oxidation.

[b]Asphalt oxidized 24 hr, 130 C, 15 psi air inlet pressure.

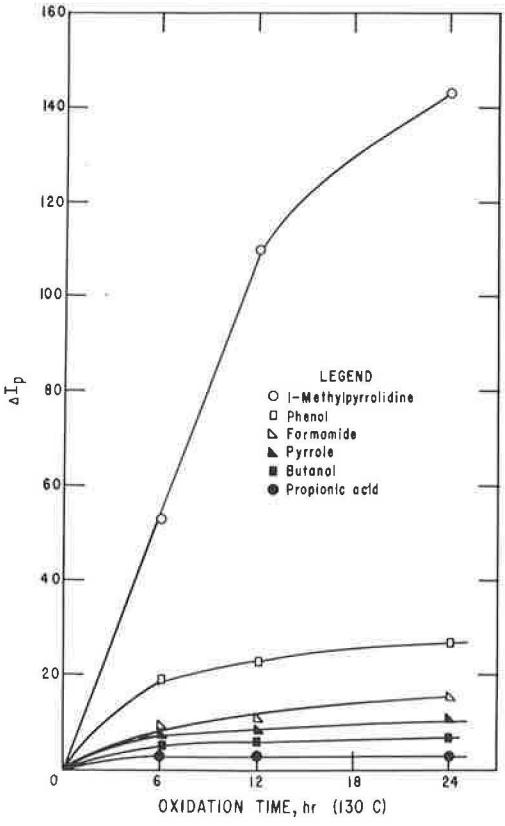

Figure 2. Changes in interaction coefficient (ΔI_p) on oxidation (asphalt No. 4).

compounds also show significant ΔI_p's. In addition, the strongly basic amines would be expected to interact with acid groups produced on oxidation, and the data do show 1-methylpyrrolidine to be held more tightly (higher ΔI_p's) than the acidic test compounds. Although not shown in Table 1, the additional strong bases, triethylamine, piperidine, and cyclohexylamine, were usually held so tightly by the oxidized columns that ΔI_p's were not obtained. In contrast, the weaker base 2-methylpyridine showed relatively small ΔI_p's. These differences in behavior of the organic bases may be indicative of the acid strength of the oxidation products.

The changes in the interaction coefficients resulting from the oxidation of asphalt No. 4, as a function of oxidation time, are shown in Figure 2. The change in the interaction coefficient of the basic 1-methylpyrrolidine is in sharp contrast to the changes produced with the remainder of the test compounds shown. 1-Methylpyrrolidine has a high rate of increase in ΔI_p and does not begin to show a significant change in the rate of increase until after 12-hr oxidation. The other test compounds which contain more acidic groups show maximum change in ΔI_p during the first 6 hr of oxidation and then level off. These data suggest that different oxidation products are detected by the basic and acidic test compounds, and that the concentrations of these products vary with the level of oxidation.

The oxidation-inverse GLC technique was able to show differences in the chemical characteristics of asphalts that were not observable by most common characterization tests. Asphalts Nos. 1 and 2 in Table 1 showed similar softening points, penetrations, carbon residues, elemental analyses, and oil, resin, and asphaltene contents (1). Their interaction coefficients prior to oxidation were also similar. However, their oxidation characteristics were not the same, as shown by the differences in the ΔI_p values. Asphalt No. 2 is apparently much more susceptible to oxidation, and may have significantly different weathering properties.

A well-known path in the oxidation of hydrocarbons involves the removal of a hydrogen atom from a carbon atom, followed by the uptake of oxygen by the hydrocarbon radical formed, ultimately leading to polar, oxygen-containing functional groups. The presence of reactive hydrogen labile toward this reaction would probably not be detected by inverse GLC prior to oxidation, because of the weak interaction forces of the hydrocarbon fragment. It is not surprising, therefore, that two asphalts may have similar interaction coefficients prior to oxidation, and different interaction coefficients following oxidation. Inverse GLC should be useful in detecting this type of reactivity; however, the changes in I_p observed on oxidation are by no means restricted to interactions with the products of hydrocarbon oxidation as in the example cited.

Correlation with Durability

Greenfeld and Wright (2) showed correlative trends between asphalt durability (as measured by the carbon-arc accelerated-weathering machine) and asphaltene content,

TABLE 2

PROPERTIES OF GREENFELD AND WRIGHT ASPHALTS[a]

Asphalt No.[b]	Softening Point, °F	Penetration, 0.1 mm, 75 F	Specific Gravity at 77 F	Durability, Days[c]
GW-2, Tia Juana-Lago Colon	220	17	1.017	69
GW-3, California Coastal (catalyzed)	221	18	1.032	53
GW-5, Kansas-Indiana	212	21	1.010	95
GW-9, California Coastal (fluxed)	230	20	1.026	32
GW-19, Kansas	223	16	1.005	95
GW-22, Lagunillas	224	14	1.030	60

[a]Data from Greenfeld and Wright (2).
[b]Sample designations are Greenfeld and Wright numbers prefixed with GW.
[c]Using carbon-arc accelerated weathering machine in accordance with daily cycle A in Recommended Practice for Accelerated-Weathering Test of Bituminous Materials (D529-59T), 1961 Book of ASTM Standards, Part 4, p. 1233.

TABLE 3

INVERSE GLC RESULTS ON GREENFELD AND WRIGHT ASPHALTS

Test Compound	Interaction Coefficient (I_p)[a]						Change on Oxidation (ΔI_p)					
	Asphalt No.						Asphalt No.					
	GW-9	GW-3	GW-22	GW-2	GW-5	GW-19	GW-9	GW-3	GW-22	GW-2	GW-5	GW-19
Triethylamine	2	28	-3	-4	1	-1	>150	107	111	104	42	39
1-Decane	3	2	2	2	2	2	-1	1	1	0	0	1
Methylcyclohexane	21	21	20	20	20	19	0	1	1	0	1	1
Butanol	51	51	48	40	44	43	7	4	6	10	3	4
Pyrrole	94	94	91	82	86	82	16	11	11	15	6	7
Propionic acid	96	87	81	65	71	66	17	18	10	16	2	5
Phenol	137	126	129	108	117	110	31	27	22	33	9	12
Formamide	149	150	141	123	136	131	28	12	16	23	15	10

[a]Before oxidation.

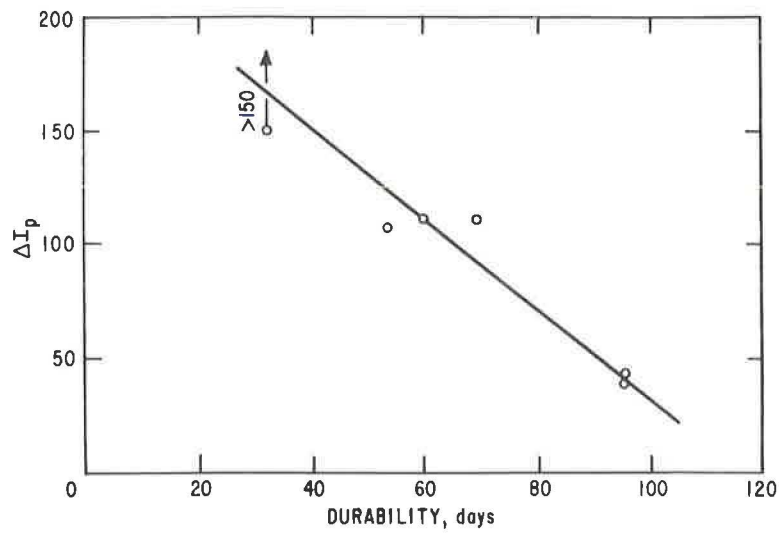

Figure 3. Relationship between accelerated weathering durability and change in interaction coefficient (ΔI_p) for triethylamine on 130 C air oxidation (durability data obtained by Greenfeld and Wright).

rate of filtration, solubility parameter, and carbonyl index. These investigators studied air-blown roofing asphalts.

To determine if inverse GLC retention data correlated with asphalt durability, a survey was conducted on six of the asphalts investigated by Greenfeld and Wright. These asphalts were chosen to cover a wide range of durabilities. Selected properties are shown in Table 2. Interaction coefficients for the six asphalts and the change in these coefficients on oxidation, using test compounds representing a wide range of activity, are shown in Table 3. Asphalts are arranged from left to right in order of increasing durability. Test compounds are arranged according to increasing I_p on asphalt GW-9.

Correlative trends were found between durability and the change in interaction coefficients on oxidation (ΔI_p) with several of the test compounds. For example, results obtained with triethylamine, plotted in Figure 3, show an inverse relationship between the variables. While the primary purpose of this paper is to report the inverse GLC oxidation technique and to suggest its usefulness in studying chemical changes occurring in asphalt on oxidation, the correlation with durability indicates its usefulness in establishing empirical relationships.

SUMMARY AND CONCLUSIONS

Inverse GLC offers a new technique for the study of the oxidation of asphalts. Differences among asphalts, and differences in their behavior on oxidation, are readily detectable. By following the changes in interaction coefficients, changes in asphalt chemical functionality on oxidation (and thus differences in the oxidation characteristics of asphalts) may be detected. An understanding of these changes should be useful in studying the initial chemical composition of the asphalt. Results of accelerated weathering of asphalts indicate inverse GLC to be useful in predicting asphalt durability.

REFERENCES

1. Davis, T. C., Petersen, J. C., and Haines, W. E. Amal. Chem., Vol. 38, No. 2, pp. 241-243, 1966.
2. Greenfeld, S. H., and Wright, J. R. Materials Research and Standards. Vol. 2, No. 9, pp. 738-745, 1962.
3. Keulemans, A. I. M. Gas Chromatography. Reinhold, New York, p. 165, 1959.

On Flow of Asphalt

F. MOAVENZADEH and R. R. STANDER, JR.
Respectively, Assistant Professor and Research Assistant, Department of Civil Engineering, Massachusetts Institute of Technology, Cambridge

This paper reviews some concepts suggested to analyze the flow characteristics of rheological materials with emphasis on those which are promising in the analysis of flow of asphalts. The suggested concepts are categorized as experimental, mathematical, structural, and physical-chemical. It is shown that for the two asphalts used in this study, it is possible to construct flow diagrams over a wide range of shear stress, rate of shear, and temperature by using three different viscometers and the principle of reduced variables. The application of Eyring's rate process theory to the analysis of asphalt flow is examined and the variation of viscosity, determined at constant shear stress or constant shear rate, with temperature is discussed.

•KNOWLEDGE OF the flow properties of asphaltic materials is of special interest in the design of asphaltic mixtures. Such knowledge should lead to a better understanding of the properties of the asphalt-aggregate mixture which in turn should result in the development of a more rational method of mixture design. An understanding of the effect of loading and climatic variables on the flow properties of the binder could be of great assistance in the selection of the most suitable asphalt for a specified job.

The complex chemical structure and numerous varieties of asphalts have, thus far, prevented development of a specific mechanism for describing its flow behavior over the useful range of loading and climatic variables. There are, however, a great number of empirical models, relatively few semi-empirical models, and few theoretical models proposed to describe the flow behavior of asphaltic materials over a limited range of some specific variables. The extent of work in this area was well reviewed by Schweyer in 1958 (1), who said, "Acceptance of the statement that 'knowledge in a field is measured by the brevity with which the concepts can be presented' makes the asphalt technologist pause when the voluminous literature on asphalt is considered." This, in other words, indicates that the "art of asphalt" is a very real and necessary part of asphalt technology, and in order to achieve a scientific base for this art, fundamental concepts involving the flow properties of asphalt must be developed. Thus, it is the general objective of this paper to contribute to the development of such concepts by briefly reviewing the fundamentals involved in analyzing the flow behavior of materials and discussing the difficulties encountered in their application to asphalt. The response of certain asphalts under loading as measured by different methods is presented and the applicability of some rheologic concepts to the analysis of the results is discussed.

CURRENT TRENDS

The objective of rheology is to yield a distinct fundamental, or rational, description of the deformation and flow of matter. To achieve this end the physical chemist has approached the problem by considering the molecular characteristic of materials. The quantum mechanics mathematician approaches the problem by formulating constitutive

Paper sponsored by Committee on Characteristics of Bituminous Materials and presented at the 45th Annual Meeting.

equations and/or conservation relations for particular materials. Although advances in both of these fields are quite evident, the practical requirements of industry have outrun basic research. This situation has created analytical and empirical solutions based on simplifying assumptions as applied to observed flow conditions. More and more, the applied approach has become that of using as much as possible of the physical-chemical and continuum mechanic works. This is quite evident from the recent works of Herrin and Jones (2) and Majidzadeh and Schweyer(3). The former have used the advances in the application of rate process theory (4) to the rheological studies of asphalt, and the latter have used a kinetic approach (5) to analyze the flow behavior of the asphalt.

FLOW REPRESENTATION

In general, there are two basic methods to represent the flow of a fluid, by using a shear stress-rate of shear diagram or by using a viscosity-shear rate diagram. It might also be argued that the single point viscosity (coefficient of viscosity) is sufficient to represent the data; however, for research purposes, the use of this parameter is limited to Newtonian materials which, unfortunately, do not include a great number of paving asphalts.

The simplest plot of flow data is that of shear stress vs rate of shear on arithmetic coordinates. A Newtonian material will plot as a straight line passing through the origin. If the material is non-Newtonian, the data will, in general, pass through the origin but will not be linear. The disadvantage of this plot is that the degree of deviation from Newtonian characteristics cannot be determined. This can be accomplished in most cases by using a log-log plot. Generally, the data will describe a straight line which may be represented by a power formula

$$\tau = A\ (\dot{\gamma})^n \qquad (1)$$

where n is a measure of the deviation from Newtonian behavior. For a Newtonian material, n is equal to unity.

Consistency cannot be represented by A because of the dimensional difficulties; however, the viscosity, defined as $\tau/\dot{\gamma}$ for a given $\dot{\gamma}$ (sometimes referred to as apparent viscosity), may be used. Since the $\dot{\gamma}$ used is arbitrary, and not standardized, confusion may result. An alternate method is proposed by Traxler (6) in which viscosities are compared at a particular power input per volume of sample. Although the power input is arbitrary ($\tau \times \dot{\gamma}$/unit volume = 1,000 given as convenient), the method has the advantage that very little extrapolation of data is necessary to determine values over a wide range of materials and test temperatures. The degree of data treatment required to arrive at the basic shear stress-rate of shear diagram, generally depends on the geometry of the test apparatus used.

An alternate method of flow representation is in terms of the viscosity-shear rate diagram. For Newtonian materials, viscosity is defined as the ratio of shear stress to shear rate which at constant temperature is independent of the shear stress level. For non-Newtonian materials, the ratio is defined as apparent viscosity, and is shear-dependent. The slope of the shear diagram, also used to define viscosity, is called the differential viscosity, $\eta_D = \partial\tau/\partial\dot{\gamma}$. For a power law material the plots of both apparent viscosity and differential viscosity vs shear rate should be straight and parallel lines. A third term, referred to as plastic viscosity, is defined as the slope of the straight line portion of $\dot{\gamma}$ vs τ on arithmetic scales. This viscosity is independent of shear rate and is generally used to determine the yield stress of pseudoplastic materials.

Materials exhibiting rheologic behavior are usually divided into different groups according to their flow characteristics. The general division is that of Newtonian and non-Newtonian flow behavior. Although Reiner (7) objects to this division and believes that all materials showing viscosity should be called Newtonian fluids, and those with variable viscosity, generalized Newtonian fluids, in most rheologic work and for the purpose of this discussion, the Newtonian and non-Newtonian division is used.

Non-Newtonian flow is generally either shear thinning or shear thickening. The first group would include the ideal Bingham plastic and the pseudoplastics, as they both exhibit

decreasing apparent viscosity with increasing shear rate The term thixotropy, as sometimes applied to this whole group, is used here to describe a special case of shear thinning in that it is time-dependent. The structure, which is broken down by shear, is recoverable with time, or, in other words, the process is reversible. Dilatancy is sometimes used to describe shear thickening material; however, this is a misnomer in that many materials which show increasing viscosity with increasing shear do not dilate at all. Thus, dilatancy is a special case of shear thickening. Another unfortunate misuse of terms results by describing time-dependent, shear thickening behavior as rheopectic. There may exist a material which displays shear thickening with time, but rheopexy is the process by which certain thixotropic materials regain their structure faster with the application of a gentle shear. This is analogous to the flocculation process which is speeded by a gentle stirring action. In both cases, increasing the shear beyond a certain limit will start to destroy the structure.

DATA INTERPRETATION

The basic objective of data interpretation is the prediction of flow properties, given limited information.

Experimental Representation

Until the development of a fundamental concept describing the flow behavior of materials in general, use of the existing models is generally limited to the range of variables incorporated in the development of such models. Thus application of these models, while showing good results when properly employed, is limited to the exact test conditions and materials as those used in the development of the particular relationship. In other words, these equations are usually developed to cover a very specific range of data. This can, perhaps, best be illustrated by allusion to the developments for a pseudoplastic material as defined by the flow diagram below.

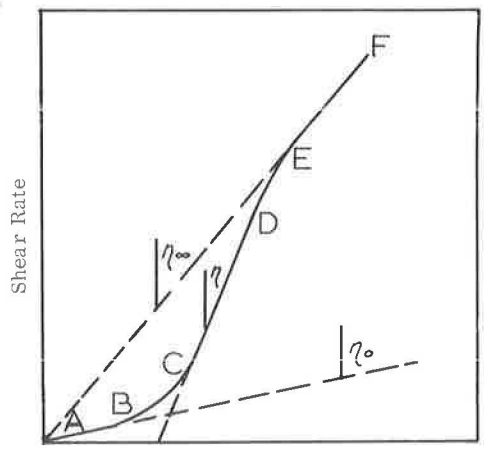

In this figure, the total flow diagram is the line ABCDEF; however, for many cases, description of only part of this line is necessary. For the straight line portion AB, the material is Newtonian and can be described by

$$\tau = \eta_0 \dot{\gamma} \qquad (2)$$

This is again true for EF with η_0 replaced by η_∞ where $\eta_\infty < \eta_0$. In the portion CD, the data are described by the Bingham plastic relationship

$$\tau - \tau_0 = \eta \dot{\gamma} \tag{3}$$

The power function, first proposed by Ostwald and described by Reiner (7) is a good approximation of the portion AC, where

$$\tau = A (\dot{\gamma})^n \tag{4}$$

and n for a pseudoplastic is less than unity. To extend the description to point D, the relationship

$$\dot{\gamma} = A \sinh B \tau \tag{5}$$

gives a very good approximation. Finally, to describe the entire curve, the equation

$$\eta = \frac{(\eta_0 - \eta_\infty)}{1 + A\dot{\gamma} + B\dot{\gamma}^n} + \eta_\infty \tag{6}$$

has been suggested (8).

Each equation is valid only within the range of the variables considered in its development and subsequent substantiation. Each has served and will continue to serve its purpose, but their limitations and conditions must be thoroughly known before they can be applied with meaning.

Mathematical Representation

To examine the flow behavior from the standpoint of continuum mechanics, certain relationships regarding the state of the material must be derived. These equations, commonly called the equations of change, are the relationships for conservation of mass, momentum, and mechanical and thermal energy, each of which is covered for both isothermal and non-isothermal systems.

The general procedure for developing any one of the equations of change is to assume a volume element of dimensions Δx, Δy, and Δz. The flow of the quantity of interest is then formulated for each face of the element, and the dimensions Δx, Δy, Δz are allowed to approach zero. This result, with some simple manipulation, is the final form of interest.

With this general procedure, each case can be taken in turn. For conservation of mass, the mass balance equations result in

$$\frac{\partial \rho}{\partial t} = -(\nabla \cdot \rho v) \tag{7}$$

where $\nabla = \left(\frac{\partial}{\partial x} + \frac{\partial}{\partial y} + \frac{\partial}{\partial z}\right)$. An important form of this equation is for a fluid of constant density, or

$$(\nabla \cdot v) = 0 \tag{8}$$

Considering conservation of momentum, the problem of momentum balance across any face becomes more involved, since momentum terms must be accounted for in all three coordinate directions for each face. The momentum balance equation not only

includes momentum in and out, but also the sum of the forces acting on the face such that

$$\frac{\partial}{\partial t} \rho v = -[\nabla \cdot \rho vv] - [\nabla \cdot \tau] - \nabla p + \rho g \tag{9}$$

where $[\nabla \cdot \rho vv]$ and $[\nabla \cdot \tau]$ are vectors because of the tensoral nature of ρvv and τ. To use Eq. 9 for flow analysis, the expressions for the components of τ must be known. For a Newtonian fluid, they are of the form

$$\tau_{xx} = -2\mu \frac{\partial v_x}{\partial x} + \left(\frac{2}{3}\mu - K\right)(\nabla \cdot v) \tag{10}$$

and

$$\tau_{xy} = \tau_{yx} = -\mu \left(\frac{\partial v_x}{\partial y} + \frac{\partial v_y}{\partial x}\right) \tag{11}$$

where μ and K are the coefficient of Newtonian viscosity and the coefficient of bulk viscosity, respectively. Some authors (9) suggest that the K term can be dropped as negligible, while others (7) are of the opinion that K is of the same order of magnitude as μ.

A useful form of Eq. 9 is for flow between parallel plates

$$\tau_{xx} = \tau_{yy} = \tau_{zz} = \tau_{yz} = \tau_{xz} = 0 \tag{12}$$

and

$$\tau_{xy} = -\mu \left(\frac{dv_x}{dy}\right) \tag{13}$$

which is Newton's law of viscosity.

The rate of change of kinetic energy per unit mass is found by considering the scalar product of local velocity with the equation for conservation of momentum

$$\frac{\partial}{\partial t}\left(\frac{1}{2}\rho v^2\right) = -\left(\nabla \cdot \frac{1}{2}\rho v^2 v\right) - (\nabla \cdot pv) - p(-\nabla \cdot v) - \nabla \cdot (\tau \cdot v) - (-\tau : \nabla v) + \rho(v \cdot g) \tag{14}$$

So far, this analysis is based on an isothermal system; however, the term $(-\tau : \nabla v)$ describes the irreversible conversion of internal energy. Since some mechanical energy is thus obviously degraded to thermal, the system is not strictly isothermal unless an isothermal system is defined as one in which generated heat does not cause appreciable temperature change. This is true in all but high-speed flow systems with large velocity gradients. After examining the equation for mechanical energy, the subject can now be expanded to thermal energy which also allows the examination of non-isothermal systems. Again assuming the general procedure as first set forth, the energy balance equation, including the effects of kinetic and heat energy and the rate of work done on the system, may be written as

$$\frac{\partial}{\partial t} \rho \left(U + \frac{1}{2} v^2\right) = -\left(\nabla \cdot \rho v \left(U + \frac{1}{2} v^2\right)\right) - (\nabla \cdot q) + \rho (v \cdot g) - (\nabla \cdot pv) - (\nabla \cdot [\tau \cdot v]) \tag{15}$$

where U is the internal energy per unit mass of the fluid within the original volume element.

By using the five equations shown here, alone or in combination, flow problems may be set up. With the help of numerous assumptions, the resulting equations may be reduced to a solution. The difficulty in applying the equations of change to practical flow problems is that in all but a few select and simple cases, the simplifying assumptions that are necessary damage the validity of the analysis so much that the results are of questionable value. It is the current trend of research in this area to apply as much as possible the mathematical approach to empirically developed models.

Structural Representation

In recent years, the most promising approach for developing a general theory of flow has been through a structural explanation. Three basic procedures have been suggested depending on whether colloidal theory, rate theory, or kinetic theory is taken as the basis of the argument. The colloidal theory is the oldest and simplest of the three. The approach is based on low concentrations of particles in a solvent. Einstein first deduced the equation

$$\eta = \eta_0 (1 + 2.5 \phi) \tag{16}$$

for solutions below about two-tenths percent of spherical particles. Here, η_0 is the viscosity of the pure solvent and ϕ is the volume of spherical particles per unit volume of suspension. The only assumption is that there is no interaction between the individual spheres. Guth, Gold, and Simha (10) later amended the relationship as

$$\eta = \eta_0 (1 + 2.5 \phi + 14.1 \phi^2) \tag{17}$$

which has been experimentally validated for up to 6 percent solutions. Using the basic idea that relative viscosity—the solution viscosity divided by the solvent viscosity—is a function of the energy dissipation caused by the presence of the suspended particles, relationships have been developed for particles of varied shapes at a range of concentrations. The effects of particle interaction, absorption of the solvent, particle deformability, system thermodynamic conditions, and system electrical conditions are also investigated in the light of colloidal theory (10).

The second approach is that of Eyring and his co-workers. As stated by Brodkey, "their work is based on the application of the theory of rate processes to the relaxation processes that are believed to play an important part in determining the nature of the flow... Very briefly, the theory postulates an activated complex as an intermediate unstable state, which would be formed from the reactants and decompose into the products. The assumption is made that the decomposition of the complex is the rate controlling step, and that there is an activation energy associated with this (11)." To expand this argument, the following is presented as digested from Glasstone et al. (4).

Liquids and gases may be considered as opposites, one consisting of matter moving around holes (gases), and the other, holes moving around matter. The energy necessary to provide molecular movement is made up of two parts, the energy to create a hole, and the energy to move a molecule into it. Taking E as the energy required to vaporize the molecule and leave behind a hole, then $\frac{1}{2}$ E is required if the hole is closed, and E - $\frac{1}{2}$ E or $\frac{1}{2}$ E is required merely to make the hole; $\frac{1}{2}$ E is then the energy of vaporization of the molecule.

In order to extend this development to viscosity, reference is made to the figure on the following page. For a molecule to move the distance δ, it must be transported across an energy barrier, E_0, the energy of activation. The net rate of flow in terms of shear rate is

$$\dot{\gamma} = \frac{2\delta}{\delta_1} k \sinh \frac{F\delta\delta_2\delta_3}{2KT} \tag{18}$$

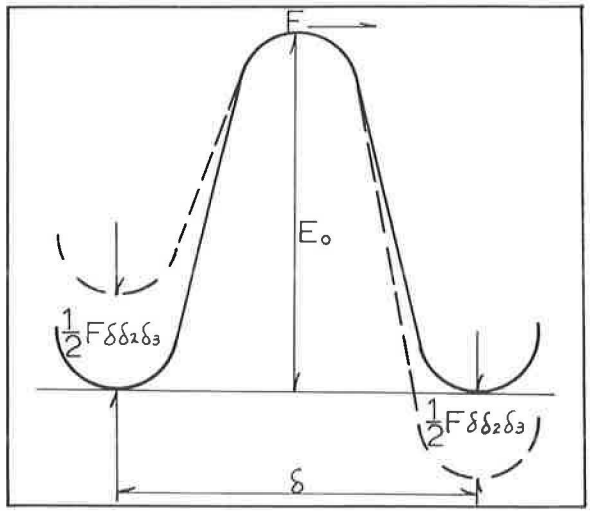

where k is the initial rate of motion and F is the applied shearing force. Using statistical mechanics, k may be shown to be

$$k = \frac{KT}{h} \exp\left(\frac{-E_O}{RT}\right) \tag{19}$$

where K, h, and R are respectively the Boltzmann, Planck, and universal gas constants. Then

$$\dot{\gamma} = A \sinh B\tau \tag{20}$$

where

$$A = \frac{2KT}{h} \exp\left(\frac{-E_O}{RT}\right) \tag{21}$$

and

$$B = \frac{\delta\delta_2\delta_3}{2KT} \tag{22}$$

The third concept of structural flow is that based on a homogeneous reaction kinetic approach as developed by Denny and Brodkey (5, 11, 12). The basic hypothesis is that non-Newtonian behavior is caused by a structural breakdown of the forces between particles. At very low shear rates, the viscosity is a constant, η_O, and at high shear rates, the viscosity of the material again approaches a constant η_∞. These two represent the limiting cases of no breakdown and complete breakdown. At any point between these extremes, the viscosity η is some function of the portion of unbroken forces within the material. By applying the inverse lever principle, the portion of broken forces may be taken as

$$F = \frac{f(\eta_O) - f(\eta)}{f(\eta) - f(\eta_\infty)} \tag{23}$$

and the unbroken portion is 1 - F. The function f (η) is a relationship for the concentration of changing structure to viscosity and for polymer melts and polymers in solution the proper form would be (11)

$$f(\eta) = A\,\eta^{1/3.5} \tag{24}$$

It is noted that all viscosities are the true apparent viscosities, or the arctangent of a straight line drawn from the origin to the point on the flow diagram in consideration.

In order to establish the kinetic reaction rate, consider the reaction

$$\text{unbroken forces} \underset{k_1}{\overset{k_2}{\rightleftharpoons}} \text{broken forces} \tag{25}$$

which has the kinetric reaction equation

$$-\frac{d(1 - F)}{dt} = k_1'(1 - F)^n - k_2 F^m \tag{26}$$

where k_1' must include the effect of shear stress. Therefore

$$k_1' = k_1(\tau)^p \tag{27}$$

Brodkey (11) has suggested the use of shear stress rather than shear rate so as to separate the effect of temperature on viscosity from the effect of shear rate on the structural reaction. The reasoning is that if shear rate is used, then the reaction rate would be affected by both changes in the F and k terms, whereas, if shear stress is used, the F term is constant with constant temperature, and the rate is changed only by changes in the k's.

Following this development, then

$$-\frac{d(1 - F)}{dt} = k_1(1 - F)^n(\tau)^p - k_2 F^m \tag{28}$$

At the limiting viscosity

$$\frac{-d(1 - F)}{dt} = 0 \tag{29}$$

and

$$K = \frac{k_1}{k_2} = \frac{F^m}{(1 - F)^n \tau^p} \tag{30}$$

where K is of the form of an equilibrium constant. The integer constants, m and n, may be taken from initial rates, or in the case of time-dependent materials, by integration with assumed values for m and n along a constant shear line.

The attractions of this theory are that the exact nature of the fundamental mechanism is not assumed, and that the constants are easy to determine and interpret. It is suggested that ultimately all of the parameters should eventually be related to the specific breakdown mechanism involved for each material or type of material, but it is emphasized that this relation need not be known to apply the method.

The application of these theories, especially rate process theory and kinetic theory, to any specific group of materials such as paving asphalts requires some further assumptions and mathematical treatments. The following is a brief review of such applications to the analysis of flow behavior of asphalts.

Herrin and Jones (2) applied the absolute rate theory, or rate process theory, to asphalts. Using Eq. 18, they assumed that the values of δ and δ_1 may be considered of the same order of magnitude, and $2\delta/\delta_1$ may be taken ≈ 1. Further, the term $\delta\delta_2\delta_3$ was taken as equal to V_f, the effective volume of the flow unit. Using these assumptions and considering the equation

$$\Delta F = \Delta H - T\Delta S \tag{31}$$

where F is the free energy, H is the heat of activation, T is the temperature in absolute degrees, and S is the system entropy, they found

$$\dot{\gamma} = \dot{\gamma}_o \sinh \frac{\tau}{\tau_o} \tag{32}$$

where $\tau_o = V_f/2KT$ and $\dot{\gamma}_o = (KT/h) \exp(-\Delta H/RT) \exp(\Delta S/R)$. Rewriting the expression for $\dot{\gamma}_o$ in logarithmic form

$$\log \frac{\dot{\gamma}_o}{T} = \log \frac{K}{h} + \frac{\Delta S}{2.303R} - \frac{\Delta H}{2.303R}\left(\frac{1}{T}\right) \tag{33}$$

Then if $\dot{\gamma}_o$ is constant at any given T, the plot of $\log \dot{\gamma}_o/T$ vs $1/T$ should be a straight line. The work of Herrin and Jones showed this relationship to be valid for their material.

It can also be shown that if τ_o is taken as large then the quantity $\dot{\gamma} = \dot{\gamma}_o (\tau/\tau_o)$ may be calculated at any test temperature from the semilog plot, $\dot{\gamma}_o/T$ vs $1/T$ for any selected $\dot{\gamma}_o$. Using this τ_o in the expression $1/\tau_o = V_f/2KT$, the size of the flow unit at any temperature may be found. It can also be shown that ΔS is not a function of temperature, and thus the heat of activation ΔH can be found as the slope of the plot. Since the intercept of the line is ΔS, the free energy of activation ΔF can then be found and is a linear function of temperature.

This analysis applied to one asphalt showed that the flow behavior of asphalt can be predicted using absolute rate theory. It also showed that the flow unit size is much larger than the individual molecules, and that they decrease in size as the temperature increases.

Majidzadeh and Schweyer (3), working with thirteen different asphalts, applied kinetic reaction theory to their data to determine the equilibrium constants, K, as a function of shear rate. For each asphalt, a hyperbolic sine relationship was assumed in the form

$$\dot{\gamma} = A \sinh B\tau, \tag{34}$$

and the constants A and B were determined. The limiting viscosities were found and the equilibrium viscosity for any constant rate of shear was then

$$\eta = \frac{1}{AB \cosh B\tau} \tag{35}$$

which is the inverse of the first derivative of $\dot{\gamma} = A \sinh B\tau$ for any stress level. Eq. 30 may be written in log form as

$$\log \frac{(\eta_o - \eta)^m}{(\eta - \eta_\infty)^n} = p \log \dot{\gamma} + \log K (\eta_o - \eta_\infty)^{m-n} \tag{36}$$

Thus, the slope of the straight line plot of log $(\eta_o - \eta)^m/(\eta - \eta_\infty)^n$ vs log $\dot{\gamma}$ will be p and the intercept at $\dot{\gamma} = 1$ will make possible the calculation of K. Of course, in order to obtain a straight line, the proper choice of m and n must be made. In this case, as with the case of many polymer melts (11), m = 2 and n = 1.

Thus, if the equilibrium constant of a material and its limiting viscosities are known, the viscosity for any shear rate within the range of the study may be calculated knowing one additional point. The only requirements on the material are that it must be represented by a hyperbolic sine relationship, and that the proper choice of the integers m and n can be made such that the log-log plot of $(\eta_o - \eta)^m/(\eta - \eta_\infty)^n$ vs $\dot{\gamma}$ is a straight line.

Physical-Chemical Representation

Early attempts to arrive at a rational explanation for the flow behavior of bitumens assumed a colloidal system. This theory, postulated by Nellensteyn (13), was based on observations of solutions of bitumens in benzene. Mack (6) questions the validity of extrapolation of Nellensteyn findings to a solvent-free material because evidence indicates that asphaltenes are not completely dissolved in benzene but exist in the solution as partially saturated associated particles. This is not compatible with the assumption that the asphaltic bitumens are solutions of asphaltenes in petrolenes which, at low temperatures (less than 120 C), form molecular complexes. Mack shows qualitatively that non-Newtonian flow increases as the aromaticity of the oil constituents decreases. Thus, it would seem that non-Newtonian flow is some function of the concentration of the asphaltenes and aromaticity or the ability of the petrolenes to dissolve the asphaltenes.

This work is substantiated by several studies on asphalt using the electron microscope. Katz and Betu (14) found that photographs of films of bitumens formed from benzene solutions showed associated particles of asphaltenes. Swanson (15) found that to form a homogeneous bitumen film by the same process, the ratio of resins to asphaltenes had to be at least three to one. Finally, if the film is not formed by evaporation of benzene from a bitumen-benzene solution, examination indicates no particles of typical colloidal dimensions.

Although most of the molecular forces in bitumens are dispersion forces of attraction produced by carbon and hydrogen, electron microscope studies seem to indicate that strong polar bonds are also operative. The structural buildup is then somewhat like crystallization in that molecular orientation takes place. On the other hand, unlike crystallization, the operative forces are unable to attract like neighbors because of the relatively large distances over which attractive forces would have to act. Thus, bitumen structure is rather random with unlike molecules attracting each other only if their forces and shapes are such that they can adapt to each other. Molecules with aromatic rings, because of their side groups, lend well to cavity formation in which other molecules, if they are of the right shape, may be trapped. Therefore, again the structure of bitumen is dependent on asphaltene concentration and the aromatic properties of the other constituents.

To relate structure to flow properties, it is necessary to consider the shape of the associated complexes. Considering the internal thermodynamics of the system, change will take place spontaneously only if the free energy is diminished. This decrease is associated with a decrease in surface area, and thus it could be expected that the complexes are spherical in shape. On application of a shear stress the particles elongate into ellipsoids and flow through the oily medium. In the case of Newtonian materials, the association bonds within the particles are too strong to be broken by the applied stress. On application of higher stresses, some point is reached where these bonds begin to break, and continue to break until breakup is in equilibrium with the applied stress. The material then shows Newtonian behavior in two ranges, one of no breakdown (low shear stress) and one of breakdown in equilibrium with stresses (high shear stress). Thus, chemical structure can be related to physical behavior.

THERMAL EFFECTS

Asphaltic materials are thermoplastic and, therefore, will show variation in consistency with change in test temperature. Since climatic variations and construction

conditions represent wide variations in temperature, the prediction of flow behavior with temperature is of great importance. The general method used to represent the viscosity-temperature relationship is some form of graphical plot that produces a straight-line relationship for the particular data. Neppe (16) has listed six different plots along with a description of the equations and useful temperature ranges.

To date, the most commonly used graphical representation of viscosity-temperature data is the Walther plot of log-log viscosity vs log absolute temperature (16). Following the general objective of finding a straight line relationship, this method has been by far the most successful. Another plot, log viscosity vs reciprocal absolute test temperature, was used by the authors in a previous study with good results over a temperature range of 10 C to 60 C (17).

The viscosity-temperature relationship may be explained structurally by considering conditions within the material at low temperatures. In this state the asphaltenes are precipitated from solution and exist as relatively large associated complexes. As the temperature increases, thermal activity forces the individual molecules farther and farther apart. Since the attractive forces diminish rapidly with distance, the complexes subjected to shear stresses begin to break down and thus the viscosity is reduced. Another contributing factor is that at low temperatures varying amounts of oily constituents are held within the asphaltene complexes by association bonds. As the thermal energy increases the strength of the bonds decrease, and the oils are freed to give added lubrication to the system.

Perhaps the most significant advance in the study of temperature effects is the development of the time-temperature superposition principle. The principle was originally developed in the field of polymeric sciences and was successfully used by Ferry (18) to obtain shear diagrams over a wide range of shear rates. The technique is such that the shear diagrams of a temperature-susceptible material like asphalt, determined over a wide range of temperatures, are reduced to a common arbitrary temperature. The result is a shear stress-rate of shear diagram of the material over a wide range of shear rate at that particular temperature.

The procedure involves determining a shift factor, a_T, either analytically or graphically such that when the shear diagram curves for different temperatures are multiplied by their respective a_T's, the curves superimpose on each other in one continuous curve at an arbitrary base temperature. The applicability of the principle to asphaltic materials has been well substantiated. Sisko (19) obtained a master curve of viscosity vs shear rate for a wide range of shear rates. Phillippoff et al. (20) developed a master curve for the dynamic properties of asphalt. The authors (17) have shown a reduced shear diagram over seven decades of shear rate.

GENERAL FLOW MEASURING DEVICES

The measurement of viscosity is a field more widely investigated than the theory of viscosity itself, a fact to which present literature will attest. Viscometers themselves present quite a large variety ranging from small simple rising-bubble types to quite large sophisticated rheometers. The basic problem with most instruments is that they are designed to do a specific job, and in most studies, unless the more sophisticated instruments are available, more than one type of instrument is necessary.

Viscometers are divided into three basic types: rotational, capillary, and miscellaneous. Rotational viscometers may be of the coaxial cylinder type or the cone and plate type. The first is characterized by two concentric cylinders with a small gap between them in which the sample is placed. A constant rotation, or a constant torque is applied to one or both of the cylinders, and the viscosity coefficient is calculated from the torque required to maintain a constant shear, or to keep the other cylinder stationary. These instruments are simple of design and easy to use; however, the data relationships are derived for Newtonian fluids.

For non-Newtonian materials, Brodkey (21) has suggested the following procedure. The correction factor n' may be found by plotting τ vs

$$\frac{\eta^2 r_1^2 \Omega h}{r_1^2 - r_2^2} \tag{37}$$

on a log-log scale where η is the apparent viscosity, r_1 and r_2 are the inner and outer cylinder radii, respectively, Ω is the angular velocity at the face of the inner cylinder, and h is the inner cylinder height. Then for any value of τ, n' is the slope of the line, and

$$\dot{\gamma} = \left[\frac{1 - (r_2/r_1)^2}{n'\left[1 - (r_2/r_1)^{2/n'}\right]}\right]\left[\frac{2r_1^2\Omega h}{(r_1^2 - r_2^2)}\right] \tag{38}$$

If n' is unity, then

$$\dot{\gamma} = \frac{2r_1^2\Omega h}{(r_1^2 - r_2^2)} = \frac{\tau}{\eta} \tag{39}$$

which is the Newtonian case. The measured τ and calculated $\dot{\gamma}$ are then used to construct the shear stress-rate of shear diagram.

The second basic group, capillary viscometers, consists of a fluid reservoir, a capillary tube, a pressure control device, a rate of flow measuring device, and a temperature control device. Rheometers are part of this general group and are distinguished by a piston used to drive the fluid through the capillary tube. Their particular advantage is that their high driving pressures allow viscosity measurements at high shear rates. Orifice viscometers are the simplest and most widely used of the capillary group. Their simplicity makes them highly adaptable to industrial uses, but for research, the difficulties of analyzing the flow mechanism of such a short capillary exclude their use.

Glass capillary tubes are of two types, pressure flow type and gravity flow type. The gravity flow types are generally limited to materials of low viscosity, but are convenient in that the driving force is usually the hydrostatic head of the test liquid itself. The kinematic viscosity may thus be measured directly.

Again, for the capillary viscometer, the relationships are derived for Newtonian materials such that

$$\dot{\gamma}_{wall} = \left(-\frac{dv}{dr}\right)_{wall} = \frac{A}{t} \tag{40}$$

where A is taken as constant and t is fill time, and

$$\tau_{wall} = \dot{\gamma}\left[K_2 (H - h)\, t\right] \tag{41}$$

where K_2 is a calibrated instrument constant and (H - h) is a vacuum head term. For non-Newtonian materials, A is not a constant. Brodkey (21) has suggested the following analysis

$$\dot{\gamma}_{wall} = \left[(3n' + 1)/4n'\right]\,(4\bar{v}/r_o) \tag{42}$$

where n' should satisfy the relationship

$$\tau_{wall} = (-r_o\Delta p/2L) = K'(4\bar{v}/r_o)^{n'} \tag{43}$$

Thus, n' can be obtained from the slope of a log-log plot of $(-r_o\Delta p/2L)$ vs $(4\bar{v}/r_o)$. The corrected shear rate at the wall may then be calculated using n' and its corresponding value of $(4\bar{v}/r_o)$. It should be noted that n' is not necessarily a constant and may have to be found for each value of shear stress at the wall. Shear stress may then be easily

calculated point by point from the relationship

$$\tau = \overset{\circ}{\gamma}\,\eta \tag{44}$$

and the shear stress-rate of shear diagram constructed.

Of all the miscellaneous group, the most useful and widely used is the sliding plate microviscometer. The procedure for this instrument is relatively simple as the geometry is that used to define viscosity. The data, therefore, may be used as taken for both Newtonian and non-Newtonian materials. The instrument produces most favorable results when applied to studies on asphaltic cement. It has the advantage of requiring a small sample, and the viscosity is measured in very thin films of the same order of magnitude as those maintained around aggregates in bituminous mixtures.

MATERIALS AND PROCEDURE

The two asphalt cements used in this study are a 60/70 penetration asphalt cement from a Venezuelan crude and an AC-20 grade asphalt cement used in the "Asphalt Institute Bureau of Public Roads Cooperative Study of Viscosity-Graded Asphalts" coded as B-3056. The results of conventional tests on these asphalts are given in Table 1. The 60-70 penetration asphalt (No. 1) is nearly Newtonian in behavior and the second asphalt (No. 2) is non-Newtonian, as indicated from their viscosity results (Table 1).

Three different instruments were used to obtain viscosity data over a range of temperature of 10 C to 160 C and a range of shear rates of 10^{-4} to 10^{4} reciprocal seconds.

A sliding plate microviscometer, made by Hallikainen Instruments, and a Varian Model G-14 graphic recorder were used to obtain data in a shear rate range of 10^{-4} to 10^{-1} reciprocal seconds and a temperature range of 10 C to 45 C. Specimen preparation and testing were done following the procedure described by ASTM (22) with one exception—each specimen was loaded only once. This exception was used because in the upper range of shear rates, and especially with more complex asphalt, a considerable deformation was necessary to establish a measured constant slope. In many cases this deformation was 200 microns, which represents a one-percent change in area of the plates and was thus used as the maximum deformation permitted on any one specimen.

In order to provide data for low shear rates at higher temperatures, a Haake Rotovisco with coaxial cylinders was used. This instrument and its test procedure is well described by Van Wazer et al. (8). Briefly, the Rotovisco consists of a control unit and a measuring head. The control unit houses electrical circuitry for converting torque to potential difference, the drive motor, and a ten-speed reduction transmission. The measuring head is connected to the control unit with a flexible shaft which acts as both an electrical and mechanical connection.

TABLE 1

STANDARD SPECIFICATION TESTS ON ASPHALTS

Test	Asphalt No. 1	Asphalt No. 2
Specific gravity 77/77 F	1.010	1.020
Softening point, ring and ball	123 F	
Ductility 77 F	150 + cm	250 + cm
Penetration		
100 gm, 5 sec, 77 F	63	30
200 gm, 60 sec, 39.4 F	23.5	
Flash point, Cleveland open cup	455 F	545 F

The sample was introduced into a circular gap between two coaxial concentric cylinders at the base of the measuring head. The cylinders were surrounded by an oil jacket heated to within ±0.1 C of test temperature by a Haake Model F oil bath. The outer cylinder was held stationary while the inner cylinder was caused to rotate at a constant rate by the drive motor through the flexible shaft. Located in the measuring head, between the flexible shaft and the rotating cylinder, is an electrical torsion dynamometer consisting of two coaxial shafts mechanically coupled by a creep-resistant torsion spring. The angular displacement of the spring caused by the torque created on the cylinder immersed in the test material is transmitted electronically through the flexible shaft to the control unit. This torque is then a measurement of viscosity.

The Rotovisco may be equipped with several sizes of inner and outer cylinders of which two, denoted MV and SV, were used depending on the expected viscosity of the material at the particular test temperature. Any one of three measuring heads, 50, 500, or 5000, was used depending on the expected level of stress (the numbers indicate the approximate torque measured in gm-cm). The ten basic rotation speeds may be reduced by 10, 100, or 1000 times using a 10-to-1 and/or 100-to-1 gear reducer in the mechanical transmission line. This provides a minimum shear rate of 3×10^{-3} reciprocal seconds. The minimum test temperature used with this instrument and coaxial cylinders was 45 C. Below this, stress levels exceed the instrument limits.

To obtain the viscosity at high shear rates Cannon-Manning vacuum viscometers were used in conjuction with the Cannon vacuum regulator, and a model H-1 high temperature oil bath. Accuracy is maintained to ±0.5 mm Hg for a range 5-50 cm Hg with the regulator, and to ±0.01 C for a range of 68 to 400 F in the bath. The geometry of the viscometers is described in detail elsewhere (8).

At least three tests were run at each test temperature to describe the range of shear rates available. Test temperatures varying from 45 C to 150 C were used.

RESULTS AND DISCUSSION OF RESULTS

The values of viscosity obtained for the two asphalts used in this study are tabulated in Table 2. As mentioned before, these values were obtained using a capillary, a sliding plate, and a rotational viscometer. Due to the instrument limitations, each type of viscometer could be used only for a certain range of temperature, shear stress, and rate of shear. However, as shown in Figure 1, it was possible to obtain values of viscosity for the asphalts at a test temperature of 45 C with all three viscometers. Figure 1, which shows the variation in the viscosity of asphalt No. 1 with rate of shear, indicates that the three viscometers used gave overlapping data, and there exists a continuity in their results. The slight deviation observed at low rates of shear is believed to be due to an error in the viscosity measurement of the sliding plate viscometer. At the test temperature of 45 C the magnitude of load required to cause flow of the asphalt between the two parallel plates was of the order of a few grams, as shown in Table 2. For such small shear stresses, any small error in the balancing system

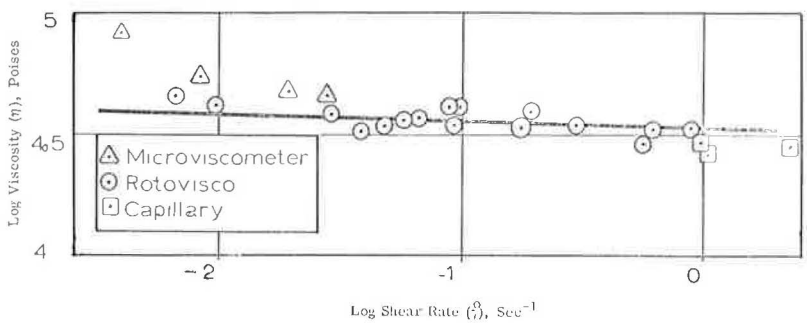

Figure 1. Viscosity vs shear rate for asphalt No. 1 at 45 C with all viscometers.

TABLE 2

VISCOMETRY RESULTS OF ASPHALTS

Description	Shear Stress τ (dynes/cm^2)	Shear Rate $\dot{\gamma}$ (sec^{-1})	Viscosity η Poises
Asphalt No. 1			
T = 5 C	3.30×10^5	6.70×10^{-4}	4.93×10^8
	5.00×10^5	8.55×10^{-4}	5.85×10^8
	7.00×10^5	1.11×10^{-3}	6.31×10^8
	1.00×10^6	1.58×10^{-3}	6.33×10^8
	1.65×10^6	3.08×10^{-3}	5.36×10^8
T = 10 C	1.61×10^5	1.42×10^{-3}	1.13×10^8
	3.50×10^5	2.67×10^{-3}	1.31×10^8
	6.00×10^5	4.68×10^{-3}	1.28×10^8
	1.20×10^5	1.12×10^{-2}	1.07×10^8
	1.65×10^5	1.73×10^{-2}	9.54×10^7
T = 20 C	1.60×10^4	1.31×10^{-3}	1.22×10^7
	3.00×10^4	2.56×10^{-3}	1.17×10^7
	5.50×10^4	4.90×10^{-3}	1.12×10^7
	1.30×10^5	1.23×10^{-2}	1.06×10^7
	3.55×10^5	3.62×10^{-2}	9.81×10^6
T = 25 C	2.50×10^3	8.75×10^{-4}	2.86×10^6
	6.00×10^3	2.29×10^{-3}	2.62×10^6
	1.20×10^4	4.59×10^{-3}	2.62×10^6
	3.50×10^4	1.43×10^{-2}	2.45×10^6
	8.10×10^5	3.43×10^{-2}	2.36×10^6
T = 35 C	8.10×10^2	2.37×10^{-3}	3.42×10^5
	1.50×10^3	4.70×10^{-3}	3.19×10^5
	4.00×10^3	1.39×10^{-2}	2.88×10^5
	9.00×10^3	3.40×10^{-2}	2.65×10^5
	1.63×10^4	6.55×10^{-2}	2.49×10^5
T = 45 C	2.80×10^2	6.48×10^{-3}	4.32×10^4
	9.00×10^2	2.21×10^{-2}	4.07×10^4
	2.80×10^3	7.45×10^{-2}	3.76×10^4
	9.50×10^3	2.67×10^{-1}	3.56×10^4
	3.00×10^4	9.10×10^{-1}	3.30×10^4
T = 80 C	2.38×10^2	7.40×10^{-1}	3.22×10^2
	7.00×10^2	2.17×10^0	3.23×10^2
	1.80×10^3	5.55×10^0	3.24×10^2
	5.50×10^3	1.68×10^1	3.27×10^2
	1.78×10^4	5.43×10^1	3.28×10^2
T = 120 C	4.10×10^2	2.68×10^1	1.53×10^1
	9.00×10^2	5.88×10^1	1.53×10^1
	1.80×10^3	1.19×10^2	1.51×10^1
	4.00×10^3	2.60×10^2	1.53×10^1
	7.70×10^3	5.00×10^2	1.54×10^1
T = 160 C	8.15×10^2	5.22×10^2	1.56×10^0
	1.40×10^3	8.95×10^2	1.56×10^0
	2.80×10^3	1.79×10^3	1.56×10^0
	4.00×10^3	2.56×10^3	1.56×10^0
	5.00×10^3	3.20×10^3	1.56×10^0

TABLE 2 (Cont'd)

VISCOMETRY RESULTS OF ASPHALTS

Description	Shear Stress τ (dynes/cm^2)	Shear Rate $\dot{\gamma}$ (sec^{-1})	Viscosity η Poises
Asphalt No. 2			
T = 10 C	4.00×10^5	2.70×10^{-4}	1.48×10^9
	6.50×10^5	5.15×10^{-4}	1.26×10^9
	9.50×10^5	1.02×10^{-3}	9.31×10^8
	1.30×10^5	1.77×10^{-3}	7.34×10^8
	1.64×10^6	2.68×10^{-3}	6.12×10^8
T = 20 C	1.15×10^5	1.84×10^{-3}	6.25×10^7
	2.20×10^5	4.40×10^{-3}	5.00×10^7
	3.80×10^5	9.35×10^{-3}	4.06×10^7
	7.00×10^5	2.07×10^{-2}	3.38×10^7
	1.16×10^6	4.08×10^{-2}	2.84×10^7
T = 25 C	4.80×10^4	2.08×10^{-3}	2.31×10^7
	8.00×10^4	3.81×10^{-3}	2.10×10^7
	1.50×10^5	8.15×10^{-3}	1.84×10^7
	2.70×10^5	1.62×10^{-2}	1.66×10^7
	4.90×10^5	3.35×10^{-2}	1.46×10^7
T = 35 C	3.28×10^3	2.40×10^{-3}	1.37×10^6
	6.00×10^3	4.77×10^{-3}	1.26×10^6
	1.00×10^4	8.53×10^{-3}	1.17×10^6
	1.80×10^4	1.66×10^{-2}	1.08×10^6
	3.20×10^4	3.15×10^{-2}	1.02×10^6
T = 45 C	7.10×10^2	1.83×10^{-2}	3.88×10^4
	2.00×10^3	4.01×10^{-2}	4.99×10^4
	5.00×10^3	1.39×10^{-1}	3.60×10^4
	1.50×10^4	4.38×10^{-1}	3.42×10^4
	2.90×10^4	8.65×10^{-1}	3.35×10^4
T = 80 C	2.68×10^2	8.80×10^{-1}	3.05×10^2
	7.00×10^2	2.38×10^0	2.94×10^2
	1.80×10^3	5.90×10^0	3.05×10^2
	3.20×10^3	1.03×10^0	3.11×10^2
	7.50×10^3	2.44×10^1	3.07×10^2
T = 120 C	2.28×10^2	1.87×10^1	1.22×10^1
	5.00×10^2	4.10×10^1	1.22×10^1
	1.20×10^3	9.95×10^1	1.21×10^1
	2.50×10^3	2.04×10^2	1.23×10^1
	6.50×10^3	5.35×10^2	1.21×10^1
T = 140 C	2.16×10^3	6.65×10^2	3.25×10^0
	3.40×10^3	1.03×10^3	3.30×10^0
	4.50×10^3	1.36×10^3	3.31×10^0
T = 160 C	1.18×10^3	9.25×10^2	1.28×10^0
	2.00×10^3	1.60×10^3	1.25×10^0
	2.93×10^3	2.32×10^3	1.26×10^0

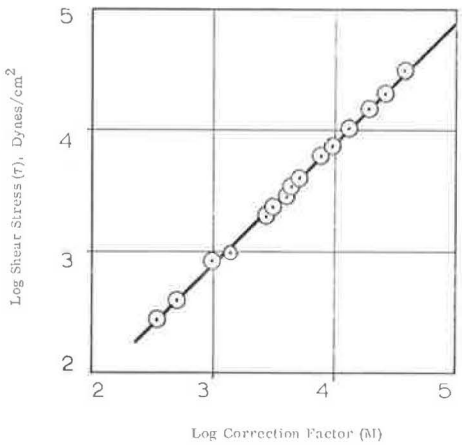

Figure 2. Correction factor vs shear stress for the rotovisco on asphalt No. 1 at 45 C.

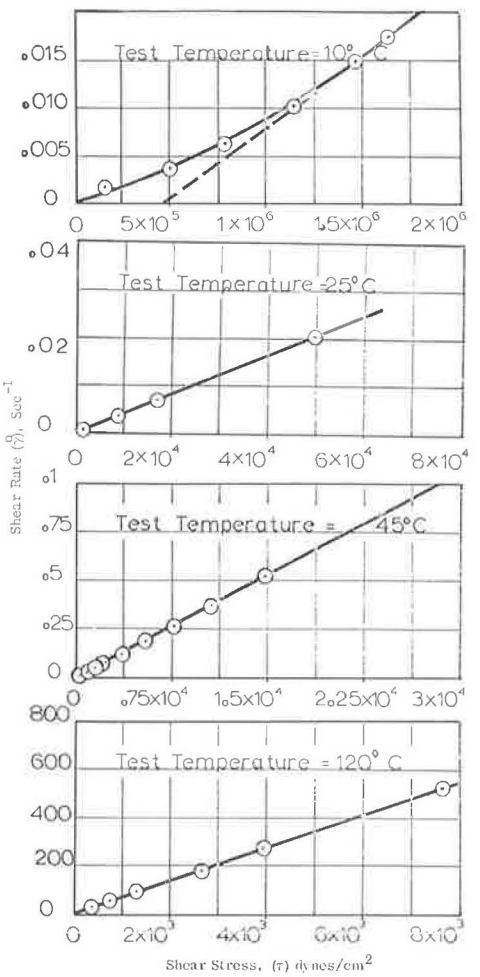

Figure 3. Shear rate vs shear stress on arithmetic scales for asphalt No. 1 at various test temperatures.

of the viscometer would result in significant variation in the calculated values of viscosity.

It was mentioned previously that for capillary and rotational viscometers the calculation of viscosity is based on Newtonian flow. In order to determine the viscosity of non-Newtonian materials, some corrections are necessary. Following the correction procedure as suggested by Brodkey, Figure 2 was constructed. This figure shows the log of shear stress vs log of correction factor M for asphalt No. 1 as obtained by the rotational viscometer where

$$M = \frac{\eta^2 r_1^2 \Omega h}{r_1^2 - r_2^2}. \qquad (45)$$

This figure shows not only that the results generate a straight line, but the slope of such a line is unity, which indicates that the Newtonian analysis is sufficient for determination of viscosity using the rotational viscometer. Similar analysis was used to determine the correction factors for the capillary viscometers, and it was found that for the test temperatures used in this study, the results of capillary viscometers could also be treated as Newtonian.

Figures 3 and 4 show the flow diagrams at different temperatures for the two asphalts used in this study. These figures, which are the plots of rate of shear vs shear stress on arithmetic scales, show that asphalt No. 1 behaves as a Newtonian material at temperatures above 25 C, while asphalt No. 2 exhibits some non-Newtonian behavior up to 45 C. These results when plotted on logarithmic scales generally give straight lines as shown in Figures 5 and 6. This suggests that, over the range of shear stress and for the temperatures used in this study, the shear stress-rate of shear relationship can be approximated by a power formula as

$$\tau = A\,(\dot{\gamma})^n \qquad (46)$$

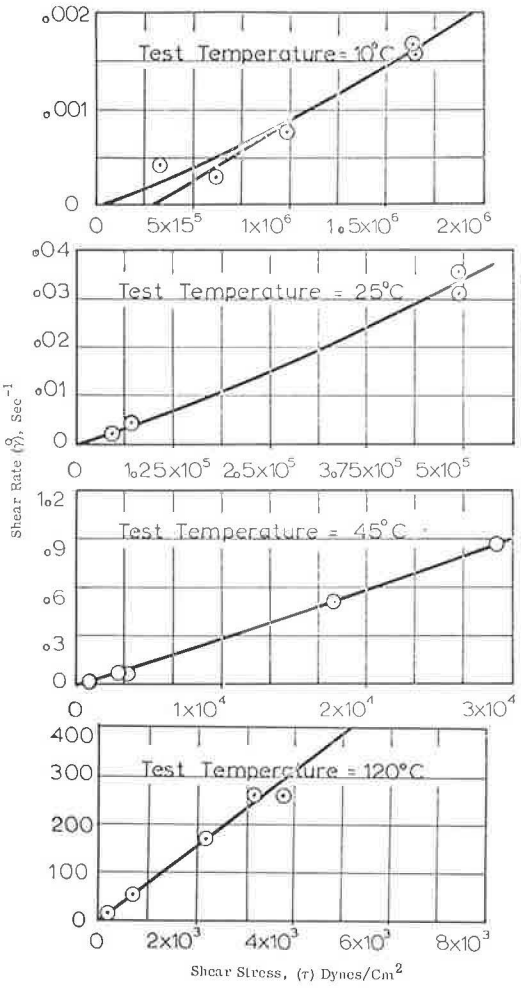

Figure 4. Shear rate vs shear stress on arithmetic scales for asphalt No. 2 at various test temperatures.

where A and n are constants whose values vary with temperature. For both asphalts, at low temperatures the slope of the line is not equal to unity, which indicates that the asphalts exhibit non-Newtonian behavior in that temperature range.

Figures 7 and 8 show master flow curves obtained by reducing the curves of Figures 5 and 6 with a horizontal shift factor (a_T) determined as

$$a_T = \frac{\eta}{\eta_o} \frac{T_o}{T} \qquad (47)$$

where T_o = 318 K is the arbitrary base temperature, and η and η_o are the viscosities of the asphalts at temperatures T and T_o, respectively. The master curves show that when the log $\dot{\gamma}$ vs log τ curves of Figures 5 and 6 were multiplied by the appropriate a_T's, they superimposed in a continuous straight line. These results substantiate the usefulness of the superposition principle in the prediction of the response of materials over wide ranges of shear rate from the results of relatively few tests.

Figure 9 is a plot of log a_T vs $1/T - 1/T_o$ where T_o = 318 K. The curve of each material is made up of two straight-line portions that intersect at a temperature slightly above the softening point of the materials. This inflection is also found in Figure 10, which is a log viscosity vs reciprocal absolute temperature plot for both asphalts. Traxler and Schweyer (24), noticing similar behavior, attributed this change in slope near the softening point to the colloidal nature of the asphalt. They suggested that the colloidal structure of asphalt changes more rapidly with temperature in the region of the softening point than in other temperature regions, which should result in a difference in temperature susceptibility of the material in that region.

TEMPERATURE EFFECT

For Newtonian materials, it is shown that viscosity is not dependent on shear stress and/or rate of shear, and is a constant at any one temperature. For such a material, the relationship showing the temperature dependency of viscosity is independent of shear rate or shear stress, and as shown before (17) this relationship can be expressed satisfactorily by the Arrhenius equation

$$\eta = A \exp(-\Delta E/RT) \qquad (48)$$

where R is the gas constant, and A and ΔE can be considered as constants over limited temperature ranges.

For non-Newtonian materials, however, the viscosity at fixed temperatures is dependent on shear stress or rate of shear. Therefore, in order to develop an expression

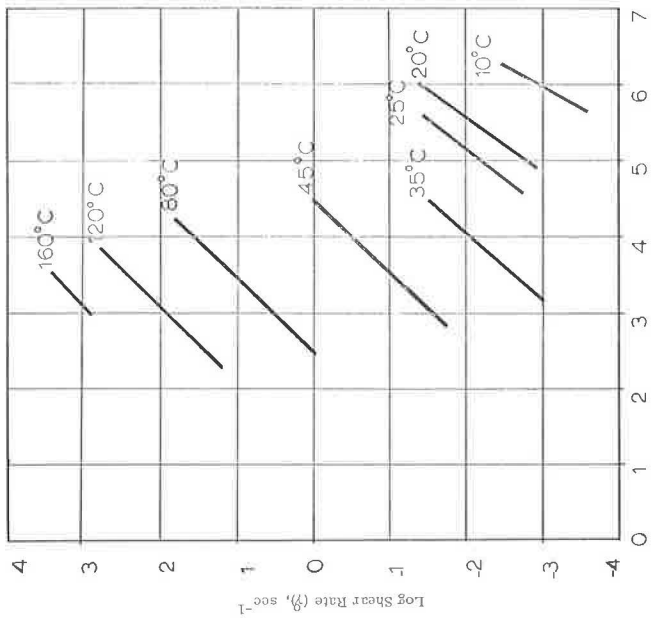

Figure 6. Shear rate vs shear stress on log-log scales for asphalt No. 2 at all test temperatures.

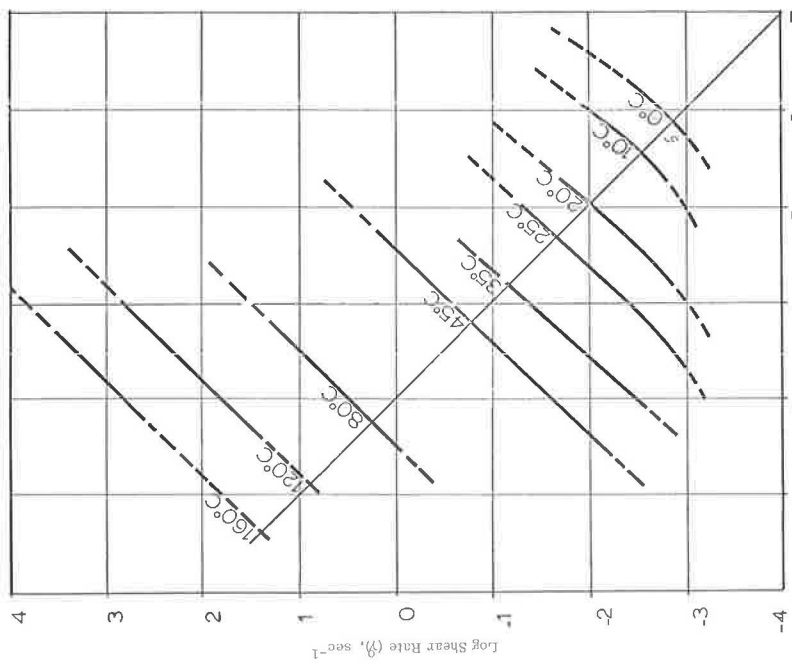

Figure 5. Shear rate vs shear stress on log-log scales for asphalt No. 1 at all test temperatures.

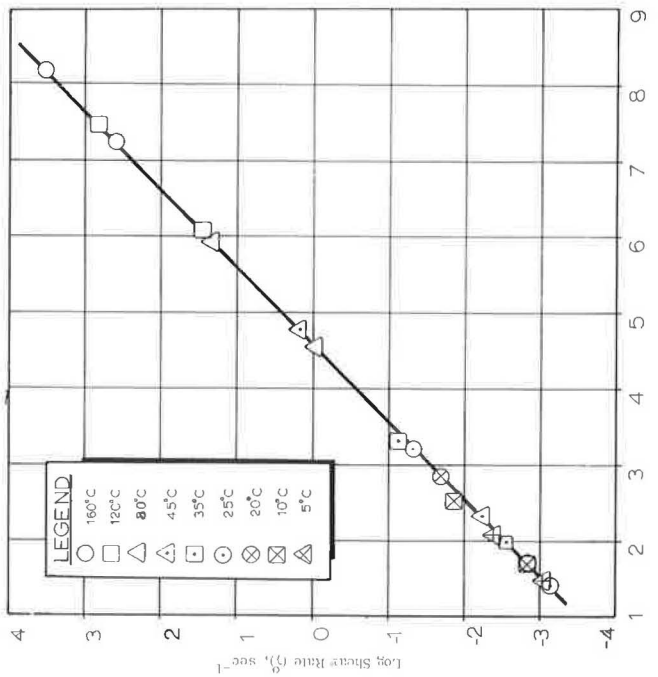

Figure 7. Master flow diagram for asphalt No. 1.

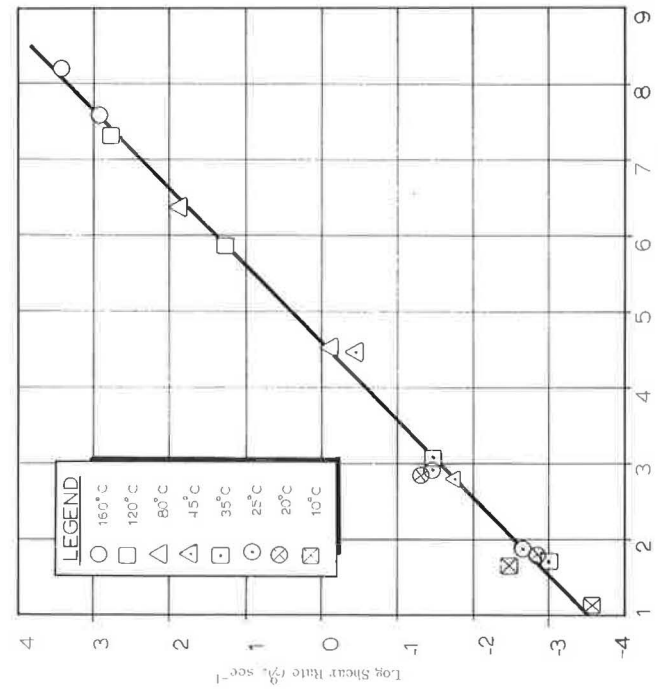

Figure 8. Master flow diagram for asphalt No. 2.

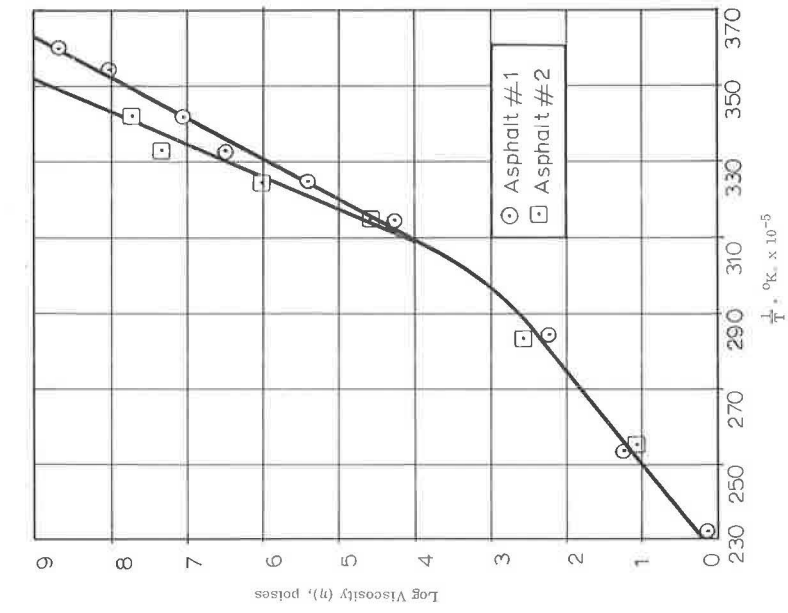

Figure 10. Viscosity vs reciprocal absolute test temperature for both asphalts at a constant power input.

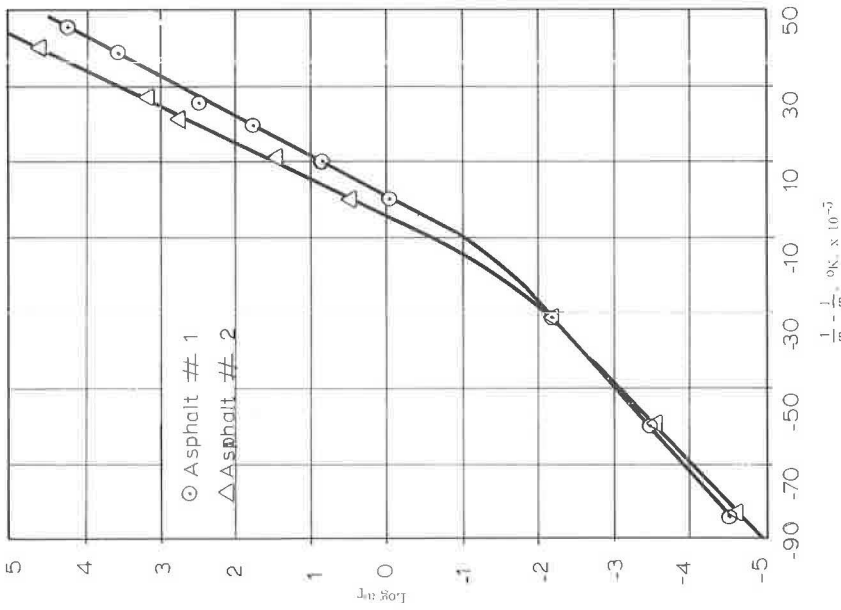

Figure 9. Shift factor vs $1/T - 1/T_o$ for both asphalts at $T_o = 318$ K.

like Eq. 12 to represent the temperature dependency of the viscosity of a non-Newtonian material, either A or ΔE or both must be considered as functions of shear stress or rate of shear. This, in most cases, is avoided by using viscosity at a constant shear rate, a constant shear stress, or a constant power input.

At a fixed shear rate, the viscosity can be expressed as

$$\eta\,(\dot{\gamma},\ T) = \frac{\tau\,(\dot{\gamma},\ T)}{\dot{\gamma}} \tag{49}$$

and at a fixed shear stress as

$$\eta\,(\tau,\ T) = \frac{\tau}{\dot{\gamma}\,(\tau,\ T)}. \tag{50}$$

Formal differentiation of these two equations with respect to temperature at fixed shear stress and fixed shear rate, respectively, results in (23)

$$\frac{(\partial\eta/\partial T)_{\dot{\gamma}}}{(\partial\eta/\partial T)_{\tau}} = \left(\frac{\partial \ln\eta}{\partial \ln\dot{\gamma}}\right)_T + 1 \tag{51}$$

and

$$\frac{(\partial\eta/\partial T)_{\tau}}{(\partial\eta/\partial T)_{\dot{\gamma}}} = 1 - \dot{\gamma}\left(\frac{\partial\eta}{\partial\tau}\right)_T \tag{52}$$

For materials such as asphalt which show a decrease in viscosity with an increase in shear rate and/or increase in shear stress, $(\partial\eta/\partial\tau)_T$ and $(\partial \ln\eta/\partial \ln\dot{\gamma})_T$ are negative.

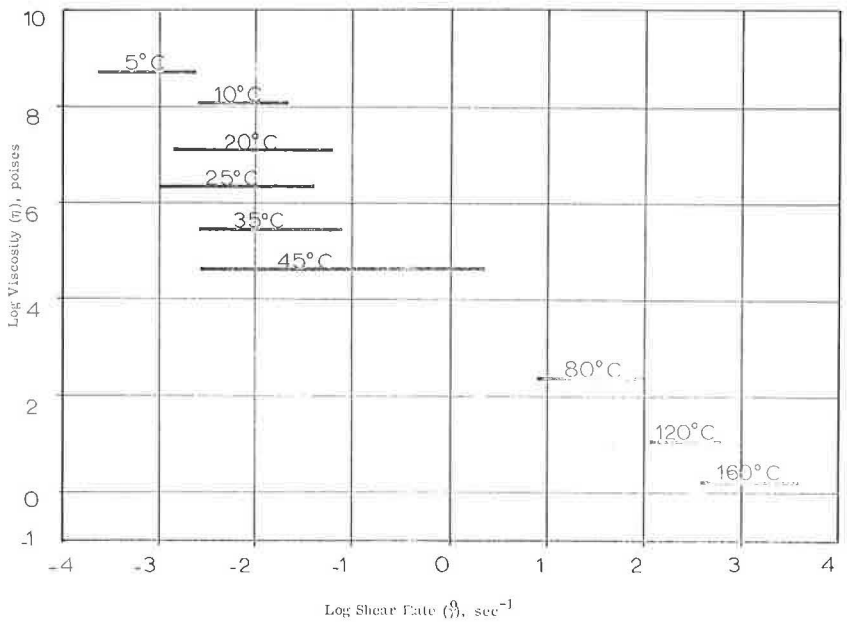

Figure 11. Viscosity vs shear rate for asphalt No. 1 at all test temperatures.

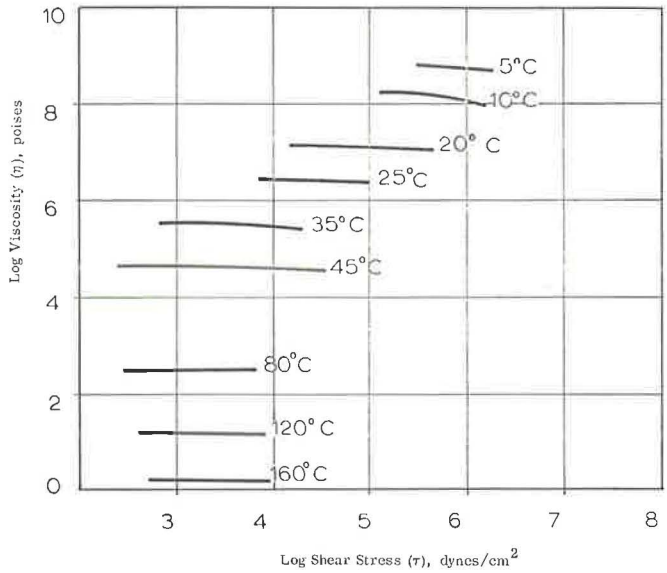

Figure 12. Viscosity vs shear stress for asphalt No. 1 at all test temperatures.

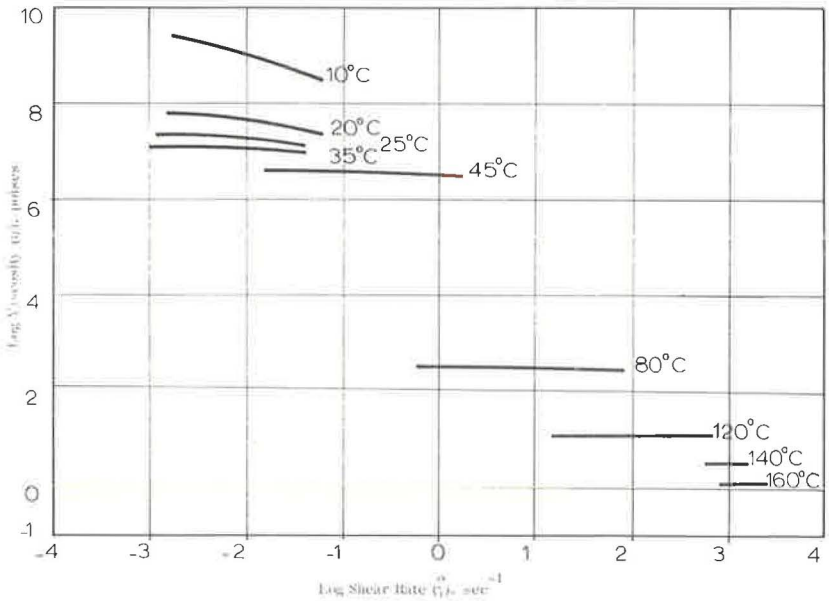

Figure 13. Viscosity vs shear rate for asphalt No. 2 at all test temperatures.

Therefore, the $\left(\frac{\partial \eta}{\partial T}\right)_\tau \Big/ \left(\frac{\partial \eta}{\partial T}\right)_{\dot{\gamma}}$ is larger than or equal to one, or $\left(\frac{\partial \eta}{\partial T}\right)_{\dot{\gamma}} \Big/ \left(\frac{\partial \eta}{\partial T}\right)_\tau$ is smaller than one, which indicates that the temperature variation of viscosity at fixed shear stress is greater than this variation at fixed rate of shear.

The above-mentioned relation can readily be observed from Figures 5, 11, and 12 for asphalt No. 1, and Figures 6, 13, and 14 for asphalt No. 2. Figures 11 and 13 are plots of log viscosity vs log shear rate and Figures 12 and 14 are log viscosity vs log shear

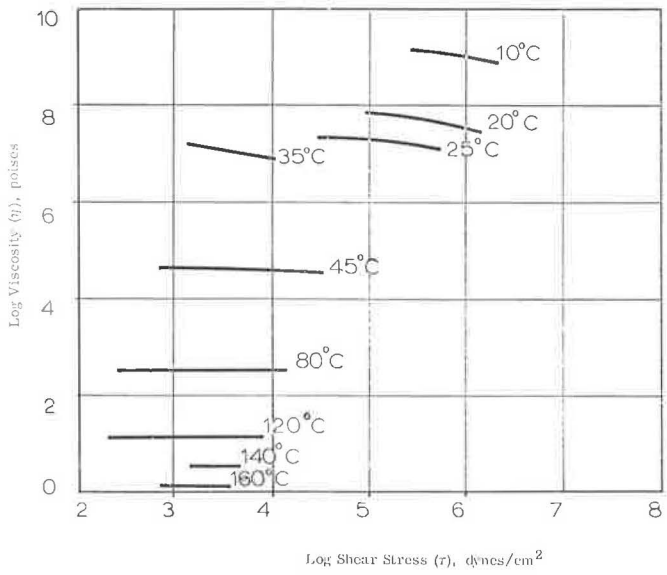

Figure 14. Viscosity vs shear stress for asphalt No. 2 at all test temperatures.

stress for asphalts No. 1 and No. 2, respectively. Using Figures 5 and 6, it can be seen that the variation at fixed shear stress is obtained by a vertical cross plot, whereas the variation at fixed rate of shear is obtained by a horizontal cross plot. It is clear that the distances between the different temperatures are greater along the vertical cross plots than along the horizontal cross plots. This relation results because the slopes of the lines in Figures 5 and 6 are greater than or equal to one, and the plots for different temperatures tend to lie roughly parallel to each other.

EXAMINATION OF HYPERBOLIC SINE FLOW EQUATION

It is believed that the study of the effect of variation of temperature on the viscous behavior of materials may lead to some important information about the molecular structure and mechanism involved in the flow behavior of asphalts. One approach to such a study is the examination of the suggested structural models for the flow of materials through the effect of temperature on their parameters. One of the structural models suggested for the flow behavior of viscous material is the hyperbolic sine equation of Eyring, which has also been applied to flow of asphalt.

Eyring's rate process theory develops a flow relation as given by Eq. 10. This equation can also be written as

$$\vartheta = A \sinh B\tau \tag{53}$$

where, at a fixed temperature, the values of A and B are constant. It is shown by Herrin and Jones (2) that when the flow behavior of asphalt can be represented by this equation, the size of the flow units and their dependency on temperature can be determined using

$$B = \frac{V_f}{2KT} \tag{54}$$

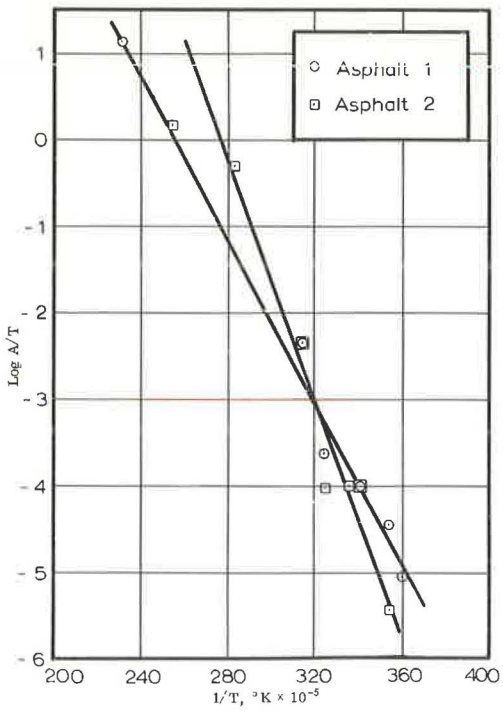

Figure 15. A/T vs reciprocal absolute test temperature for both asphalts.

where V_f is the size of flow unit and T is the absolute test temperature. Furthermore, it is shown that considering a hyperbolic sine relation for flow leads to the calculation of the heat of activation ΔH and the free energy of activation.

In order to examine the validity of such an analysis for the asphalts used in this study, a curve-fitting procedure was used to calculate the values of A and B at each test temperature for the two asphalts. For asphalt No. 1 and No. 2 a plot of log A/T vs 1/T, where T is the absolute temperature, is shown in Figure 15. Herrin and Jones have shown that this plot should be a straight line

$$\log\left(\frac{A}{T}\right) = p - \frac{\Delta H}{2.303R}\left(\frac{1}{T}\right) \qquad (55)$$

where p is a constant over a normal range of temperature, R is the universal gas constant, and ΔH is the heat of activation. This indicates that the slope of the curve representing log A/T vs 1/T is a measure of the heat of activation. Using the corresponding values of B at each temperature for each asphalt, the size of flow units and its variation with temperature were calculated as shown in Figure 16.

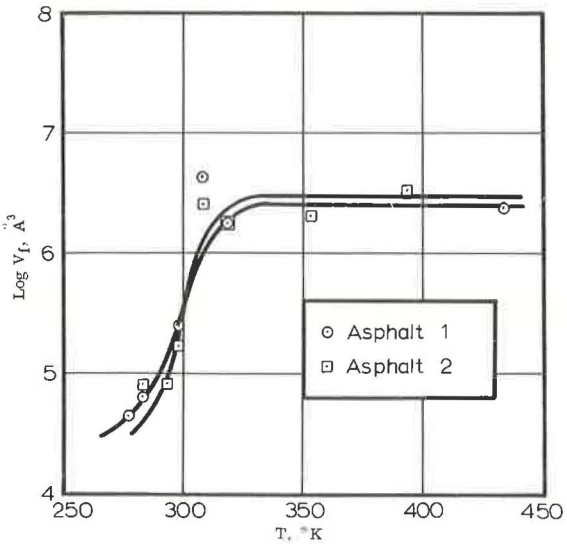

Figure 16. Flow unit volume vs absolute test temperature for both asphalts.

This figure shows that the size of the flow units of both the asphalts increased with temperature to a leveling-off point at about 45 C. According to presently accepted ideas, the flow units should break down and become smaller with increasing temperature. Because of the apparent contradiction shown in Figure 16, a further examination of the validity of using the hyperbolic sine to represent the flow behavior of asphalts was made.

Eyring's flow relation, given by Eq. 18, can be written as

$$\eta = \frac{\tau\delta_1}{2\delta}\left(\frac{h}{kT}\right)\exp\left(\frac{\Delta H - T\Delta S}{kT}\right)\text{cs ch}\left(\frac{\tau\delta\delta_2\delta_3}{2kT}\right) \tag{56}$$

where $\Delta F = \Delta H - T\Delta S$ and $\eta = \tau/\dot{\gamma}$.

Differentiating this expression with respect to 1/T once at constant shear stress and once at constant rate of shear gives

$$\frac{\Delta F_\tau}{R} \equiv \left[\partial \ln\eta/d(1/T)\right]_\tau = \frac{\Delta H}{R} + T - (\tau\delta\delta_2\delta_3/2k)\coth(\tau\delta\delta_2\delta_3/2kT) \tag{57}$$

and

$$\frac{\Delta F_{\dot{\gamma}}}{R} \equiv \left[\partial \ln\eta/d(1/T)\right]_{\dot{\gamma}} = -T + (\Delta H/RT + 1)(2kT^2/\tau\delta\delta_2\delta_3)\tanh(\tau\delta\delta_2\delta_3/2kT) \tag{58}$$

These two equations indicate that if Eyring's flow equation is valid for a material, then the change in logarithm of viscosity, at constant shear stress and/or constant shear rate, with the change in the reciprocal of absolute temperature is not only temperature-dependent but also depends on the shear stress or rate of shear used for the viscosity calculation. Furthermore, these equations show that there exists a certain shear stress at which $\partial \ln\eta/\partial(1/T)$ will go through zero and change sign. For asphaltic materials it is shown that the viscosity always decreases with an increase in shear rate, while the above equations predict a shear stress beyond which the viscosity would start increasing with an increase in shear rate. It is obvious that at shear stresses around this value, the hyperbolic sine function cannot represent the flow behavior of asphalt. In order to obtain an approximate numerical value for this critical shear stress, the following calculated values of the flow unit size and the heat of activation were used at a temperature of 300 K as taken from Figures 15 and 16:

	Temperature °K	H cal/mole °K	V_f $(A^o)^3$
Asphalt No. 1	300	21,400	3.70×10^5
Asphalt No. 2	300	32,000	3.55×10^5

Substitution of these values in the equations and setting the right side equal to zero will result in $\partial \ln\eta/\partial(1/T)_\tau$ and $\partial \ln\eta/\partial(1/T)_{\dot{\gamma}}$ going through zero at $\tau = 7.4 \times 10^5$ dynes/cm^2 for the first asphalt, and $\tau = 2.4 \times 10^6$ dynes/cm^2 for the second asphalt.

Figure 17 shows the variation of $\partial \ln\eta/\partial(1/T)_\tau$ with shear stress for the two asphalts used as determined by Eq. 13. This figure indicates that up to a shear stress of about 10^4 dynes/cm^2 for the asphalts, the behavior of the materials can probably be approximated by a hyperbolic sine relation. This is probably the reason that values of B in $\dot{\gamma} = A \sinh B\tau$ were contradictory. This point is further substantiated by considering that shear stresses below 10^4 dynes/cm^2 could be used only at high temperatures where the behavior of the materials is Newtonian, and the hyperbolic sine relation degenerates into $\tau = \eta\dot{\gamma}$.

The results discussed above indicate that Eyring's hyperbolic sine relation may provide an excellent means to correlate experimental data to a structural analysis of flow

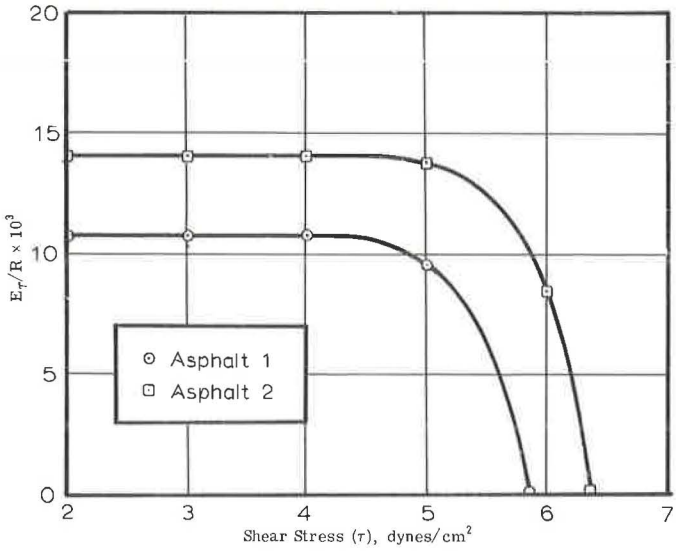

Figure 17. Temperature variation of viscosity at fixed shear stresses according to hyperbolic sine flow equation.

of asphalts in some cases, but not in others. As shown, for both of the asphalts used, such a hypothesis fails to establish conceptually consistant values of the constants necessary to define the expression.

SUMMARY AND CONCLUSIONS

This paper reviews some concepts suggested to analyze the flow characteristics of rheological materials with emphasis on those which are promising in the analysis of flow of asphalts. The suggested concepts are categorized as experimental, mathematical, structural, and physical-chemical. It is shown that for the two asphalts used in this study, it is possible to construct flow diagrams over a wide range of shear stress, rate of shear, and temperature by using three different viscometers and the principle of reduced variables. The application of Eyring's rate process theory to the analysis of asphalt flow is examined and the variation of viscosity, determined at constant shear stress or constant shear rate, with temperature is discussed. From this study, the following conclusions are drawn:

1. The flow data, when obtained by different viscometers, are consistent. Therefore, different viscometers can be used to obtain shear data over a wide range of shear rate or shear stress. The principle of reduced variables will further extend these ranges by reducing the data obtained at different temperatures to an arbitrary base temperature.
2. The temperature dependency of viscosity requires that viscosity variation with temperature at fixed shear stress be larger than that at fixed rate.
3. An examination of the applicability of Eyring's hyperbolic sine relation to analysis of the flow of the two asphalts used reveals that (a) for these two materials there exist critical shear stresses, beyond which the hyperbolic sine relation fails to represent the flow behavior of each material, and (b) when these critical shear stresses are within the experimental range, the flow results cannot be represented by such a relationship.

ACKNOWLEDGMENTS

This research was performed as a part of a project entitled "Durability Characteristics of Asphaltic Materials" sponsored by The Ohio Department of Highways in cooperation with the U. S. Bureau of Public Roads, at the Department of Civil Engineering, The Ohio State University. The authors are grateful to the above agencies for their financial support of this study.

REFERENCES

1. Schweyer, H. E. Asphalt Composition and Properties. HRB Bull. 192, p. 33, 1958.
2. Herrin, M., and Jones, G. E. The Behavior of Bituminous Materials from the Viewpoint of the Absolute Rate Theory. Proc. AAPT, Vol. 32, 1963.
3. Majidzadeh, K., and Schweyer, H. E. Non-Newtonian Behavior of Asphalt Cements. Paper presented at the annual meeting of the AAPT, Feb. 1965.
4. Glasstone, S., Laidler, K., and Eyring, H. The Theory of Rate Processes. McGraw-Hill, New York, 1941.
5. Denny, D. A., and Brodkey, R. S. Kinetic Interpretation of Non-Newtonian Flow. Jour. Appl. Phys., Vol. 33, No. 7, p. 2269, 1962.
6. Hoiberg, Arnold J. (ed.). Bituminous Materials: Asphalts, Tars, and Pitches, Vol. 1. Interscience Pub., New York, 1964.
7. Reiner, Markus. Deformation, Strain, and Flow. Interscience Pub., New York, 1960.
8. Van Wazer, J. R., Lyons, J. W., Kim, K. Y., and Colwell, R. E. Viscosity and Flow Measurement. Interscience Pub., New York, 1963.
9. Bird, R. B., Stewart, Warren E., and Lightfoot, Edwin N. Transport Phenomena. John Wiley and Sons, New York, 1960.
10. Andrade, E. N. da C. Viscosity and Plasticity. Chemical Pub. Co., New York, 1951.
11. Brodkey, Robert S. Unpublished notes.
12. Denny, D. A., Kim, H. T., and Brodkey, R. S. Kinetic Interpretation of Non-Newtonian Flow. Paper presented at the annual meeting of the Society of Rheology, Oct. 1964.
13. Nellensteyn, F. J. Jour. Inst. of Petroleum Technology, 1924.
14. Katz, D. L., and Betu, K. E. Ind. Eng. Chem., 1945.
15. Swanson, J. M. Jour. Phys. Chem., 1942
16. Neppe, S. L. Classification of Bitumens in Asphalt Technology by Certain Rheological Properties. Jour. Inst. of Petroleum, Part 1, p. 38, 1952.
17. Moavenzadeh, F., and Stander, R. R., Jr. Effect of Aging of Asphalt on Its Rheological Properties. Paper presented at the annual meeting of ASTM, June 1965.
18. Ferry, John D. Viscoelastic Properties of Polymers. John Wiley and Sons, New York, 1961.
19. Sisko, A. W. Determination and Treatment of Asphalt Viscosity Data. Highway Research Record 67, p. 27, 1965.
20. Gaskins, F. H., Brodnyan, J. G., Phillippoff, W., and Thelen, E. The Rheology of Asphalt, II. Flow Characteristics of Asphalt. Trans. Society of Rheology, Vol. 4, p. 265, 1960.
21. Brodkey, R. S. Translating Terms for Non-Newtonian Flow. Ind. Eng. Chem., Vol. 54, p. 44, Sept. 1962.
22. ASTM Standards. Proposed Method of Test for Aging Index of Bituminous Materials. 1964.
23. Bestul, A. B., and Belcher, H. V. Temperature Coefficients of Non-Newtonian Viscosity at Fixed Rate of Shear. Jour. Appl. Phys., Vol. 24, No. 6, June 1953.
24. Traxler, R. N., and Schweyer, H. E. Physics, Vol. 7, p. 67, 1936.

Changes in Properties of Bitumen in the Surface Layers of Rolled-Asphalt Wearing-Courses

Part I. Dependence of the Surface Texture of the Asphalt on the Type of Bitumen

A. PLEASE and F. E. MAYER, Road Research Laboratory, Harmondsworth, Middlesex, England

The influence of the type of bitumen on durability and surface texture of rolled-asphalt surfacing has been examined in a full-scale experiment using binders from ten different crude sources. It has been found for the majority of the binders that, provided sufficient binder is used, rolled-asphalt surfacings are very durable but that very different surface textures, and hence resistances to skidding, were developed by the surfacings. Materials made with some bitumens became very smooth, others became very rough although still durable, and the remainder developed a texture intermediate between these two extremes. The performances of the materials in this respect are traced to the susceptibility of the constituent binders (a) to harden by weathering, (b) to be fluxed with lubricating oil dropped by vehicles, and (c) to resist the leaching action of water. The effect of these processes has been examined by a technique involving recovery and measurement of viscosity of very small quantities of bitumen from the top few hundredths of an inch of the surface.

•ANALYSIS OF road accidents occurring in the United Kingdom has shown that in 33 percent of the personal-injury accidents on wet roads skidding has been reported. The United Kingdom has one of the highest densities of traffic in the world, and with the increased speed and braking power of modern vehicles the demands made by the frictional contact between tire and surface have risen and surfacings that at one time were regarded as acceptable are now unacceptable. Research has been in progress for many years with the aims of setting minimum standards of resistance to skidding for various types of site and of improving bituminous materials so that these standards can be met reliably and economically.

The most important type of wearing-course material in the United Kingdom, particularly for heavily used high-speed roads, is rolled asphalt. Although this is a dense material, it differs from asphaltic concrete in that a gap-graded aggregate is employed, the fine aggregate being a fine natural sand. Moreover, the binder employed is harder, usually of 40-60 penetration. For motorway surfacings, a rolled asphalt of low stone content (30 percent of coarse aggregate) is the only material permitted; a heavy application of coated chippings of ½-in. or ¾-in. size is made to the hot surfacing immediately after laying.

The resistance to skidding of rolled asphalts depends both on the surface properties of the exposed coarse aggregate (including any applied chippings) and on those of the bituminous matrix, which is a fine-textured mixture of natural sand, mineral filler and

Paper sponsored by Committee on Characteristics of Bituminous Materials and presented at the 45th Annual Meeting.

TABLE 1

PROPERTIES OF ASPHALTIC CEMENTS[a]

Bitumen	Pen. at 25 C	Pen. Index	Viscosity at 25 C (10^6 poises)	Viscosity at 45 C (10^6 poises)	Logarithmic Temp. Coeff.	Equiviscous Mixing Temp. (viscosity 1.6 poises), Deg C	Plastic Flow Index	Angle of Elastic Recovery (deg)	Asphaltene Content (percent)	Insolubles Content (percent)
Californian	66	-1.75	2.08	0.022	11.9	142	1.01	0.5	4.6	0
Venezuelan	64	-0.6	2.58	0.032	11.5	160	1.10	1.8	13	0.05
Mexican	67	-0.1	4.51	0.060	11.2	177	1.19	3.8	20	0.05
Lobitos	65	-1.1	2.71	0.030	11.7	142	1.06	0.4	1.1	0
Egyptian (waxy)	65	-0.1	3.71	0.016	13.9	150	1.01	1.6	18.8	0
Egyptian (cracked)	66	-0.7	1.86	0.017	12.5	123	1.02	–	29	0
Trinidad 5A[b]	59	-0.5	3.6	0.057	10.8	–	1.21	1.4	15	29.9
Trinidad 5A (soluble fraction)	143	–	0.6	0.011	10.3	–	1.11	2.9	18.7	0
Trinidad 5B[c]	66	-0.6	2.08	0.038	10.8	–	1.06	0.5	13	20.8
Trinidad 5B (soluble fraction)	107	–	1.21	0.019	10.8	–	1.06	2.4	15	0
Cuban	67	+1.5	84.1	0.423	13.8	–	1.89	2.6	16	20

[a] A blown Venezuelan bitumen of 65 pen. was used in addition to these 9 asphaltic cements in the full-scale experiment; no data are available on its rheological behavior.
[b] The Trinidad 5A contained 83.5 percent Trinidad Epuré and 16.5 percent Golden Flux.
[c] The Trinidad 5B contained 49.5 percent Trinidad Epuré, 5 percent Golden Flux and 45.5 percent 200-pen. bitumen.
Note: The shearing stress for the determination of the flow properties was 2000 dynes/cm^2.

hard bitumen. Methods are well established for selecting coarse aggregate which maintains good resistance to skidding under the action of traffic. The present report gives the results of several years of research aimed at determining the properties of bituminous binder that affect resistance to skidding by the matrix, as well as those influencing the degree to which the coarse aggregate projects above the matrix.

Between 1937 and 1940 a series of full-scale experimental sections of rolled asphalt were laid to examine the effect of binder properties on performance. For this purpose ten asphaltic cements of 60-70 penetration, drawn from several different sources, were used. The sections of rolled asphalt in the course of time developed very different surface textures (a fact having considerable bearing on the means whereby rolled asphalts might be designed to retain good non-skid characteristics). This paper describes work undertaken to examine the changes that occurred in the properties of the bitumen in the surface layers of these rolled asphalts and connects these changes with the textures finally developed.

Physical and Chemical Properties of Binders

Details of the ten bitumens or asphaltic cements in this investigation are given in Table 1. Further data on the viscosity of the binders have been given elsewhere (1, 2).

Scope of the Full-Scale Experiment

The site chosen for the experimental surfacings was a straight 30-ft-wide three-lane carriageway, carrying in 1938 about 23,000 tons a day; by May 1956 the traffic had increased to 32,000 tons a day. The experimental surfacings were dense rolled asphalt 2 in. thick containing 50 percent coarse aggregate, 34 percent fine silica sand, 8.5 percent filler (portland cement) and 7.5 percent soluble bitumen. This composition would conform to the medium-rich Schedule 2 of the British Standard 594:1961 (3) for rolled asphalt.

To examine the effect of reducing the bitumen content, five of the binders were used in an additional series of rolled asphalts laid in 1940. Each binder was used at two binder contents, making a total of ten extra sections.

Performance

The performance of the experimental sections was assessed by an inspection panel (4) at various times up to and including 1956, when the experiment was terminated. The results of these assessments showed that the main factor influencing the durability of the surfacings was the binder content. The five leanest asphalts made with 3.5 to 5 percent bitumen disintegrated within 5 years, while the slightly richer asphalts made with 5.25 to 5.75 percent bitumen were in only fair-to-poor condition after 14 years with severe fretting. On the other hand, with the higher binder content of 7.5 percent, durability was normally no problem; eight out of the ten sections were still in fairly good condition after 16 to 19 years' service and only one section, that made with the

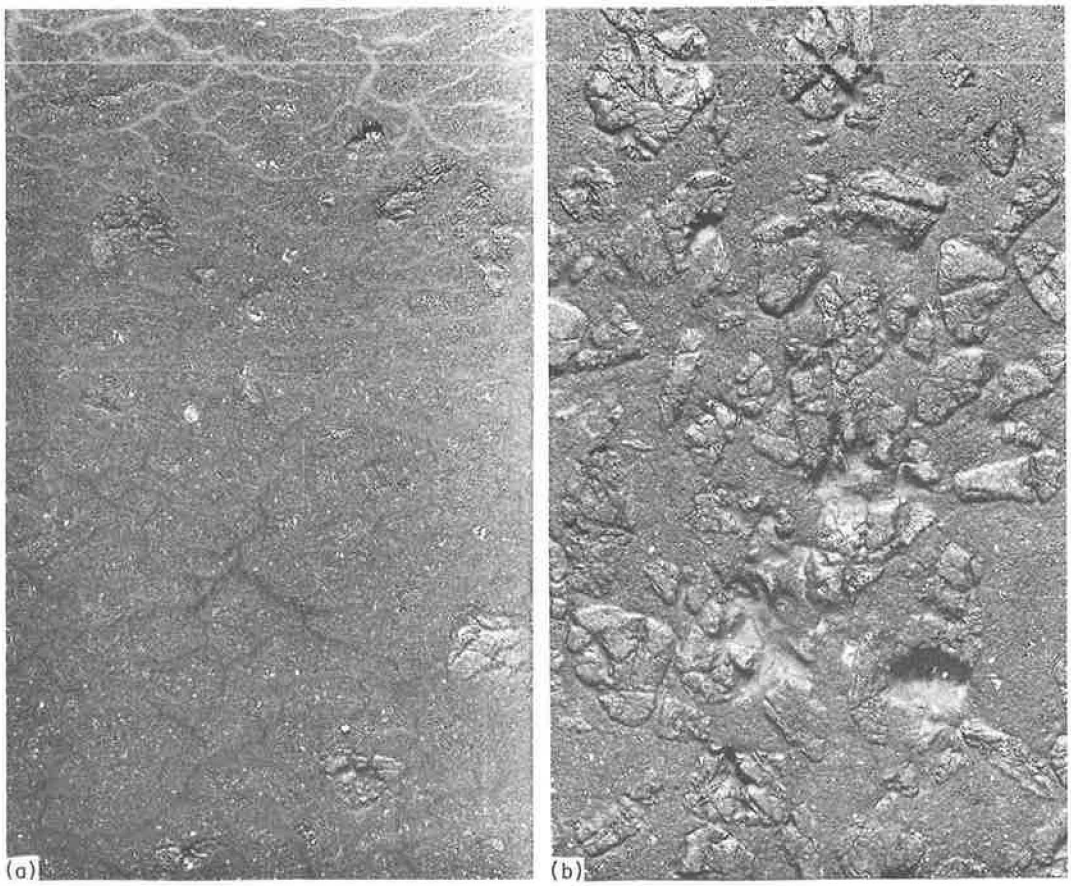

Figure 1. Surface textures developed by rolled asphalts. A—Smooth texture of rolled asphalt containing Venezuelan 60-70 pen. bitumen after 19 years (50 percent coarse aggregate). B—Rough texture of rolled asphalt containing Trinidad 5A 60-70 pen. asphaltic cement after 19 years (50 percent coarse aggregate).

Egyptian cracked bitumen, proved less durable in that it began to fret within 5 years of laying.

Surface Texture

The main difference in the performance of the ten rolled asphalts containing 7. 5 percent bitumen lies in the surface textures they developed. The three sections made with the Lobitos, Californian and Venezuelan bitumens had, after 15 to 18 years, a very closely-knit mortar which was level with the exposed surfaces of a few particles of coarse aggregate. Although these surfacings contained 50 percent coarse aggregate, they eventually had the same appearance as very lightly chipped sand asphalts. Figure 1A illustrates the typical smooth texture; a particularly noticeable feature is that thin "veins" have appeared on the surface. On the other hand , the rolled asphalts made with the blown Venezuelan, the Trinidad lake asphalt 5A and the Egyptian "cracked" binders are very rough-textured with a sandpapery mortar, leaving the coarse aggregate well-exposed and proud of the surface (Fig. 1B). Between these two extremes of surface texture are the rolled asphalts made with the remaining four binders—Trinidad lake asphalt 5B, Mexican, Cuban and Egyptian waxy.

The importance of surface texture lies primarily in its influence on resistance to skidding. All the sections in the experiment were too short for the measurement of

TABLE 2

HARDENING OF THIN FILMS OF BITUMEN DURING EXPOSURE ON ROOF

Binder	Penetration at 25 C		Ratio Pen. 2 Yr/ Pen. Original
	Original	2 Yr	
Californian	63	26	0. 41
Venezuelan[a]	65	27	0. 42
Mexican	69	30	0. 43
Soluble Cuban	75	32	0. 43
Egyptian (waxy)	65	22	0. 34
Soluble Trinidad 5B	107	35	0. 33
Soluble Trinidad 5A[a]	143	37	0. 26
Cuban	67	34	0. 51
Trinidad 5B	65	24	0. 37
Trinidad 5A	60	17	0. 28

[a]A 143-pen. Venezuelan bitumen hardened to 56 pen. after 2 yr exposure to give a ratio of final to original penetration of 0.39.

resistance to skidding by methods then available but experience gained in other full-scale experiments shows that a rough texture is desirable for maximum friction between smooth rubber-tired wheels and the road surface, particularly at high speeds (5).

Weathering of Binders

In the present work the influence that weathering of binders had on the performance of the experimental surfacings was examined. First, a measure was obtained of the extent to which the binders themselves hardened on exposure to weather in the absence of traffic. Second, the hardening of the binders in the bulk of the road surfacings was studied over a period of years by measurements of penetration on the recovered binders and determinations of their asphaltene contents. Finally, the change in the flow properties of the binders, recovered after many years from the top few hundredths of an inch of asphalt surfacing, was studied by using a microviscometer.

Thin Films of Binders

The weathering of thin films of binder was carried out in the following way. A tray, 20 cm by 20 cm, was filled with binder to a depth of 0. 1 cm and exposed on the laboratory roof. A muslin cover was placed over the film to give some protection against dust but allowing full exposure to the effects of light, water, oxidation and evaporation. Six trays of each of ten binders were exposed to weathering; these comprised all the binders used in the full-scale experiment except for the Lobitos, blown Venezuelan and Egyptian cracked. The three remaining bitumens were the soluble fractions of the three asphaltic cements. The penetrations of the weathered binders were measured over a period of two years (Table 2).

The ten binders became more viscous with age; the rates of hardening were extremely rapid within the first three months, but became slower as the time of exposure increased. Within the first 36 days of exposure, the binder films had discolored progressively and developed extensive cracks, and although protection from dust was given by the muslin covers, increases in weight ranging from 0. 27 to 0. 50 percent were observed. It is thought that oxidation was probably the main cause for the changes in appearance, consistency and weight. This suggestion is supported by tests using an

TABLE 3

EFFECT OF WEATHERING ON RECOVERED BINDERS

Binder	Penetration[a]								
	From Tank	Before Traffic	½ Yr	1 Yr	2 Yr	10 Yr	12 Yr	14½ Yr	17 Yr
Californian (26)	59	58	56	—	—	—	—	60	52
Venezuelan (27)	60	47	54	54	50	60	67	64	50
Mexican (30)	57	50	52	49	49	47	—	46	41
Trinidad 5A (37)	192	145	123	127	105	93	75	67	45
Trinidad 5B (35)	117	98	86	87	78	80	—	60	48
	Asphaltene Content (percent)								
Californian	6	7	—	—	—	—	—	7	7
Venezuelan	13	14	14	15	13	—	—	16	14
Mexican	20	21	21	22	21	—	—	24	25
Trinidad 5A	15	18	19	18	18	—	—	24	24
Trinidad 5B	12	14	15	16	16	—	—	18	20

[a]The penetration of the bitumen weathered for 2 years in the form of thin films is given in brackets for comparison.

Ostwald-type viscometer which showed that the temperature susceptibilities of the weathered binders were lower than the temperature susceptibilities of binders hardened by loss of volatiles. Also, there was an approximate relationship between increase in weight and increase in viscosity—the binders with the greatest increase in weight (0. 5 percent) hardened most. Further, the increase observed in the asphaltene content of bitumens recovered from weathered road surfacings suggest that chemical changes have been brought about by oxidation.

In Table 2, the average rates of hardening of the bitumens are expressed in the form of the ratio of penetration after two years' weathering to the original penetration—the lower this ratio, the higher the rate of hardening. It can also be seen from Table 2 that the greatest rates of hardening are found with the soluble portions of the Trinidad lake asphalt 5A and 5B asphaltic cements and the Egyptian waxy bitumen. Their ratios of penetration after two years to original penetration ranged from 0. 26 to 0. 34, whereas the corresponding ratios for all the other soluble bitumens ranged from 0. 39 to 0. 43.

Recovered Bitumens

At intervals throughout the lives of the road surfacings, bitumens were recovered from the bulk of road samples by the solvent extraction method described in B. S. 598: 1950. This work has been reported by Gough and Green (6) and by Lee and Nicholas (7). It is summarized here in Table 3.

After two years, bitumens weathered in the form of thin films are considerably harder than the corresponding binders recovered from the bulk samples of the road surfacings—showing that a large measure of protection from weathering is given to the binder in the body of the surfacing.

Measurements were also made of the changes in asphaltene content of the binders recovered from road samples following weathering. The summary of these results (Table 3) shows that, for some binders, in particular the two Trinidad lake asphalt binders, the asphaltene contents increased markedly with age and in general the hardening of the recovered binders is associated with an increase in asphaltene content. The conclusion that chemical changes such as oxidation are responsible for some of the change in the consistency of the weathered binders agrees with the results of the tests on the thin films of binders exposed on the laboratory roof.

It will be shown in the next section that, in rolled asphalts, the main changes in the consistencies of the weathered binders occur in quite thin layers near the exposed surface and it is therefore not surprising that these determinations of penetration, which have been obtained on bitumens recovered from the bulk of the surfacings, do not explain the different performance of the asphalts. Nevertheless, the tests described in this section have shown that Trinidad lake asphalt 5A, Trinidad lake asphalt 5B and Egyptian waxy bitumen are far more susceptible to hardening by weathering than the other binders. It should, however, be noted that the Egyptian cracked, the blown Venezuelan and the Lobitos bitumens were not included in this comparison.

Changes in Viscosity

By 1955, although it had been shown that the bitumens in the road surfacings changed their properties owing to weathering, the reasons for the varying surface-texture of the experimental sections were not clear. For example, after 17 years' service, the binder recovered from the bulk of the rough-textured asphalt made with Trinidad lake asphalt 5A had a penetration of 45, which is not significantly different from the value of 50 obtained for the Venezuelan bitumen recovered from the veined, smooth-textured asphalt. Apparently binder properties on the top surfacing layers, which are the most exposed to the atmosphere, were almost completely concealed by properties of larger quantities of binder in the body of the material protected from the weather. Accordingly a new method involving the use of a small-scale solvent-recovery and a simple-shear microviscometer, needing only 0. 2 g of bitumen, was developed to study the variation of viscosity of the recovered binder with depth below the top surface (8).

The properties of binders recovered from the six rolled asphalts made with Trinidad lake asphalt 5A and 5B cements and the Mexican, Lobitos, Californian and Venezuelan bitumens were studied in relation to depth within the surfacing and location across the road. The results are shown in diagrammatical form in Figure 2 for the rough-textured rolled asphalts, and in Figure 3 for the smooth-textured rolled asphalts. Each single result is the mean of three independent determinations of viscosity. There are four main features of the results.

1. The viscosities of the six binders recovered from the three top layers cover a considerable range of values (10^3 to 10^9 poises at 25 C). At any particular point across the road the binder from the top layer (0 to 0. 02 in. below the surface) which is most exposed to weather is always harder than the binder from the layers immediately below (0. 02 to 0. 06 in. below the surface).
2. At depths exceeding 0. 5 in. below the surface, the fluxed Trinidad lake asphalt 5A is the only binder of the six which has hardened significantly. In 18 years the viscosity of its soluble portion increased from 0. 5 $\times$ 10^6 poises to about 3 $\times$ 10^6 poises. The Trinidad lake asphalt 5B shows a considerably smaller increase, and the remaining five binders recovered from the interior of the surfacings have very nearly the same viscosities after 18 years as the corresponding original binders. Furthermore, the viscosities of all six binders recovered from the body of the surfacing do not depend on the position of the sample across the road.
3. For the three upper layers (i. e., at depths of up to 0. 06 in. below the surface) the viscosities of the recovered binders depend on the position across the road from which the sample was taken. In the "oil lane" (a strip at a distance of 6 to 7 ft from the curb darkened by oil droppings from vehicles) the bitumens are softer than the bitumens recovered from the curb or the crown of the road. This effect is most marked for the smooth-textured rolled asphalts.
4. For the sections which have become smooth and veined, namely those made with the Lobitos, Californian and Venezuelan bitumens, the viscosities of all three top layers in the oil lane of each section have decreased from the original values of about 2 $\times$ 10^6 poises to very low values between 10^3 and 10^5 poises.

The investigation shows that in these six rolled asphalts the greatest changes in the viscosities of the binders occur at the surface. For five of the six binders no significant change has occurred in the body of the rolled asphalt after 19 years.

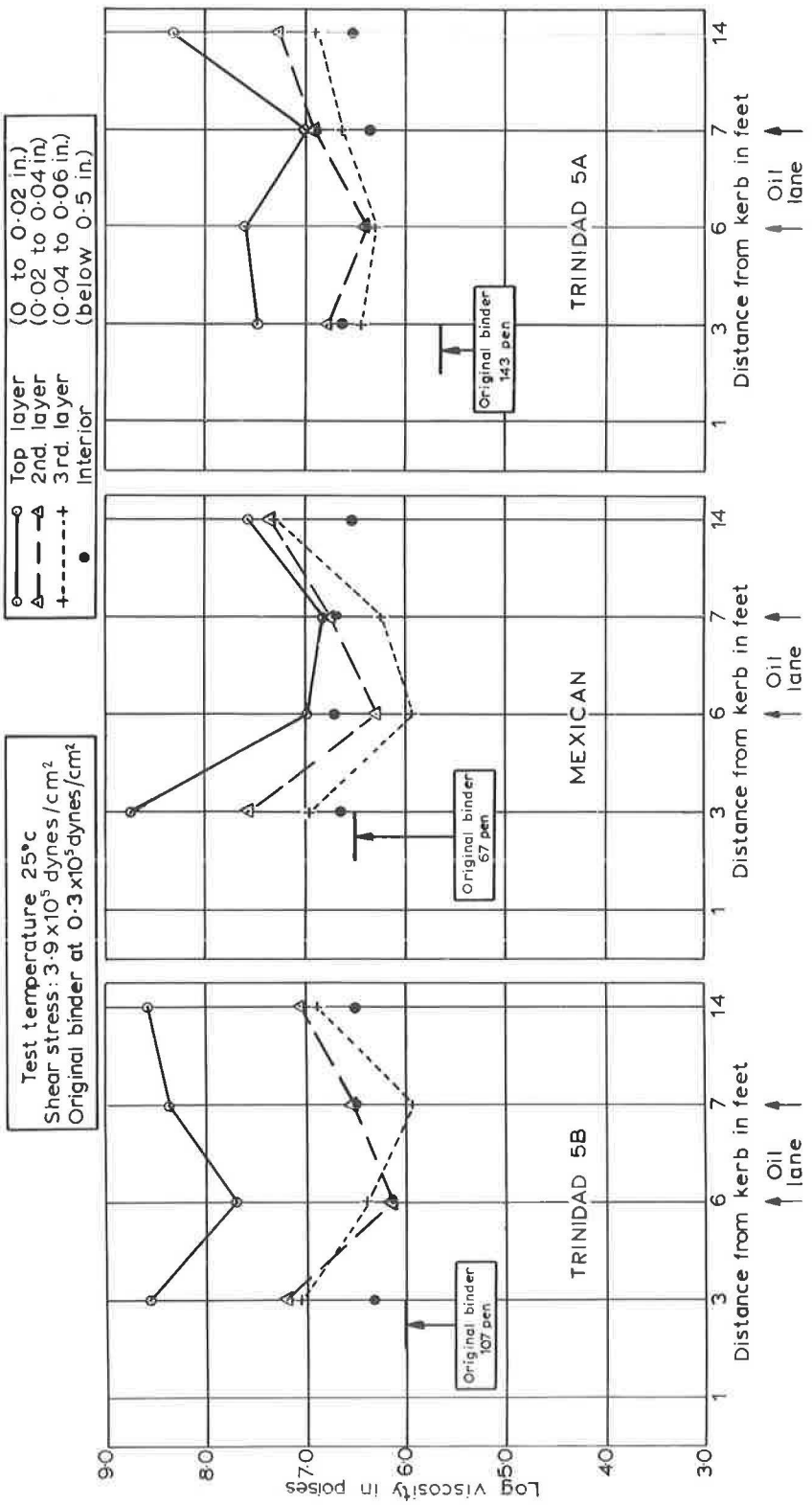

Figure 2. Viscosity of bitumen recovered from thin layers of mortar abraded from the surface of rough-textured rolled asphalts.

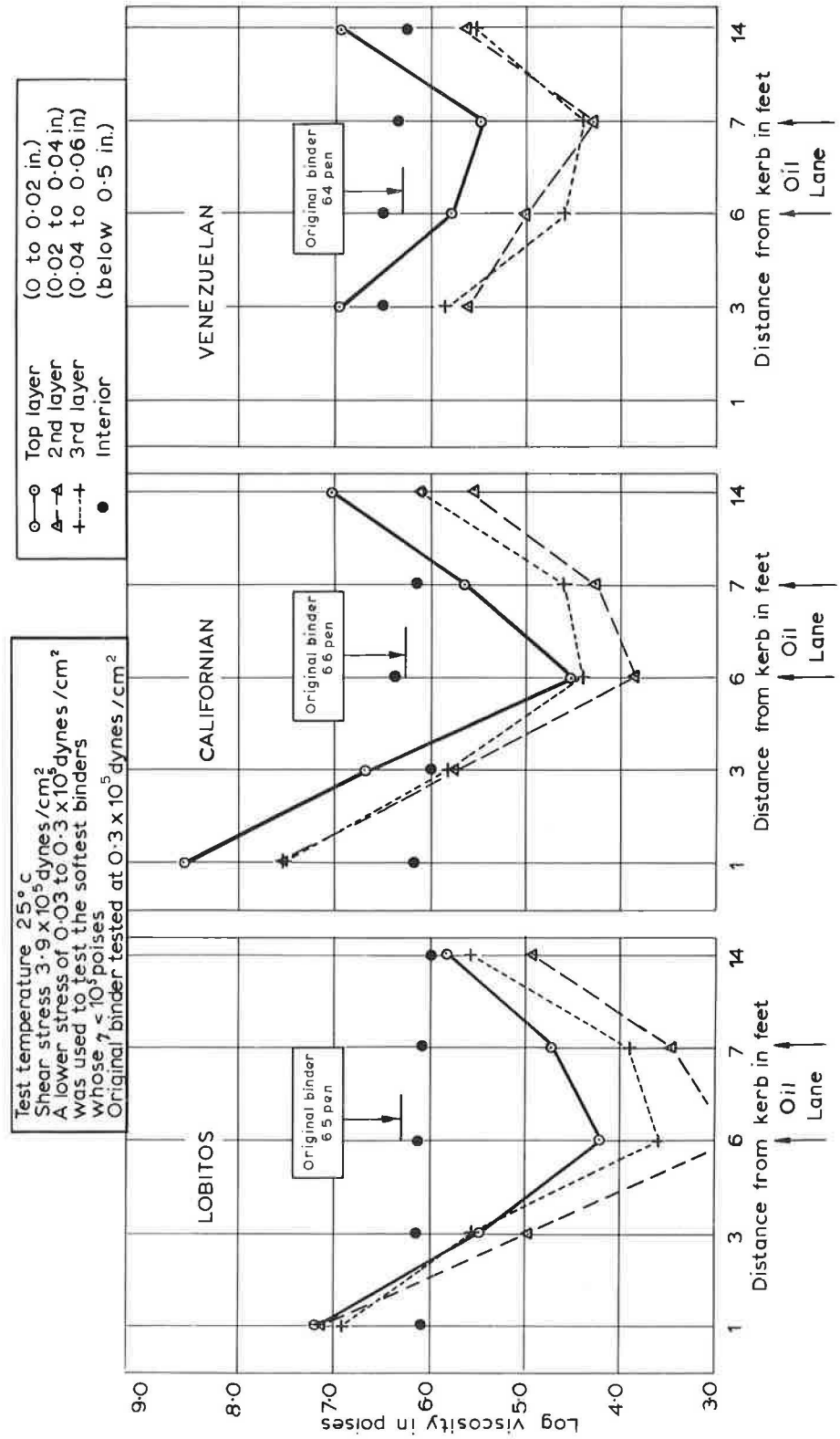

Figure 3. Viscosity of bitumen recovered from thin layers of mortar abraded from the surface of veined, smooth-textured rolled asphalts.

TABLE 4

VISCOSITY OF BITUMEN RECOVERED FROM THIN LAYERS OF MORTAR ABRADED FROM THE SURFACE OF ROLLED ASPHALTS—SAMPLES TAKEN FROM OIL LANE AFTER 16 YEARS

Source	Viscosity at 25 C (10^6 poises)			
	Egyptian Waxy (intermediate-textured)	Egyptian Cracked (rough-textured)	Cuban A. C. (intermediate-textured)	Blown Venezuelan (rough-textured)
Top layer	34. 4	--[a]	3. 7	No quantitative result
2nd layer	12. 8	25. 0	2. 8	No quantitative result
3rd layer	3. 6	15. 3	1. 4	No quantitative result
Interior	3. 7	6. 6	1. 3	10. 3
Original soluble binder	2. 9	1. 8	4 to 8	?

[a]This binder separated into two phases on recovery.

It should be remembered that the Venezuelan and Californian bitumens exposed to weather for two years on a roof as thin films increased their viscosities at 25 C from 2×10^6 poises to about 13×10^6 poises, a value estimated using Saal's formula (9) from the values of penetration given in Table 2. It would be expected that, if weathering were the only factor affecting the viscosity of the bitumens in the road mixtures, the combined viscosities of the binders in the two top layers would be considerably greater than 10^7 poises after 18 years. Referring to Figure 3, it will be seen that in the Californian and Venezuelan asphalts the viscosities of the binders recovered from the two top layers of the inner and outer wheel tracks are in fact significantly lower than 10^7 poises, and the corresponding viscosities for the two top layers in the oil lane are even lower. The general pattern of results is consistent with the fluxing action of lubricating oils dropped from vehicles opposing the tendency of binders to harden with weathering.

The study of the viscosity/depth dependence for the bitumens recovered from the rolled asphalts made with the two Egyptian bitumens, the blown Venezuelan bitumen and the Cuban asphaltic cement has been less extensive; it was restricted to the investigation of samples from the oil lane with the objectives of confirming the general pattern of viscosity distribution with depth, and of finding out whether the test method is suitable with these rheologically-more-complicated binders.

The wax content of the steam-reduced Egyptian bitumen presented no difficulty in the measurement of viscosity, and the dependence of viscosity on depth for the bitumen recovered from the oil lane followed the same pattern, i. e., there has been no significant change of binder viscosity in the interior, and binder from the three top layers has high viscosity which is in accord with the previous results for bitumens producing rough-textured asphalts.

The test method has not been entirely successful with the three remaining binders, because (a) the Egyptian cracked bitumen recovered from the topmost layer (0 to 0.02 in.) of mortar consisted of two separate phases—a continuous lightly colored medium and a darker dispersed phase, and (b) the Cuban and the blown Venezuelan binders recovered from the two top layers formed a hard elastic skin which made the preparation of the viscometers difficult for the Cuban and often impossible for the blown Venezuelan. In all tests on these two weathered binders there was evidence of nonlinear deformation/

TABLE 5

VISCOSITY OF BITUMEN RECOVERED FROM SAND ASPHALTS EXPOSED ON THE LABORATORY ROOF FOR 10 MONTHS

Specimen		Viscosity at 25 C (10^6 poises)	
		Venezuelan 75 Pen.	Fluxed Trinidad 75 Pen.
Original soluble binder (stress 3500 dynes/cm^2)		2. 3	0. 45
Recovered bitumens from weathered sand asphalts (stress 3. 9 × 10^5 dynes/cm^2)	Top layer	2240	252
	2nd layer	31	17
	3rd layer	10	3. 6
	Interior	7	0. 9

time relationships, making the determination of viscosity rather doubtful with this viscometer.

When these qualifications have been made the results for these binders do show a pattern of viscosity distribution similar to that obtained for the rough- and intermediate-textured rolled asphalts.

The results collected in Table 4 show that:

1. Where obtainable, the viscosities of the four binders recovered from the upper layers of mortar (0 to 0. 06 in.) in the oil lane are either greater than or (for the Cuban A. C.) about equal to the corresponding original viscosities.
2. In the intermediate-textured asphalts made with the Egyptian waxy and the Cuban binders, the viscosities of the soluble bitumens in the interior of the surfacing are approximately equal to the viscosities of the original binders.
3. The viscosity of the Egyptian cracked binder that was recovered from the interior of a rough-textured asphalt has increased by about four times—a result similar to that obtained on the rough-textured asphalt made with the fluxed Trinidad lake asphalt 5A. The separation into phases of the weathered binder recovered from the top surface of the asphalt is evidence of very marked changes produced by weathering. Changes of this magnitude may well account for the fretting and early disintegration of the asphalt made with this binder.

Results for Laboratory-Prepared Mixtures

The behavior of the asphalt on the road has been influenced by the fluxing action of motor oil. Specimens of sand asphalts conforming to B. S. 594 and containing a Venezuelan and a fluxed Trinidad lake asphalt of 75 penetration were therefore prepared in the laboratory and weathered on the roof in order to study the effect of weathering alone without the action of traffic. The results for these sand asphalts after 10 months' exposure to the action of weather (Table 5) show that both the Venezuelan and the fluxed Trinidad lake asphalt hardened considerably—by a factor of 1,000 for the top layer of the Venezuelan and a factor of about 500 for the top layer of the Trinidad. These hardening factors are considerably higher than those obtained on the corresponding binders weathered in the form of thin films of pure binder (hardening factor of 6 for Venezuelan and 18 for Trinidad lake asphalt 5A), which is not unexpected, because the exposed pure binders were voidless and their film thickness was considerably greater. What is surprising, however, is that the susceptibilities of the two binders to hardening by weather in the surface of the asphalts are in the reverse order to those observed for the thin films. In the form of thin films, the Trinidad lake asphalt binder had the higher rate of hardening (Table 2); in the bituminous mortars, on the other hand, it was the Venezuelan binder which had the higher rate of hardening. The explanation for this apparent discrepancy probably lies in the fact that a portion of the weathered binder

Figure 4. Leaching of weathered mortar from the untrafficked surface of sand asphalt—magnified view after ten months' exposure on laboratory roof.

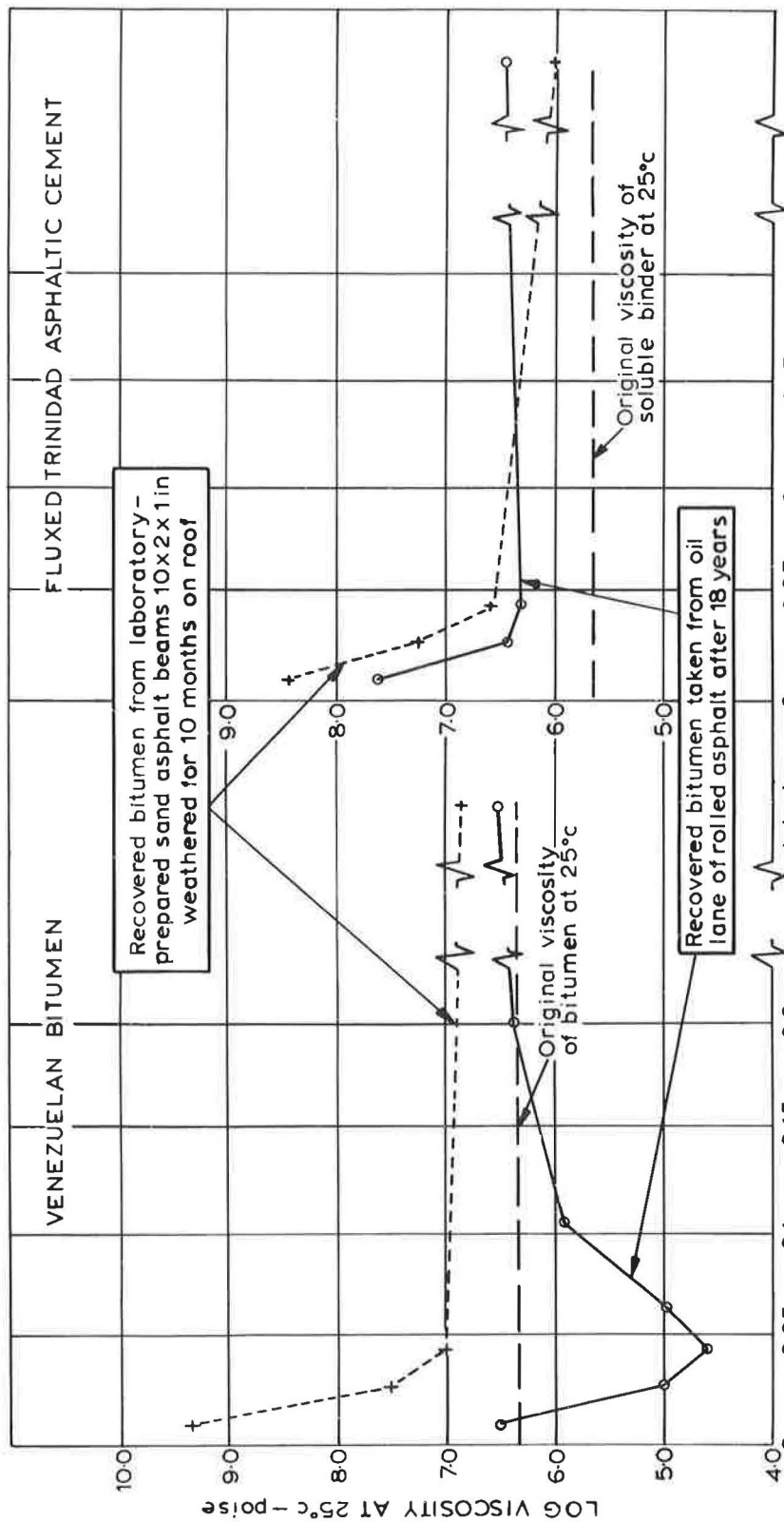

Figure 5. Variation of viscosity with depth for Venezuelan bitumen and fluxed Trinidad asphaltic cement recovered from road surface after 18 years and from laboratory-prepared sand asphalt after 10 months.

TABLE 6

RESISTANCE TO SKIDDING OF ROLLED ASPHALTS ON A. 40, LONDON-FISHGUARD TRUNK ROAD

Binder Type	Binder Content (%)	Sideway Force Coefficient at 30 mph On Wet Surface						
		Mar. 1953	May 1954	Aug. 1954	May 1955	Sept. 1955	May 1956	Aug. 1956
Venezuelan Petroleum Bitumen	5.8	0.72	—	0.41	—	0.32	0.45	0.45
	7.7	0.58	0.29	0.34	0.35	0.25	0.39	0.37
Fluxed Trinidad Lake Asphalt	5.8	0.63	—	0.51	0.55	0.54	0.54	0.62
	7.7	0.58	0.45	0.47	0.50	0.49	0.52	0.57

in the bituminous mortars had been eroded, presumably by the action of water, leaving the clean sand particles on the surface (Fig. 4). This effect is considerably more marked in the case of the mortar made with the Trinidad lake asphalt binder, so that the Trinidad binder recovered from the topmost layer, for which the viscosity was measured, had not been subjected to the full ten months' weathering. It was at first protected by a thin layer of bituminous mortar and subsequently by the residual layer of clean sand particles from which the weathered binder had been leached away. This observation shows clearly that a sandpaper texture can be brought about without the action of traffic being necessary, presumably by the leaching of weathered binder from the surface.

Comparison of the changes in the viscosities of these binders by weathering alone and by weathering in conjunction with road traffic is shown in Figure 5, where it will be seen that at the surface of the asphalts, down to a depth of about 0.1 in., the binders from the road surfacings are softer, after 18 years, than the corresponding binders in the laboratory-prepared mixtures which were weathered on the roof for only ten months. This result is consistent with the suggestion already made that the fluxing action of lubricating oil spilled by vehicles opposes the hardening of the binders by weathering.

Another Full-Scale Experiment

A study similar to that described has been made of rolled asphalts on another heavily trafficked road in southern England, with similar results (8). On this road mixtures were laid with a range of binder contents and were given an extra application of chippings, to give a rougher surface texture. Nevertheless, within 5 years of laying, sections made with a Venezuelan petroleum bitumen became smooth and lightly veined, whereas similar materials made with fluxed Trinidad lake asphalt became even more rough-textured, with the mortar worn down slightly to leave the coarse-aggregate particles proud of the surfacing. The association of these differences in texture with differences in resistance to skidding were reported elsewhere (5). The results are summarized in Table 6, where it can be seen that whereas the sections with fluxed Trinidad lake asphalt have maintained a fairly high value for the sideway-force-coefficient[a] the sections made with the Venezuelan petroleum bitumen have fallen to significantly lower values (5).

DISCUSSION

The investigation has shown that there are differences between the viscosities of the different binders within the top few hundredths of an inch of the asphalt surfacings and that these changes are reflected by differences in surface texture.

[a]The coefficient of friction between a smooth rubber-tired wheel and the road surface is assessed by measuring the sideway thrust on the loaded wheel while it is skidding in a direction inclined to its plane of rotation; the ratio of sideway force to wheel load is defined as the Sideway Force Coefficient.

Smooth-Textured Asphalts

Smooth-textured rolled asphalts were produced by the Californian, Venezuelan and Lobitos bitumens. The Californian and Venezuelan bitumens have been shown by the weathering tests on the thin films of binder to have fairly low rates of oxidation, and, in the case of the Venezuelan, a relatively low susceptibility to leaching by water. Lubricating oil dropped by traffic tends to slow down the hardening produced by weathering; traffic tends to knit the mortar into a closer texture thereby reducing further the effects of oxidation. A fair proportion of the lubricating oil dropped by traffic will penetrate the surface of the rolled asphalt and be largely protected from the action of weather by the closely knit skin of mortar at the surface; the oil-fluxed bitumen immediately below the surface attains in time a very low viscosity. At an early stage in the life of the surfacing, traffic stresses produce fine cracks in the upper hardened skin through which the soft oil-fluxed bitumen exudes to form a strongly defined pattern on the surface resembling a network of veins. The process is continuous, developing after some years into the characteristic texture shown in Figure 1A.

Rough-Textured Asphalts

Rough-textured rolled asphalts were produced by the Egyptian cracked bitumen, the Trinidad lake asphalt 5A and the blown Venezuelan. Although the soluble bitumen of the Trinidad lake asphalt 5A originally had a comparatively low viscosity, it has a high rate of oxidation and during weathering shows a high susceptibility to leaching by water. In this case the first drops of lubricating oil tend to produce a softer bitumen at the surface but, because of the higher rates of oxidation and erosion, some of the bitumen in the top skin begins to be removed by the action of the weather. The coarser mortar at the surface permits the weathering of a higher proportion of the lubricating oils which in turn tends to reduce the extent to which the binder at the surface is fluxed. The process is slow but continuous, developing after some years to give a sand-papery mortar and a well-exposed coarse aggregate (Fig. 1B).

The other two binders giving rough-textured asphalts are the Egyptian cracked and the blown Venezuelan. No evidence has been obtained to show whether either of these two binders are leached by water when weathered in the same way as the Trinidad lake asphalt 5A. The Egyptian cracked bitumen is unstable when weathered and separates into two distinct phases when recovered in carbon disulfide. This may well account for a friable mortar at the top surface. The lack of durability of the rolled asphalt containing this binder shows that its susceptibility to hardening by weathering (and the associated phase-separation that occurs) is too pronounced. A binder having this susceptibility to a more moderate degree may well be of practical value.

Intermediate-Textured Asphalts

Rolled asphalts with an intermediate texture are given by Trinidad lake asphalt 5B, Egyptian waxy, Mexican and Cuban bitumens. Of these four binders both the Trinidad lake asphalt 5B and the Egyptian waxy bitumen have intermediate rates of hardening as shown by the weathering tests on thin films. The Mexican and Cuban bitumens have rates of hardening of the same magnitude as the Californian and Lobitos bitumen.

CONCLUSIONS

The full-scale experiment has shown that, in the climatic conditions prevailing in southern England, rolled-asphalt surfacings conforming to Schedule 2 of B. S. 594:1958 are very durable. With nine binders of 60-70 penetration obtained from various sources, a satisfactory life exceeding 15 years has been obtained and only one binder, the Egyptian cracked bitumen, gave an unsatisfactory material of poor durability.

There are, however, important differences in the surface texture developed by the rolled asphalt made with these binders--some developed a smooth texture whereas others became rough. The development of different surface textures cannot be explained in terms of the original rheological properties of the binders but results from new properties brought about in the top surface of the rolled asphalt.

The type of surface texture developed after some years is related to the hardening of the bitumen within the surface layers. Three processes affect the development of surface texture: (a) changes produced by weathering, giving increases in viscosity by a factor of up to 1,000 in some cases; (b) fluxing by lubricating oil, giving decreases in viscosity in a ratio of up to 1,000 despite the opposing action of oxidation; and (c) leaching by water of the weathered binder to produce a friable condition in the exposed surface of the sand/filler/binder mortar.

The rough-textured asphalts are those made with the binders having a low resistance to weathering; binder at the surface has hardened despite the fluxing action of motor oil, and erosion of the top skin of mortar gives the typical sandpapery mortar. The smooth-textured rolled asphalts are those made with binders having the highest resistance to weathering. Fluxing by motor oil offsets the action of weather sometimes to such an extent that softened binder immediately below the top skin exudes to the surface in the form of veins giving a smooth, rich appearance.

ACKNOWLEDGMENT

The work was carried out as part of the program of the Road Research Board. The paper is contributed by permission of the Director of Road Research. Crown copyright reserved. Reproduced by permission of the Controller of Her Britannic Majesty's Stationery Office.

REFERENCES

1. Lee, A. R., and Warren, J. B. A Coni-Cylindrical Viscometer for Measuring the Visco-Elastic Characteristics of Highly Viscous Liquids. Jour. Sci. Instrum., Vol. 17, No. 3, p. 63, 1940.
2. Lee, A. R., Warren, J. B., and Waters, D. B. The Flow Properties of Bituminous Materials. Jour. Inst. Petrol., Vol. 26, No. 197, p. 101, 1940.
3. British Standards Institution. British Standard 594:1961. Rolled Asphalt (Hot Process). London, 1961.
4. Lee, A. R. A Method of Assessing the Condition of Experimental Surfacings. Road Tar, Vol. 11, No. 3, p. 11, 1957.
5. Giles, C. G. The Skidding Resistance of Roads and the Requirements of Modern Traffic. Inst. of Civil Eng., Road Paper No. 52, London, 1956.
6. Gough, C. M., and Green, E. H. Changes in the Composition, and in the Viscosity and Asphaltene Content of the Binders, of Rolled Asphalts and Medium-Textured Macadams Laid on the Colnbrook By-Pass (A. 4), Middlesex, in 1937 and 1938. Dept. of Sci. and Ind. Res., Road Research Lab. Note No. RN/3023/CMG. EHG. Harmondsworth, 1957, Unpublished.
7. Lee, A. R., and Nicholas, J. H. The Properties of Asphaltic Bitumen in Relation to Its Use in Road Construction. Jour. Inst. Petrol., Vol. 43, No. 405, p. 235, 1957.
8. Please, A., Green, E. H., and Mayer, F. E. The Viscosity of the Bitumen in the Surface of Rolled Asphalts Made with Venezuelan Bitumen and Trinidad Lake Asphalt on A. 40 at Greenford, Middlesex, in 1951. Dept. of Sci. and Ind. Res. Road Research Lab., Note No. RN/3025/AP. EHG. FEM. Harmondsworth, 1957, Unpublished.
9. Saal, R. N. J., Baas, P. W., and Heukelom, W. Jour. Chem. Phys., Vol. 43, p. 235, 1946.

Part II. Changes in Bitumen Composition Causing Changes in Viscosity

E. D. TINGLE and E. H. GREEN, Road Research Laboratory, Harmondsworth, Middlesex, England

An examination has been made of experimental surfacings laid on a heavily trafficked road. These comprised asphaltic concrete sections using refinery bitumen and fluxed Trinidad lake asphalt as binders, and rolled asphalt sections using refinery bitumens from two distinct crude sources. The changes in viscosity have been determined for the bitumen recovered from the uppermost layer of the experimental surfacings and in successive 0.5-mm layers of the rolled asphalt sections. Corresponding changes in composition have been determined by a newly developed solvent fractionation technique.

Important factors in the behavior of binder in surface layers are changes in constitution brought about by atmospheric oxidation and by absorption of oil dropped from vehicles. The interaction of hardening by oxidation and softening by oil droppings helps explain why the nature of the binder plays an important role in determining the resistance to skidding of dense bituminous surfacings. A correlation has been established between the combined effects of weather and traffic, the change in properties of the binders in the surface layers, and the surface texture and skidding resistance.

•FOLLOWING THE work reported in Part I, a further full-scale experiment was carried out in 1960 designed to clarify the reasons why dense surfacings made with certain bituminous binders became slippery whereas those made with other binders retained a rough, skid-resistant texture. A laboratory investigation was begun to study in more detail the changes in the properties of the binder in service. Measurements were made of changes in viscosity and composition of binder recovered from different parts of the road surface and at successive depths below the surface. Most of the work is concerned with binders used in rolled asphalt manufactured according to B. S. 594, but an investigation is also recorded of changes occurring in binders used in asphaltic concrete with a continuously-graded-aggregate structure.

EXPERIMENTAL

The Full-Scale Road Experiment

The full-scale road experiment, begun in August 1960, comprised 38 sections, each 70 yd long. The main aim of this experiment was to compare the behavior of eleven selected bitumen binders chosen to have individual properties significant for the maintenance of good skid-resistance. Five sections containing four different binders have been studied intensively and the results presented in this paper. The composition of two of these sections was selected inside the range of the specification given in Table 7, Schedule 1 of the British Standard Specification B. S. 594:1961. They contained 25 percent (by weight) coarse aggregate, 57 percent fine silica sand, 9.5 percent filler and 8.5 percent soluble bitumen binder; ½-in. nominal-size chippings coated with bitumen were rolled into these surfacings at a rate of 185 sq yd per ton. The other three sections were to a specification similar to that of wearing-course asphaltic concrete as used on the continent of Europe and in the USA. The material used in these sections had a continuously-graded-aggregate content of ¾-in. maximum size. The coarse aggregate content was 46 percent by weight, fine aggregate 44 percent and filler 10 percent.

Since laying in 1960, the experimental surfacings have carried heavy traffic of approximately 23,000 vehicles per day, corresponding to a load of 64,000 tons per day.

TABLE 1

PROPERTIES OF THE BITUMENS

Property	X	Y	Z
Penetration	42	45	63
Softening point (ring and ball), deg C	58	54	51
Penetration index	+0.2	-0.7	-0.5
Viscosity (measured at a rate of shear of 4×10^{-4} sec^{-1})			
at 25 C ($\times 10^6$), poises	9.4	6.1	4.6
at 45 C ($\times 10^6$), poises	0.34	0.17	0.14
[a] Temperature susceptibility (m)	3.57	4.01	3.98
[b] Plasticity index (p)	1.2	1.2	1.1
[c] η_0/η_∞	1.6	1.55	1.25
[d] Aging index (air)	4.1	5.5	2.7
Aging index (nitrogen)	1.6	2.4	—
Spot test (oliensis)	-ve	-ve	-ve

[a] From Walther formula log log (V + 0.8) = -m log T + C (where V is kinematic viscosity and T the temperature, deg K).
[b] From $D = K_s P$ where D is rate of shear and s is shear stress.
[c] η_0 and η_∞ represent respectively the values for viscosity at low and high rates of shear, calculated from a plot of the shear stress against angular rotation in a conicylindrical viscometer. The ratio η_0/η_∞ gives a measure of the departure of the bitumen from Newtonian behavior.
[d] Measured by the method of Griffin, Miles and Penther (1).

All sections of the full-scale road experiment are in very good condition after five years under this heavy traffic and there is no indication that any of the sections will have a life significantly shorter than the 20 years expected from a standard rolled asphalt wearing-course.

The Bituminous Binders

The rolled asphalt sections contain two different residual bitumens of the same nominal penetration (50) and at the same nominal binder content (8.5 percent by weight). The first, bitumin X, is a product typical of road bitumen commercially available in Great Britain. The second, bitumen Y, is a specially imported road bitumen selected for the road experiment because of its particularly high sensitivity to hardening by photo-oxidation.

Two of the asphaltic concrete surfacings contain a residual bitumen Z from the same crude source as bitumen X but of a nominal 60/70 penetration. In one of these sections the binder content is 5.3 percent by weight, in the other, a little higher (5.5 percent by weight). The third section of asphaltic concrete contains fluxed Trinidad lake asphalt as binder. The naturally occurring lake asphalt after refining consists of approximately 35 percent by weight finely divided mineral matter and 55 percent by weight bitumen soluble in carbon disulfide. The remaining 10 percent consists of organic matter insoluble in carbon disulfide. The refined lake asphalt is fluxed to the appropriate penetration with about 15 percent by weight of a heavy petroleum flux oil. The soluble bitumen content of the asphaltic concrete made with fluxed lake asphalt was 5.7 percent by weight. Some properties of the bitumens X, Y and Z are given in Table 1.

Surface Characteristics

In common with most roads carrying heavy canalised traffic there is a distinct dark strip approximately 3 ft wide, about 6 ft from the curb, caused by oil droppings from passing vehicles. The oil lanes on the rolled asphalt sections containing the two bitumens are markedly different in visual appearance. On the section containing bitumen X the oil lane is very dark in color and smooth in appearance. The coated chippings applied to the surface appear to have been pushed into the mortar to a much greater extent than in the wheel tracks bordering the oil lane. On the section containing bitumen Y the oil lane is lighter in color and less clearly defined, and the whole surfacing is of more uniform appearance. The coated chippings in the oil lane are raised above the mortar to almost the same extent as in the wheel tracks.

A similar difference in appearance is noted in the asphaltic concrete surfacings containing the two different binders. In the oil lane on the section containing the residual bitumen Z, there has been considerably greater closing-up of the surfacing than in the wheel tracks. The mortar of fine aggregate is level with the exposed coarse aggregate giving the surface in the oil lane a smooth dark appearance. The section containing Trinidad lake asphalt has a surface of much more uniform roughness and color. The difference in appearance between the rough wheel track of the asphaltic concrete containing Trinidad lake asphalt and the smooth oil lane of the asphaltic concrete containing

bitumen Z is illustrated in Figure 1. Measurements of the differences in texture depth of the surfacings that were so apparent on visual inspection have been made by the "sand-patch" method. In this method a measured volume of fine, single-size, dry sand is poured in a conical heap on the road surface. It is carefully distributed to just fill the interstices; the diameter of resultant circular sand patch is then measured. The volume of sand divided by the area of the patch gives an average value of texture depth. Texture depths of less than 0. 010 in. are difficult to measure by this technique. Where necessary, on smooth surfaces, the texture depth has been measured by a complementary method similar in all ways except that a weighed quantity of soft grease replaces the sand. The results of these roughness measurements on both rolled asphalt sections and on the asphaltic concrete sections containing Trinidad lake asphalt and bitumen Z (higher binder content) are given in Table 2.

It is still too early to give a complete assessment of s. f. c. measurements. However, a preliminary assessment has been made based on monthly measurements of s. f. c. using data (2) on liability to skidding accidents of roads with different s. f. c. Table 3 gives an order of merit for the surfacings in terms of relative liability to skidding accidents. The tentative results show that the rolled asphalt containing bitumen X is 43 times as dangerous as the best surfacing, the asphaltic concrete containing fluxed Trinidad lake asphalt.

The s. f. c. measurements were made in the wheel track of the road. The resistance to skidding in the oil lane was measured by means of the Road Research Laboratory portable pendulum tester. The results are given in Table 4. The results given in Tables 2, 3, and 4 show that for both rolled asphalts and asphaltic concretes a change in the nature of the bitumen binder can lead to marked differences in the surface texture developed and in the resistance to skidding. For each pair of surfacings of the same type, the rougher the surface texture, the higher the resistance to skidding.

Examination of Bitumen Recovered from Road Sections

The general technique used for investigation of viscosity changes in the binders was similar to that reported in Part I, but the investigation was carried deeper into the surfacing and refined methods of recovery and measurement of viscosity were used. In addition, composition changes in the binder used in the rolled-asphalt sections, in layers at increasing depths below the surface, were examined by a specially developed solvent-fractionation method.

Two cores 6 in. in diameter and the full depth of the surfacing were cut from each road section of rolled asphalt, one in the wheel track (3 ft 6 in. from the curb) the other in the oil lane (6 ft from the curb).

In the laboratory the sand/filler/binder mortar was removed from between the applied coated chippings using a small sharpened steel spatula. This was done in such a way that successive layers, each approximately 0. 5 mm thick, were separately removed. The bitumen was recovered from each sample by extracting with carbon disulfide, centrifuging out the mineral matter and recovering the bitumen under controlled conditions.

The viscosity of the recovered bitumen was determined with the sliding-plate microviscometer (3) and the results are given in Table 5.

To obtain more information on the changes in composition that occur during weathering, the bitumens were divided into fractions using a series of solvents of increasing dispersing power, as recommended by Krenkler (4). The solvent-fractionation method devised by Krenkler requires 2. 5 g of bitumen for determination of a single fraction, i. e., 25 g for a complete analysis in duplicate using the five recommended solvents. For the present investigation the technique was modified to give a micro-method which uses only 400 mg of bitumen for a complete analysis. Results of the solvent fractionations of the bitumen recovered from successive layers removed from all cores from the rolled-asphalt sections are given in Table 6.

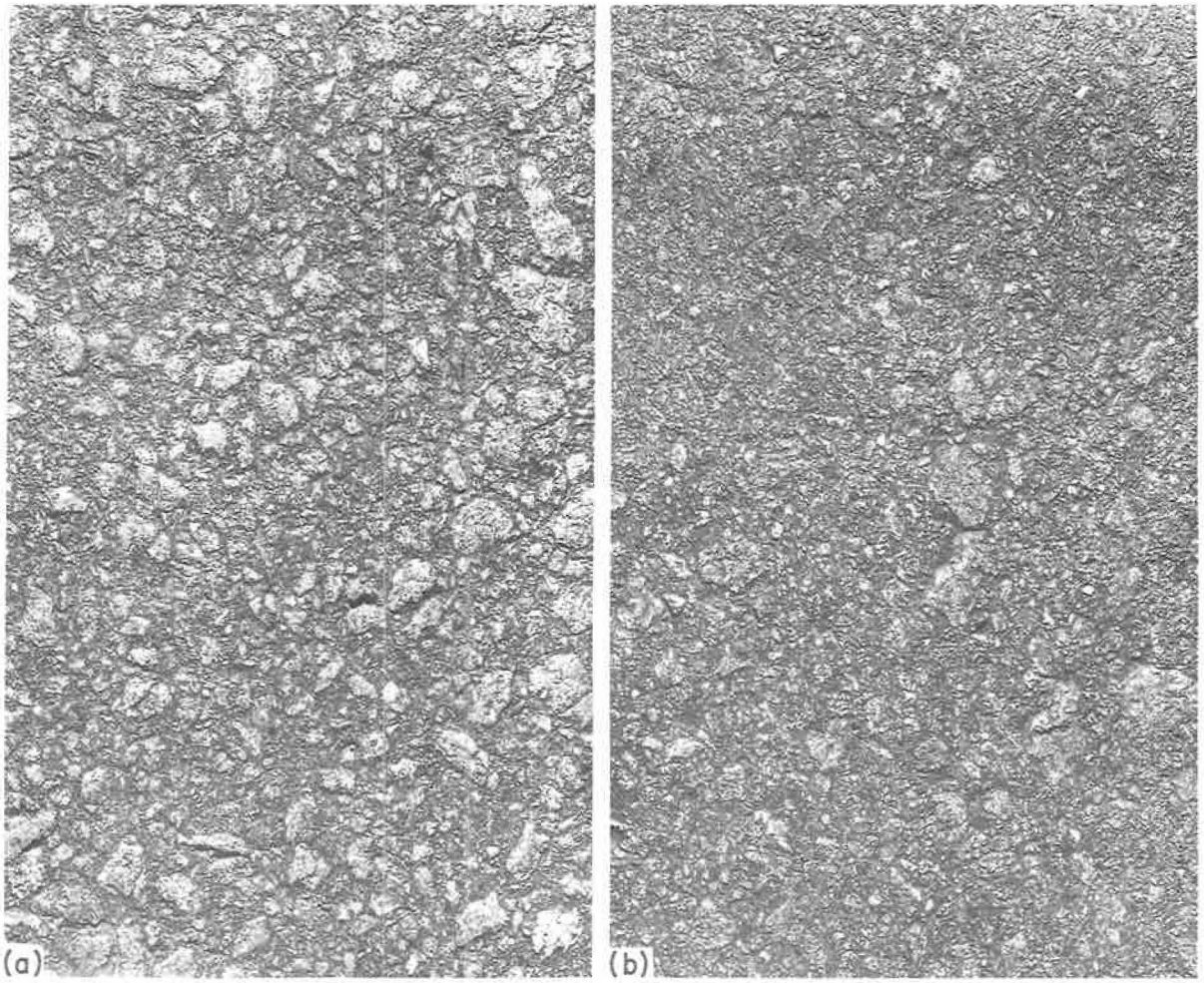

Figure 1. Appearance of asphaltic concrete surfacing after 4 years' service under heavy traffic. A—Wheel track of asphaltic concrete, Trinidad lake asphalt binder (measured texture-depth 18.3 in.$^{-3}$). B—Oil lane of asphaltic concrete, residual bitumen binder (measured texture-depth 9.0 in.$^{-3}$).

TABLE 2

TEXTURE-DEPTH MEASUREMENTS[a]

Surfacing	Binder	Texture Depth in 1/1000 in.	
		Oil Lane	Wheel Track
Rolled asphalt	Bitumen X	12.6	18.6
	Bitumen Y	14.3	16.5
Asphaltic concrete	Bitumen Z	9.0[b]	12.4[c]
	Trinidad lake asphalt	18.2	18.3

[a]All values given are the averages of at least 12 measurements.
[b]Measured by grease-patch method.
[c]Measured by both grease-patch and sand-patch method.

TABLE 3

RELATIVE LIABILITIES TO SKIDDING ACCIDENTS

Surfacing	Relative Skidding Liability	Order of Merit
Asphaltic concrete containing fluxed Trinidad lake asphalt	1	Best
Rolled asphalt containing bitumen Y	15	
Asphaltic concrete containing bitumen Z	24	
Rolled asphalt containing bitumen X	43	Worst

TABLE 4

RESULTS OF SKID-RESISTANCE MEASUREMENTS WITH PENDULUM TESTER

Surfacing	Binder	Skid Resistance in Oil Lane
Rolled asphalt	Bitumen X	47
	Bitumen Y	55
Asphaltic concrete	Bitumen Z	52
	Trinidad lake asphalt (fluxed)	60

TABLE 5

VISCOSITY OF BITUMEN RECOVERED FROM SUCCESSIVE LAYERS OF MORTAR OF ROLLED ASPHALT SECTIONS[a]

Site	Bitumen X[b]		Bitumen Y[c]	
	Wheel Track	Oil Lane	Wheel Track	Oil Lane
First layer, 0-0.5 mm	1.4	0.5	(40)	(40)
2nd layer, 0.5-1.0 mm	2.4	0.3	13	3.1
3rd layer, 1.0-1.5 mm	4.5	0.6	7.0	4.5
5th layer, 2.0-2.5 mm	8.2	4.5	9.7	9.2
10th layer, 4.5-5.0 mm	10.2	10.0	10.0	10.1
Approx. 18 mm (¾ in.)	15.5	15.0	12	—

[a] All viscosities in poises, x 10^6, at 25 C. Shear rate: 0.04 sec^{-1} except the two results in parentheses, which were interpolated from measurements at lower rates of shear or higher temperature of testing.
[b] Original binder (after recovery), 8.5. [c] Original binder (after recovery), 5.3.

TABLE 6

SOLVENT FRACTIONS OF BITUMENS RECOVERED FROM SUCCESSIVE LAYERS OF MORTAR OF ROLLED-ASPHALT SECTIONS[a]

Site	Bitumen X, Oil-Lane (percent in fraction)					Bitumen X, Wheel-Track (percent in fraction)					Bitumen Y, Oil-Lane (percent in fraction)					Bitumen Y, Wheel-Track (percent in fraction)				
	1	2	3	4	5	1	2	3	4	5	1	2	3	4	5	1	2	3	4	5
Original Bitumen	39.6	32.9	18.4	8.4	0.7	39.6	32.9	18.4	8.4	0.7	36.6	31.7	11.8	18.9	1.0	36.6	31.7	11.8	18.9	1.0
First layer, 0-0.5 mm	61.5	10.8	8.2	18.6	0.9	58.0	9.7	12.5	18.2	1.6	52.4	7.2	9.0	7.2	24.2	48.7	12.1	5.0	14.1	20.1
2nd layer, 0.5-1.0 mm	62.1	12.9	12.0	11.4	1.6	53.6	16.9	13.2	14.6	1.7	51.0	15.7	7.3	16.0	10.0	45.7	20.8	9.5	13.7	10.3
5th layer, 2.0-2.5 mm	54.0	19.5	14.5	12.0		47.3	25.3	16.9	10.5		43.6	25.2	10.7	17.8	2.7	42.8	25.7	10.7	18.0	2.8
10th layer, 4.5-5.0 mm	47.6	27.1	16.2	9.1		44.3	29.7	17.0	9.0		43.1	27.1	9.8	16.1	3.9	41.9	28.6	8.1	16.5	4.9

[a] Fraction 1. (low-molecular-weight maltenes) soluble in n-butanol. 2. (resins) soluble in n-heptane, insoluble in n-butanol. 3. (low-molecular-weight asphaltenes) soluble in 2:1 heptane/cyclohexane mixed solvent, insoluble in n-heptane. 4. (medium-molecular-weight asphaltenes) soluble in 1:2 heptane/cyclohexane, insoluble in 2:1 heptane/cyclohexane mixed solvent. 5. (high-molecular-weight asphaltenes) insoluble in 1:2 heptane/cyclohexane mixed solvent.

From each of the selected sections of asphaltic concrete four 6-in. diameter cores were cut, one pair from the oil lane, the other pair from the wheel track. Examination of recovered binder was by a different technique from that used in the case of rolled asphalt because of the stonier nature of the material. The thinnest layer that it was possible to remove from the surface and that was at all representative of the surface was on average about ¼ in. thick. This layer was removed by hand from the surface of each core heated to a temperature of 100 C. The amount of material so removed (15-20 g) was just sufficient to allow the use of a small-scale method described by Green (5) for solvent recovery of the binder. The remainder of the core was then broken down and a sample equal to a quarter of the total material was taken for recovery of the bitumen. The penetrations of the recovered bitumens were measured in calibrated small-scale cups, 14 mm in diameter; absolute viscosities were measured with the sliding-plate microviscometer. The results obtained are compared in Table 7 with those obtained on the original bitumen and fluxed lake asphalt. These original binders were submitted to the recovery process for comparison of results with those obtained with the binders from the road samples. Results of penetration tests on binder recovered from the road materials immediately after mixing at the asphalt plant are included in Table 7.

Oxidation Tests on Binders

The effect of oxidation on the consistency and composition of the bitumens used in the experimental road sections of rolled asphalt has been examined. Films, 2 mm thick, of the binders were subjected to oxidation, under conditions that allowed no evaporation of volatile components, by storing for 70 hours in a bomb in which a pressure of

TABLE 7

RESULTS OF VISCOSITY TESTS ON BITUMENS RECOVERED FROM THE ASPHALTIC-CONCRETE SECTIONS[a]

Nature of Binder	Section	Oil Lane		Wheel Track	
		Pen. at 25 C	Viscosity, Poises x 10^6	Pen. at 25 C	Viscosity, Poises x 10^6
Bitumen Z, 5.3% by wt[b]	Top 1/4 in.	210	0.17	61	3.5
	Remainder	38	11.0	27	21.8
Bitumen Z, 5.5% by wt[b]	Top 1/4 in.	174	0.26	69	3.22
	Remainder	41	8.4	41	10.4
Fluxed Trinidad lake asphalt, 5.7% by wt[c]	Top 1/4 in.	130	0.6	67	2.4
	Remainder	78	1.8	67	2.1

[a]All viscosities at rate of shear 0.04 sec^{-1}, determined at 25 C.
[b]Original bitumen (without aggregate), pen. at 25 C = 50, viscosity in poises (x 10^6) = 4.6; bitumen recovered from mixing plant sample, pen. at 25 C = 44.
[c]Original bitumen (without aggregate), pen. at 25 C = 100, viscosity in poises (x 10^6) = 0.68; bitumen recovered from mixing plant sample, pen. at 25 C = 101.

TABLE 8

CHARACTERISTICS OF PRESSURE-OXIDIZED BITUMENS

Binder		Pen. at 25 C	Softening Point (R & B), deg C	Penetration Index	Solvent Fraction[a] (% by wt)				
					1	2	3	4	5
Bitumen X	Original	42	58	+0.2	39.6	32.9	18.4	8.4	0.7
	Pressure-oxidized	19	70	+0.6	44.8	18.0	15.8	20.5	0.9
Bitumen Y	Original	45	54	-0.7	36.6	31.7	11.8	18.9	1.0
	Pressure-oxidized	16	77	+1.5	40.6	15.9	11.1	10.9	21.5

[a]For definition of fractions see Table 6.

20 atmospheres (300 psi) of oxygen and a temperature of 65 C were maintained. After this treatment the penetration and softening point of the oxidized material were measured. In addition, the composition changes as measured by the Krenkler solvent-fractionation method were determined. The results are given in Table 8.

The results show that the susceptibilities to increase of consistency of the bitumens on oxidation under these conditions are not dissimilar. Bitumen Y is a little more susceptible than bitumen X. The effect of oxidation on composition is to increase the content of the high-molecular-weight (fractions 4 or 5) at the expense of fractions of lower-molecular-weight resins (2 and 3). Surprisingly, in both cases there has been an increase in the lowest-molecular-weight oily (fraction 1) from which it might be inferred that a degradation reaction producing lower-molecular-weight material accompanies the association reactions producing higher-molecular-weight material. However, there is a marked difference between the two bitumens in the nature of the high-molecular-weight material produced in the oxidation reaction. In bitumen X practically all the increase occurs in the medium-molecular-weight asphaltene (fraction 4) whereas in bitumen Y there has been a decrease in this fraction but a large increase in the high-molecular-weight asphaltene (fraction 5).

RESULTS

It is known that the processes that lead to the changes in binder properties are most complex and in many cases interacting. Some of the most important of the processes occurring are:

1. Oxidation reactions, accelerated by the influence of light in many cases;
2. The softening or fluxing action of oil dropped on the road surfacings by passing vehicles;
3. The leaching of water-soluble oxidation products by rain; and
4. The degradation of certain bitumens by water alone that can occur in the absence of oxygen and light.

It is clear from observations of different binders that their success in providing a skid-resistant surfacing depends on some or all of these processes. It is also clear

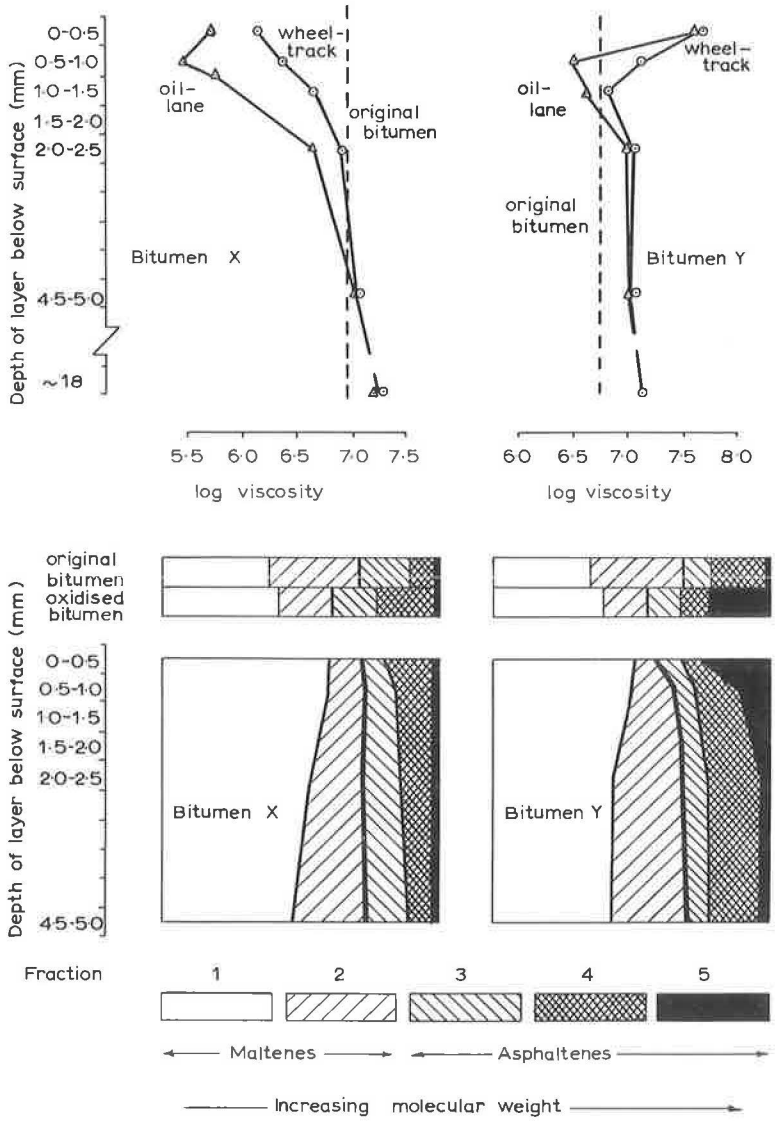

Figure 2. Viscosity and composition of bitumen in successive depths of rolled asphalt.

that the mechanisms to which binders of approximately equal performance owe their success can be very different.

Only long-term research can clarify this complex situation. The discussion here will be mainly in terms of the first two processes mentioned, i.e., oxidative hardening of the binder and softening by oil droppings.

Viscosity Changes

To facilitate the discussion of the results given in Table 5, they are shown graphically in Figure 2. Samples of bitumen X recovered from the uppermost (0.5 mm thick) layer of the mortar of both the oil-lane core and the wheel-track core are considerably softer than that recovered from the layer at the greatest depth (approx. 18 mm) below the surface, to which depths it can be assumed that the effects of neither weather nor oil droppings penetrate. The surface bitumen is, in fact, considerably softer than the original bitumen; in the case of the oil-lane sample by a factor of 17, in the wheel track somewhat less. In the second layer in the oil lane the bitumen is still softer. It is apparent that oil droppings on the road, in greater quantity in the oil lane, have penetrated and softened the binder to a considerable extent. Tests made of the effect of filtered, used, sump oil in the original bitumen show that to obtain the amount of softening observed, in the absence of other factors that might change the viscosity of the binder, approximately ten percent of oil would be required.

At a depth of around 2.5 mm the softening is much less, and at 5 mm there is no significant difference in viscosity from that of the original bitumen, i.e., this represents the limit of penetration of the oil droppings.

The second binder, bitumen Y, behaves in a quite different fashion. Both in the oil lane and in the wheel track the binder recovered from the first layer of mortar is harder by a factor of about ten than the original bitumen; it is about four times as hard as the bitumen recovered at a depth of 18 mm in the bulk of the cores. This hardening has taken place despite the fact that there is no reason to believe that the amount of vehicle-oil droppings on the road sections containing this bitumen was any different from that on the sections containing bitumen X. Evidence that oil has penetrated the surfacing is given by the fact that bitumen in the second layer is much softer than in the lower layers both in the wheel track and the oil lane. The fluxing effect of oil is apparent to a depth of 2.5 mm after which no further change in viscosity occurs.

It is deduced that the fluxing effect of oil droppings is counteracted to a much greater extent by oxidative changes in bitumen Y at the exposed surface than with bitumen X. The evidence for this is discussed later.

The changes of viscosity in successive layers of binder cannot be compared directly with those reported in Part I because different bitumens are concerned and because the length of exposure in the road was different in the two cases. However, the behavior pattern is very similar in the two cases, bitumen X behaving similarly to the Venezuelan bitumen observed by Please and Mayer, bitumen Y behaving in a fashion intermediate between the Venezuelan bitumen and the Trinidad lake asphalt.

Turning now to the results of viscosity tests on the bitumen recovered from the asphaltic-concrete sections assembled in Table 7, it can be seen that the behavior pattern is again similar to that shown in the rolled-asphalt sections. In this case the consistency of the recovered binder was measured in terms of penetration and absolute viscosity. The agreement between the measurements, although showing some slight anomalies, is satisfactory in view of the known precision of the measurements.

Here again, considerable softening has occurred in the binders in the oil lanes of all sections and in the wheel track of the sections containing the residual bitumen. The softening (to a penetration of 210) is most marked in the oil lane of the lower-binder-content section containing bitumen Z and is equivalent to the effect of addition of about ten percent oil to the original bitumen. The binder in the surface layer of the section made with Trinidad lake asphalt has the same consistency as in the thicker bottom layer and, in this case, as in that of bitumen Y in the rolled-asphalt section, it appears that the fluxing effect of oil dropped on exposed binder has been counteracted by the effect of oxidation.

Changes in Composition of the Bitumens on Exposure

The use of fractionation by selective solvents, one of the oldest methods of composition analysis of bitumens, is open to criticism on the grounds of its arbitrary nature and relatively low accuracy. Nevertheless its use has been very helpful in explaining the behavior of bitumens and, in the present case, the simple procedure adopted has been remarkably successful in providing important clues to the reasons for the differences in the viscosity changes between bitumens X and Y discussed previously.

The modified Krenkler system adopted for the investigation has been found particularly appropriate. It divides the heptane-soluble portion (maltenes) into an oil (fraction 1) soluble in butanol and a low molecular-weight resin (fraction 2). The heptane-insolubles (asphaltenes) are divided into low-molecular-weight asphaltenes (fraction 3), medium-molecular-weight asphaltenes (fraction 4) and high-molecular-weight asphaltenes (fraction 5). The fraction insoluble in cyclohexane (fraction 6) is absent or insignificantly small in all the bitumen samples observed. This division has been useful in that estimation of fraction 1 has allowed some assessment to be made of the quantity of oil dropped on the road. The division of the asphaltenes into three molecular-weight ranges has indicated important differences between the bitumens in composition changes on weathering and on laboratory oxidation.

Figure 2 shows simultaneously, in diagrammatic form, the composition changes and the viscosity changes measured in the binders in the rolled asphalt sections. Composition analyses of the bitumen in the successive layers of mortar removed in the oil lane only are given. Analyses relating to the wheel track show a similar pattern and are omitted for the sake of clarity. In Figure 2 the composition changes found on pressure oxidation of the bitumens are also illustrated.

The composition analysis of bitumen recovered from the first layer of mortar shows a striking feature common to both bitumens X and Y. The lowest-molecular-weight oil (fraction 6) has increased considerably (approximately 20 percent).

On pressure oxidation, as has been already noted, the oil fraction does increase (between 4 and 5 percent) but to a much smaller extent than the increase observed in the first layer of mortar. The data are consistent with an increase of about 15 percent in the oil fraction due to the oil dropped from vehicles onto the road surface. The changes in the other fractions of the recovered bitumens follow the same pattern as when the bitumens are subjected to pressure oxidation. Bitumen X on oxidation in the laboratory shows a large increase in the medium-molecular-weight asphaltenes (fraction 4) but an insignificant increase in the high-molecular-weight asphaltenes (fraction 5). By contrast, bitumen Y on pressure oxidation increases markedly in the high-molecular-weight asphaltenes (fraction 5) and shows a decrease in the medium-molecular-weight asphaltenes (fraction 4). The proportions of resin and asphaltene fractions in the recovered bitumen from the first layers show a close correlation with those measured after pressure oxidation; where a fraction increases on pressure oxidation, a corresponding increase is noted in that fraction in the bitumen recovered from the road surface. The results of this comparison lend strong support to the conclusion that the changes in resin and asphaltene fractions measured in the sample of recovered bitumen are due to oxidation.

Although the data are not sufficient for accurate comparison, it is clear that the degree of oxidation of the bitumen in the uppermost layers of the mortar is fairly similar to that in the corresponding laboratory-oxidized bitumens. Comparison of the proportion of that part of the asphaltene fraction that has increased on pressure oxidation with the corresponding proportions in the recovered bitumen (recalculated to take into account the assumed increase of 15 percent in fraction 1 caused by oil droppings) suggests that bitumen X has oxidized on the road rather less than in the laboratory test, bitumen Y more. This extra oxidation of bitumen Y could well be due to the known greater effect of light on the rate of oxidation of this bitumen.

The bitumen in the top layers of the road surfacing is softened by oil droppings and hardened by atmospheric oxidation. The result in terms of viscosity changes will depend on the opposition of these processes. The first simple hypothesis to explain the observed facts that bitumen X is softer than the original bitumen, and bitumen Y harder, is that in the case of bitumen X the oxidative hardening is less than the oil-fluxing action, the reverse being the case for bitumen Y.

Besides the differences in viscosity in bitumens X and Y recovered from the surface layers, there are indications that other changes which affect the binding power of the materials have taken place. The marked increase in high-molecular-weight asphaltenes and corresponding decrease in the peptising resin fraction indicate a decrease in stability of the colloidal system of bitumen Y with a transition toward the gel type of structure. The increase of penetration index on oxidation is a witness to this transformation. It must also be remembered that, because photo-oxidation is an important factor in bringing about the composition changes in bitumen Y, and because ultraviolet light penetrates only a few microns, the bitumen in the very top surface of the road is probably extremely rich in high-molecular-weight asphaltenes and therefore very unstable. The action of oil droppings, paraffinic in nature, could well be to further decrease the stability to the stage where a breakdown of the colloid structure occurs and the system ceases to function as a binder.

Discussion has centered on the behavior of the bitumens used in the rolled-asphalt sections. The differences in viscosity observed between equivalent samples of bitumen Z and fluxed Trinidad lake asphalt recovered from the asphaltic-concrete sections can be explained in a similar fashion, although in the case of Trinidad lake asphalt the presence of natural mineral filler and the effect of water on this binder are complicating factors.

Changes in Binder Properties and Surface Characteristics of the Road

The changes that occur in the appearance of the surfaces of the experimental sections have been studied by observation of enlarged photographs of a small area of each section taken at regular intervals of about six months. These photographs show clearly that in those surfacings that have become slippery the applied coated chippings have been pushed by the action of traffic into the plastic mortar. At the same time the surface of the sand/filler/binder mortar has become smoother by migration of binder to the surface. In the surfacings that retain good skid resistance, the coated chippings stand proud of the mortar which itself has a rough sandpaper appearance. It is also clearly shown that in these surfacings the mortar is suffering a continuous slight attrition as evidenced by the slow appearance of coarse aggregate from the body of the asphalt, originally hidden under a thin layer of mortar.

The measured differences in surface-texture depth reported earlier are explicable in terms of the changes in viscosity and compositions of the binders. The softening of bitumen X in the surface layers (particularly in the oil lane) favors the migration of durable bitumen to the surface of the mortar and may favor the penetration of the coated chippings. The hardening and change in composition of bitumen Y will result in the embrittlement and loss of binding power of the binder and in an abrasion of the mortar which helps to maintain the chippings proud of the surface. In addition, the penetration of the coated chippings may be counteracted to some extent.

In the asphaltic-concrete sections the photographic evidence shows that the softening observed with bitumen Z allows a greater compaction to a smooth surface in the oil lane than in the wheel track in spite of the greater compacting effect of traffic in the wheel track. The hardening of the fluxed Trinidad lake asphalt is the process that governs the greater rugosity and resistance to skidding of the asphalt made with this binder.

CONCLUSIONS

This study of the constitution changes in service goes some way to explaining why the nature of the binder plays an important role in determining the resistance to skidding of dense bituminous surfacings.

The method of constitution analysis by solvent fractionation used in the research has shown that bitumens with similar rheological properties and similar molecular weight gradings behave in very different ways on atmospheric oxidation. The differences in composition brought about by oxidation are crucial for the road performance of the bitumens.

An interacting factor, the change in composition of the binder brought about by oil droppings from vehicles, has been shown to be of great importance. Some quantitative

estimate has been made both of the quantity of oil dropped and of the depth of its penetration. It has been estimated from the observed changes in properties of the bitumens that, in four years on the heavily trafficked road studied, about 0.15 pint of oil is absorbed per square yard of the oil lane of the road. This quantity is equivalent to an addition of 15 percent flux oil to the binder in the important surface layer of asphalt mortar (with an original binder content of 8.5 percent by weight). The road concerned has three lanes carrying a total of about 24,000 vehicles per day, of which 5,000 are heavy commercial vehicles that use the near-side lanes almost exclusively. A rough calculation shows that, even if it is assumed that only the heavy vehicles are responsible, an average of 1 pint of oil deposited and absorbed for every 15,000 miles of travel would be sufficient to account for the observed action of oil droppings. There is evidence from the data of Part I to show that the effect of oil droppings can increase with the years. This factor in the behavior of bituminous surfacings has been little studied. Further research is in progress to examine the effect with the aim of including the oil-droppings factor in future performance-testing procedures.

In addition, research presently in progress will increase the understanding of the complicated weathering process on which reliable performance tests must be based. The work will also supply important clues for suitable modifications to produce binders of improved performance.

ACKNOWLEDGMENTS

This work was carried out as part of the program of the Road Research Board. The paper is contributed by permission of the Director of Road Research. Crown copyright reserved. Reproduced by permission of the Controller of Her Britannic Majesty's Stationery Office.

The authors are grateful for the help given them in the laboratory work by C. Isiksalan of the Turkish Highways Department and N. Michas of the Greek Ministry of Public Works during their secondment to the U.K. Road Research Laboratory.

REFERENCES

1. Griffin, R. L., Miles, T. K., and Penther, C. J. Microfilm Durability Test for asphalt. Proc. AAPT, Vol. 24, pp. 31-53, 1955.
2. Giles, C. G. The Skidding Resistance of Roads and the Requirements of Modern Traffic. Inst. of Civil Eng., Road Paper No. 52, London, 1956.
3. Griffin, R. L., Miles, T. K., Penther, C. J., and Simpson, W. C. Sliding Plate Microviscometer for Rapid Measurement of Asphalt Viscosity in Absolute Units. ASTM Special Tech. Pub. No. 212, 1957.
4. Krenkler, K. Bitumen Analysis by Means of Selective Solvents. Bitumen, Teere Asphalte, Peche, Vol. 2, pp. 59, 85, 105, 1951.
5. Green, E. H. A Method for Recovering Small Samples of Bitumen From Road Mixtures and Surface Dressings. Jour. Appl. Chem., Vol 11, pp. 309-312, 1961.
6. Lee, A. R., and Warren, J. B. A Coni-Cylindrical Viscometer for Measuring the Visco-Elastic Characteristics of Highly Viscous Liquids. Jour. Sci. Instrum., Vol. 17, No. 3, pp. 63-67, 1940.

Temperature-Flow Functions for Certain Asphalt Cements

S. K. SHOOR, K. MAJIDZADEH, and H. E. SCHWEYER
Engineering and Industrial Experiment Station, University of Florida, Gainesville

•ASPHALT CEMENTS and the intimately associated mineral aggregates which are used in paving operations are subjected to environments ranging from subzero to above ambient temperatures. In such extreme mixing and service conditions, the performance of the road surface may be controlled by the response of the bituminous binder to induced temperature gradients. To analyze the anticipated behavior of the bituminous binder caused by temperature variations, parameters describing its rheological response must be determined.

Among the parameters of great theoretical significance are temperatures at which flow regimes are greatly altered. One such characteristic temperature is the glass transition temperature, below which viscoelastic substances exhibit glassy, brittle behavior. The great reduction in the mobility of asphalts below this temperature results in excessive brittleness which may be a critical factor in reducing the durability of asphaltic concrete or other bituminous highway pavements.

In this paper the theoretical significance of glass transition temperature and its relation to a proposed temperature-flow function for certain asphalt cements will be presented.

REDUCED VARIABLES

Literature Background

The method of reduced variables which was initiated as an empirical technique for construction of composite curves has been applied successfully to polymeric systems as presented by Ferry (12) and Tobolsky (30) in the last decade. This method, which is now strongly supported by molecular theories, also has been used successfully by many investigators for materials other than polymers. For asphaltic materials the first investigations using this principle were made by Brodnyan (6) and Gaskins et al. (13) who showed the similarity between the behavior of asphalts and some viscoelastic polymers. The latter authors also used the Williams-Landel-Ferry relation (commonly referred to as the WLF equation) to reduce viscoelastic measurements to a common temperature. They suggested that the ASTM ring and ball softening point is very similar to the temperature of equal corresponding states on which to base the WLF equation. Among other similar work is that of Sisko (28), where the significance of this method in interpretation of rheological data was demonstrated. Similarly Wada and Hirose (33) found that the dilatometrically measured glass transition temperature was an important parameter for asphalts. They showed that the temperature-time dependence of asphalt retardation times obeys the WLF equation. The same dependence for a dynamic modulus of asphalt has been indicated by Sakanoue (25).

Theoretical Development of Method of Reduced Variables

Although the use of reduced variables developed empirically, it can be shown as a logical consequence of the Rouse theory (21, 12) where a molecule is considered as subdivided into N submolecules, each with some monomer units. The resistance en-

Paper sponsored by Committee on Characteristics of Bituminous Materials and presented at the 45th Annual Meeting.

countered by a submolecule junction moving through its surroundings is characterized by a friction coefficient. It is assumed that an average value can be used for all such junctions. It was shown that relaxation or retardation time of any relaxation or retardation process is given by

$$t_p^* = \frac{6\eta}{\pi^2 p^2 n\, kT} \tag{1}$$

where

η = steady flow viscosity,
p = summation index for all contributions to relaxation or retardation,
n = number of molecules per cc,
π = 3.1416,
k = Boltzmann's constant,
T = absolute temperature, and
t_p^* = relaxation or retardation time.

The ratio of t_p^* at temperature T to that at an arbitrary standard temperature T_o can be shown to be given by

$$\left[t_p^*\right]_T \Big/ \left[t_p^*\right]_{T_o} = a_T(T) = \frac{\eta T_o \rho_o}{\eta_o T \rho} \tag{2}$$

where $a_T(T)$ is called the shift factor, and ρ and ρ_o are densities at T and T_o, respectively.

The effect of temperature increase from T_o to T on a logarithmic plot of a viscoelastic function is to shift the curve upward by log $\rho_o T_o / a_T \rho T$ and horizontally by log a_T. It is assumed here that every contribution to the steady flow viscosity is proportional to ρRT, R being the gas constant. Thus, the reduced variables are defined as

$$\eta_R = \frac{\eta_T T_o \rho_o}{a_T T \rho} \tag{3}$$

For reduced viscosity, and for reduced rate of shear

$$\dot{\gamma}_R = a_T \dot{\gamma}_T \tag{4}$$

The datum temperature T_o serves to designate a standard reference state somewhat analogous to the standard state used in thermodynamics. A series of experimental measurements at several different temperatures, when each is reduced to T_o using the appropriate value of a_T, should superpose to give a single composite curve representing η at T_o. If η is known at T_o it can be readily obtained at any other temperature by reversing the procedure.

The molecular theories based on flexible chains (12) for polymers predict that a single composite curve will be obtained if a single average friction coefficient governs the motions reflected in the measured quantity. To apply this method it is necessary that the shapes of curves originally determined at different temperatures, each over a substantial range of the time variable (rate of shear), be similar. Further, the temerature dependence of the shift factor should be consistent with the past experience on polymers.

Significance of Shift Factor

The function log a_T when plotted against temperature gives a smooth curve with no gross fluctuations or irregularities. These empirical values can be fitted to an expres-

sion which has proved to be widely applicable for polymers. The equation is

$$\log a_T = \frac{-C_1^o (T - T_o)}{C_2^o + (T - T_o)} \tag{5}$$

C_1^o and C_2^o are constants corresponding to T_o, T_o = reference temperature.

The values of log a_T, if compared for different viscoelastic substances all based on the same T_o, generate a family of curves crossing at the same T_o, but differing in their slope. However, if a separate reference temperature T_s is suitably chosen for each system and log a_T is expressed as a function of $T - T_s$, this function turns out to be identical for a wide variety of polymers and a variety of organic and inorganic glass-forming substances over a wide temperature range above the vitrification point noted by Williams, Landel and Ferry (34).

The function expressed analytically is

$$\log a_T = \frac{-8.86 (T - T_s)}{101.6 + (T - T_s)} \tag{6}$$

where T_s is a characteristic temperature which when properly selected permits all the asphalt cements studied to superimpose on a single curve according to Eq. 6. Williams (35) and Payne (20) also have shown from a study of many materials that temperature T_s lies 50 C above the glass transition temperature T_g, with an average deviation of ±5 C. Brodnyan (6), and Gaskins et al. (13) have found the above relationship to hold for certain asphalts. Further, they found that the reference temperatures T_s are very similar in value to the ring and ball softening points.

Wada and Hirose (33) found that the temperature dependence of steady flow viscosity as well as retardation times obey the Williams-Landel-Ferry equation when the reference temperature is taken 56 C higher than the glass transition temperature T_g. Barrall et al. (1) calculated the viscosities of certain asphalts with this expression. The agreement between the calculated and experimental values was fairly good for reasonably wide temperature ranges.

Bueche (7) has shown that the WLF relation for glass-forming substances at temperatures somewhat above the glass transition temperature is not only an empirical relation, but that it has a firm theoretical foundation. The constants in the relation have been shown to have the significance assigned to them by WLF. Further, the author states that the existance of the WLF relation, together with the fact that it can be deduced from previous concepts of the glass transition region, is a very strong indication that the basic concept is correct. It would, therefore, appear that the anomalous behavior observed for materials near T_g is primarily the result of the fact that molecules within the melt must move by a cooperative effort with their neighbors.

GLASS TRANSITION TEMPERATURE

The close similarity between the behavior of asphalts and the behavior of viscoelastic polymers suggests that the glass transition temperature may be an important characteristic parameter for asphalts. Several investigators have shown the usefulness of this temperature in reducing the rheological measurements to a single temperature. Wada and Hirose (33) determined glass transition temperatures for some asphalts, and they then showed that asphalt behaves viscoelastically above T_g. They also demonstrated a definite relationship between glass transition temperature and asphaltene content of asphalts. Barrall et al. (1) determined glass softening points (T_{gsp}), which could be discussed interchangeably with T_g, by a differential thermal apparatus and maintained that this temperature was a function of both the asphaltene and petrolene content of the asphalt.

Definition and Significance

By definition the glass transition point is the temperature at which a substance shows a marked change in its physical, mechanical, and optical properties (4). One concept of the glass transition temperature is that it is the temperature below which there is insufficient space between the molecules for them to rotate or move except for in-place vibration. This means that there is very little tendency for the material to flow (1), and the elastic modulus is very high. Below this temperature the substance is characterized mainly by dimensional stability and a tendency to be relatively brittle. Above this temperature, creep and rubberlike properties make their appearance. The presence of crosslinking and orientation complicates the situation. In general the transition temperature is the dividing line between plastic and rubberlike properties (4).

Methods of Measuring Glass Transition Temperature

Numerous experimental methods have been used to determine glass transition temperatures. In each case variation with temperature of some physical, optical or mechanical property is followed. The temperature at which the particular property shows a sudden change is taken to be a glass transition temperature. Some of the more important properties include specific volume (4, 3), specific heat (2), viscosity (31), thermal expansion (1, 5, 9, 17), differential pressure (16), differential thermal analysis (8, 18, 27, 29), and penetration (10, 11, 14, 22, 23, 24).

Most of these methods are either complicated in operation, or require costly apparatus. The penetrometer method is an adaptable and inexpensive apparatus for this purpose. The results obtained are of reasonable accuracy. Therefore, this method was used for exploratory research in determining the glass transition temperature of the eight asphalt cements used in this study.

The use of the penetrometer to determine melting points and glass transition temperatures of polymers has been described by Edgar and Ellery (10, 11). Rynbikar (22, 23, 24) also used the penetrometer to obtain the temperatures for the onset of viscous flow of the amorphous polymer. Grieveson (14) used the same technique to obtain glass transition temperatures for linear polymers and concluded that they were above 5 C above the dilatometric glass transition temperature T_g.

MATERIALS AND TESTING PROCEDURE

In this investigation eight 85 to 100 penetration grade asphalt cements (AC-8) have been used. The selected group of materials includes asphalts obtained from different sources and with expected different chemical compositions; they were used as part of a research program for the Florida State Road Department. Two air-blown asphalts have also been included in this group in order to obtain properties on a type of material

TABLE 1

PROPERTIES OF ASPHALT CEMENTS

Asphalt Sample No.	Source and Type	Penetration 77 F, 100 g/5 sec	Softening Point, F	Ductility 77 F, cm	Specific Gravity 60 F/60 F	Percent Sulfur	Percent Hexasphaltene
S63-4	Smackover	90	116	125	1.021	3.56	12.9
S63-5	Steam refined Venezuelan blend	96	115	150+	1.021	3.06	12.0
S63-6	Florida AC-8	95	118	140+	1.037	5.83	19.4
S63-9	Steam refined intermediate	92	115	200+	1.033	4.24	16.8
S63-12	Steam refined gulf coast naphthenic	99	114	166	1.001	0.70	9.8
S63-13	Air blown, low sulfur naphthenic	100	119	170	0.988	0.69	12.8
S63-14	Air blown, high sulfur	92	120	160	1.017	3.94	18.7
S63-15	Steam refined	90	113	200+	1.016	3.64	8.7

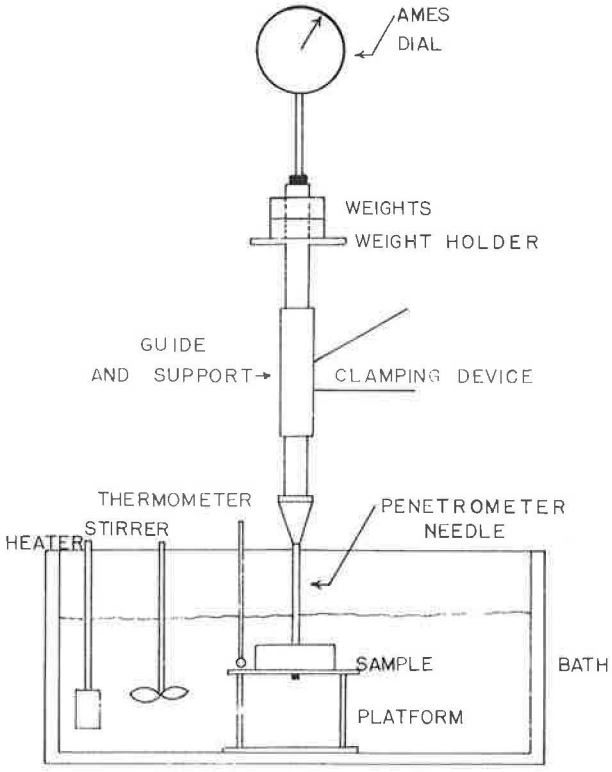

Figure 1. Schematic diagram of penetrometer for glass transition point.

demonstrating different flow characteristics from normal steam-refined asphalts. The test characteristics of these asphalts are given in Table 1 (19).

In this study the rheological data have been determined at temperatures of 15.5 C, 25 C, 35 C, 40 C and 50 C by utilizing a Shell sliding plate microviscometer described by several investigators (15, 26, 32). The testing procedure followed the recommended method described by the manufacturer. The samples were tested at different rates of shear. The velocity of movement was measured on a Varian recorder.

Glass Transition Temperature Measurement

A schematic diagram of the apparatus is shown in Figure 1. A silicone liquid (Dow-Corning 200 fluid) bath was used to control the temperature of the asphalt sample. It was made of Plexiglas and had dimensions of 8 in. square by $5\frac{1}{2}$ in. deep. It was insulated with $\frac{1}{2}$-in. Styrene plastic insulation. The bath was kept uniformly stirred. An immersion heater was used to heat the bath. The rate of heating was controlled by an autotransformer. A 4-in. high and 3-in. square platform was made as a support for the sample tray. The top perforated plate of the platform was fitted to the base plate by four bolts at the four corners. This arrangement was also used for levelling of the sample tray. The sample tray was $\frac{3}{4}$ in. in diameter and $\frac{1}{4}$ in. in height and was made of stainless steel. A screw fitted to the bottom of the tray was used to center the tray in a hole in the center of the top plate of the platform. The penetration readings were recorded by means of an Ames dial (0.001-in. divisions). The needle used was a standard penetrometer needle which had been ground to produce a right cylinder instead of a needle. Initial low temperatures were reached using dry ice.

The asphalt sample was gently heated in a 3-oz. can; care was taken that the sample was not oxidized. The sample was then poured into the sample tray to about $\frac{3}{16}$ in. height and the sample was allowed to cool to room temperature. The sample was then

placed in the silicone bath cooled to at least 30 deg below the expected glass transition temperature. The foot of the loaded penetrometer was placed on the quenched sample after approximately ten minutes. The bath was then heated at a constant temperature rate of 2 F/min. The readings of the dial gage were taken at every 2 F rise in temperature and the corresponding temperatures were recorded. A load of 50-200 gm is required to obtain the desired penetration readings. However, for the asphalt cements studied with this method, the optimum load required was found to be 200 gm.

RESULTS AND EVALUATION

Viscosity vs Rate of Shear

Figure 2 shows a plot of viscosity against rate of shear at different temperatures for a low sulfur naphthenic asphalt cement. The procedure adopted to reduce all viscosity-rate of shear data at different temperatures to an arbitrarily chosen reference temperature T_0 is the same as described by many investigators (28, 34, 35).

The reduced curves (Fig. 3) obtained are almost straight lines in the intermediate range of rate of shear, but tend to bend down at high rates of shear. The curves for asphalt cements S63-13 and S63-14, which are air-blown samples, have higher slopes than those of others. This indicates that they show greater non-Newtonian flow characteristics. In all cases the range of rate of shear has been increased because of plotting the data in terms of reduced variables.

The Shift Factor

The values of shift factors [$a_T(T)$] obtained at different temperatures have been tabulated in Table 2. They were plotted against temperature on semilog paper. The

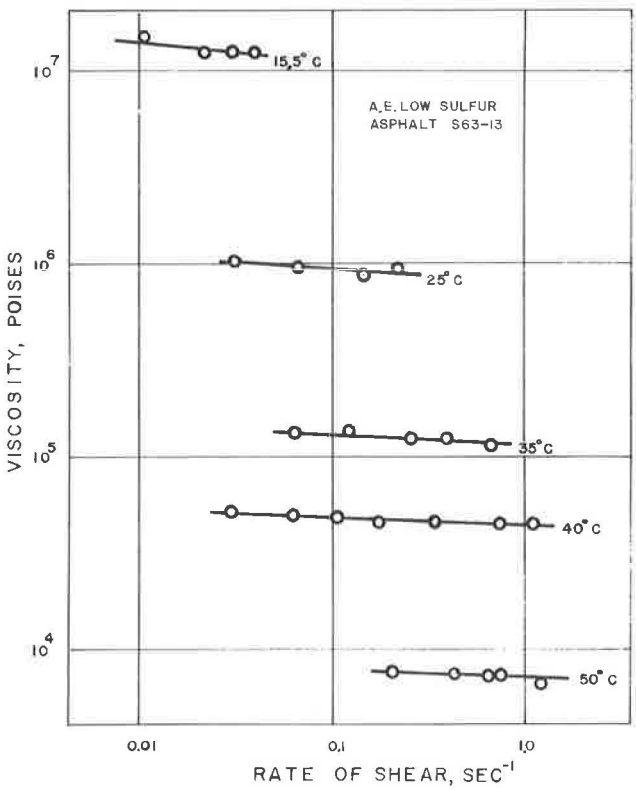

Figure 2. Rheological diagrams for air blown, low sulfur naphthenic asphalt cement, S63-13.

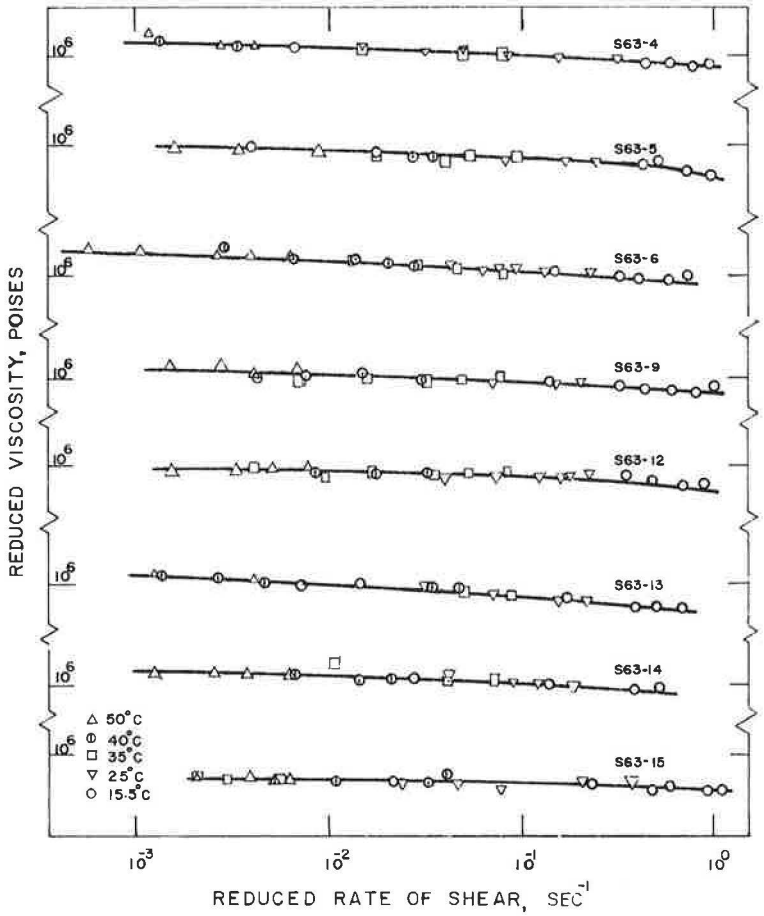

Figure 3. Reduced rheological curves for eight different asphalt cements.

TABLE 2

VARIATION OF $a_T(T)$ FUNCTION WITH TEMPERATURE

Asphalt Sample No.	15.5 C	25 C	35 C	40 C	50 C
S63-4	1.695×10^{1}	1.0	1.333×10^{-1}	4.019×10^{-2}	7.047×10^{-3}
S63-5	1.393×10^{1}	1.0	1.034×10^{-1}	3.932×10^{-2}	7.415×10^{-3}
S63-6	1.300×10^{1}	1.0	1.273×10^{-1}	4.427×10^{-2}	8.180×10^{-3}
S63-9	1.210×10^{1}	1.0	9.754×10^{-2}	3.405×10^{-2}	1.010×10^{-2}
S63-12	1.870×10^{1}	1.0	9.781×10^{-2}	3.187×10^{-2}	5.495×10^{-3}
S63-13	1.650×10^{1}	1.0	1.252×10^{-1}	4.239×10^{-2}	6.033×10^{-3}
S63-14	1.340×10^{1}	1.0	1.235×10^{-1}	5.560×10^{-2}	7.396×10^{-3}
S63-15	2.337×10^{1}	1.0	9.437×10^{-2}	4.084×10^{-2}	5.775×10^{-3}

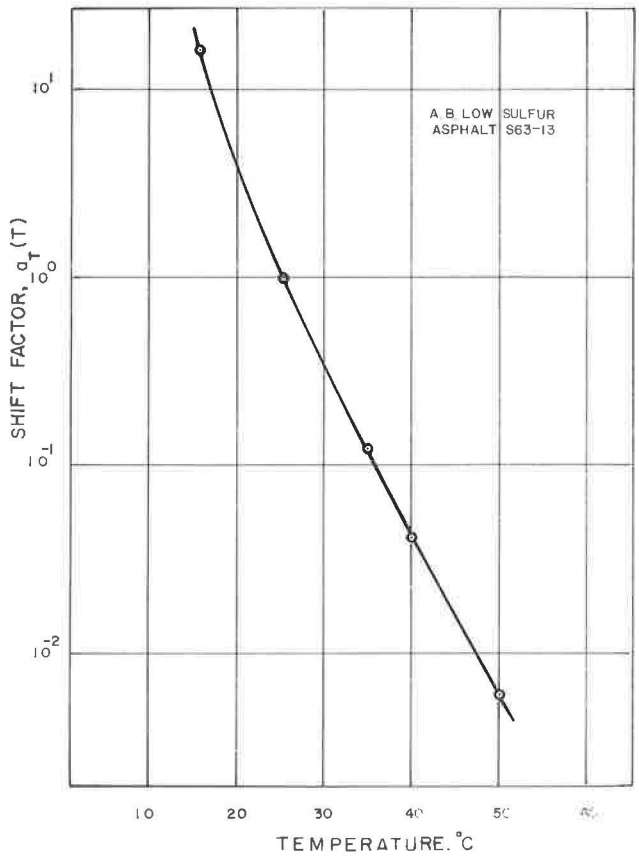

Figure 4. Variation of shift factor (a_T) with temperature for air blown, low sulfur naphthenic asphalt, S63-13.

TABLE 3

DIFFERENCE BETWEEN CHARACTERISTIC TEMPERATURE (T_S) AND GLASS TRANSITION TEMPERATURE (T_g)

Asphalt Sample No.	T_S (deg C)	T_g (deg C)	$T_S - T_g$
S63-4	38.0	-11.8	49.8
S63-5	37.5	-12.7	50.2
S63-6	36.0	-12.2	48.2
S63-9	34.0	-13.9	47.9
S63-12	40.0	- 9.7	49.7
S63-13	39.0	-10.8	49.8
S63-14	37.0	-12.8	49.8
S63-15	41.0	-12.1	53.1

curves obtained were in general smooth with a value of unity at the reference temperature T_0. Figure 4 shows such a plot for one of the asphalt cements (S63-13). These curves show that the temperature dependence of the function $a_T(T)$ is of a form which is in agreement with previous experience on polymers. In accordance with the observations of other investigators (6, 13, 33), it was found that the WLF Eq. 6 holds good for the AC-8 asphalt cements used in this study. To fit the experimental $a_T(T)$ data to the above equation, and to determine the characteristic temperature T_S (34), the experimental plots of log a_T against temperature were matched against the standard plot of Eq. 6 with horizontal and vertical adjustments to obtain the best conformance in shape. The values of T and T - T_S were read at any vertical line from which values of T_S were obtained. The values of T_S for different AC-8 asphalt cements are given in Table 3. Figure 5 shows how closely $a_T(T)$ data obey the WLF equation when it is reduced to a standard temperature T_S.

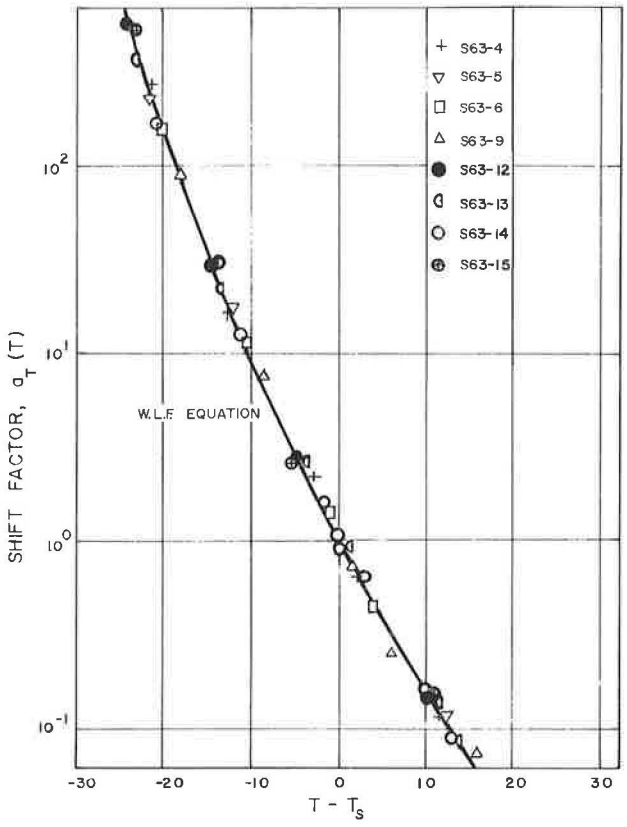

Figure 5. Comparison of asphalt data on asphalt cements with the Williams, Landel and Ferry relation.

The Glass Transition Temperature

To evaluate the glass transition temperature, penetration readings were plotted against temperature. Figure 6 shows a typical plot. In all cases the curves consist of three portions—the lower and the upper portions which are approximately straight lines and the intermediate portion where the change in penetration with temperature is gradual. This intermediate region is a transition region. The lower and upper portions were extended so as to intersect each other. The point of intersection of the two straight lines was taken to be the glass transition temperature. It may be concluded from these curves that there is a definite transition in the properties of these asphalt cements, although this is somewhat gradual rather than sudden and sharp. The relevant temperatures obtained by this method have been given in Table 3. (To obtain greater sensitivity with the available equipment, the experimental data were determined in degrees Fahrenheit. The glass transition temperatures were then converted to degrees centigrade as listed in Table 3 for subsequent use.)

To check the glass transition temperature obtained by this method with the more usual dilatometric measurements, one of the asphalt cement samples (S63-14) was sent to the California Research Corporation for test. The volumetric expansion vs temperature curve indicated a temperature of -12.5 C corresponding to the upper discontinuity in the data obtained. This agrees quite closely with the glass transition temperature of -12.8 C (9.0 F) obtained by the penetrometer method used in this study (Fig. 6).

Relation Between T_S and T_g

In accordance with the findings of other workers (6, 13, 33) it was found that the difference between T_S and T_g, i.e., $T_S - T_g$, was very close to 50 C for all the asphalt

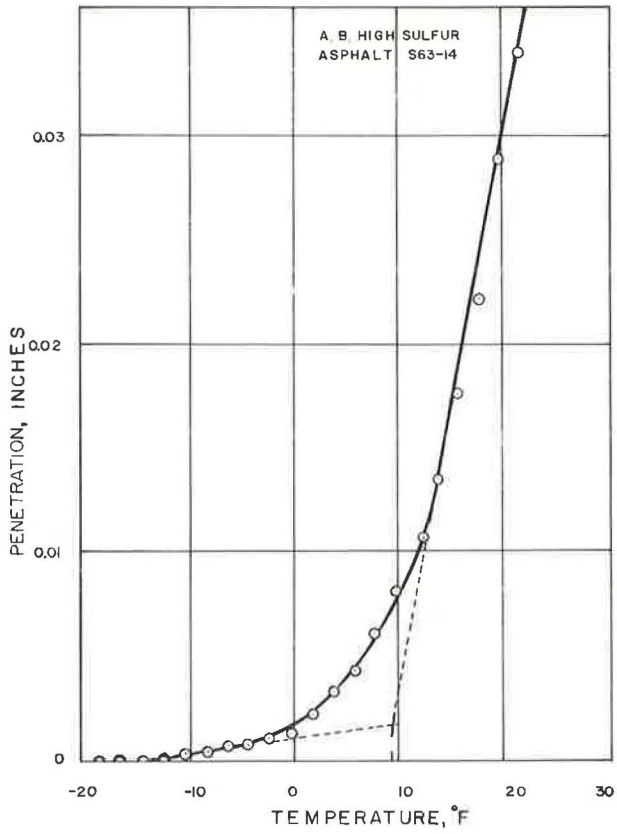

Figure 6. Typical glass transition temperature evaluation, air blown, high sulfur asphalt, S63-14.

cements used in this investigation (Table 3). This further supports the concept that discontinuities obtained in penetration vs temperature curves and by dilatometric methods represent true glass transition temperatures of the asphalt cements. It may be pointed out that the glass transition temperatures of all the asphalt cements tested lie quite close to each other. It has been found by Wada and Hirose (33) that the glass transition temperature increases with the asphaltene content for certain types of asphalts. Barrall et al. (1) maintain that this is true if the asphalts are produced from the same source. Those authors suggest that the reverse is more likely to be found because, usually where a high asphaltene content is found in a given grade of asphalt, the petrolenes will have a much lower viscosity (and a correspondingly lower molecular weight) to compensate for the high specific viscosity of asphaltenes. Such results on asphalts having a high asphaltene content and a low T_{gsp}, as indicated by Barrall et al. (1) would be explained by the presence of the lower molecular weight petrolenes having correspondingly lower viscosities. The results for the asphalts used in this study are not sufficiently broad to discuss this variable. The hexasphaltene contents of the different asphalt cements have been tabulated in Table 1 for information.

CONCLUSIONS

The method of reduced variables has been applied to viscosity-rate of shear data obtained at different temperatures for eight AC-8 asphalt cements (85 - 100 penetration) having different physical and chemical properties. The data superpose fairly well to give composite master curves for each asphalt cement. The shift factor has an anticipated temperature dependence. The data fit reasonably well with the analytical expression of Williams, Landel and Ferry which evaluates a characterizing temperature (T_S).

A penetrometric technique has been used to determine the glass transition temperature (T_g) of the asphalt cements. The (T_g) obtained by this method agrees quite closely with the dilatometric glass transition temperature for one asphalt run in another laboratory. The difference between the characterizing temperature (T_S), which permits the superposition of all $a_T(T)$ data, and the glass transition temperature (T_g) is found to be 50 ± 3 C. This constant difference checks the accuracy of T_g obtained by the penetrometric method. Since the other investigators have found the same magnitude for the difference with other polymeric systems, this emphasizes that the glass transition temperature may be an important characteristic temperature for viscoelastic substances such as asphalt.

ACKNOWLEDGMENT

This research was conducted under contract with the Florida State Road Department in cooperation with the Bureau of Public Roads of the U. S. Department of Commerce.

REFERENCES

1. Barrall, E. M., II, Schmidt, R. J., and Johnson, J. F. Asphalt Transitions at Low Temperatures: Measurement Using Thermal Expansion Apparatus. Am. Chem. Soc., Petroleum Div. preprint, Meeting April 1964, Philadelphia, Pa.
2. Bekkedahl, N., and Matheson, H. Heat Capacity, Enthalpy and Free Energy of Rubber Hydrocarbons. Jour. Res. Nat. Bur. Std., Vol. 15, p. 503, 1935.
3. Bekkedahl, N. Volum Dilatometry. Jour. Res. Nat. Bur. Std., Vol. 42, p. 145, 1949.
4. Boyer, R. F., and Spencer, R. S. Thermal Expansion and Second Order Transition Effects in High Polymers. Jour. Appl. Phys., Vol. 15, p. 398, 1944.
5. Bradford, J. An Automatic Recording Differential Dilatometer. Jour. Sci. Instr., Vol. 40, p. 444, 1963.
6. Brodnyan, J. G. Use of Rheological and Other Data in Asphalt Engineering Problems—Rheological and Adhesion Characteristics of Asphalt. HRB Bull. 192, p. 1, 1958.
7. Bueche, F. Derivation of the WLF Equation for the Mobility of Molecules in Molten Glasses. Jour. Chem. Phys., Vol. 24, p. 418, 1956.
8. Chackraburthy, D. M. Transition Temperature in Some Polymers by Differential Thermal Analysis. Jour. Chem. Phys., Vol. 26, p. 427, 1957.
9. Dannis, M. L. Thermal Expansion Measurements and Transition Temperatures, First and Second Order. Jour. Appl. Polymer Sci., Vol. 1, p. 121, 1959.
10. Edgar, O. B. Structure-Property Relationships in Polyethylene Terephthalate Co-polyesters. Part II: Second-Order Transition Temperatures. Jour. Chem. Soc., Vol. 74, p. 2638, 1952.
11. Edgar, O. B., and Ellery, E., Jr. Structure-Property Relationships in Polyethylene Terephthalate Co-polyesters. Part I: Melting Points. Jour. Chem. Soc., Vol. 74, p. 2633, 1952.
12. Ferry, John D. Viscoelastic Properties of Polymers. John Wiley and Sons, New York, 1960.
13. Gaskins, F. H., Brodnyan, J. G., Philippoff, W., and Thelen, E. The Rheology of Asphalt. II: Flow Characteristics of Asphalts. Trans. Soc. Rheol., Vol. 4, p. 265, 1960.
14. Grieveson, B. M. The Glass Transition Temperature in Homologous Series of Linear Polymers. Polymer, Vol. 1, p. 499, 1960.
15. Griffin, R. L., Miles, T. K., Penther, C. J., and Simson, W. C. Sliding Plate Microviscometer for Rapid Measurement of Asphalt Viscosity in Absolute Units. ASTM, STP 212, 1957.
16. Heller, J., and Doland, J. L. Measurement of Glass Transition Temperatures of Polymers by Differential Pressure Transducer. Jour. Polymer Sci., B1, 317, 1963.
17. Howard, W. H. The Glass Temperatures of Polyacrylonitrile and Acrylonitrile-Vinyl Acetate Copolymers. Jour. Appl. Polymer Sci., Vol. 5, p. 303, 1961.

18. Keavney, J. J., and Eberlin, E. C. The Determination of Glass Transition Temperatures by Differential Thermal Analysis. Jour. Appl. Polymer Sci., Vol. 3, p. 47, 1960.
19. Majidzadeh, K., and Schweyer, H. E. Non-Newtonian Behavior of Asphalt Cements. Proc. AAPT, 1965.
20. Payne, A. R. Rheology of Elastomers. Edited by Mason, P., and Wookey, N. Pergamon Press, London, 1958.
21. Rouse, P. E., Jr. A Theory of the Linear Viscoelastic Properties of Dilute Solutions of Coiling Polymers. Jour. Chem. Phys., Vol. 21, p. 1272, 1953.
22. Rybnikar, F. An Objective Method for the Determination of Melting Points and Softening Ranges of Macromolecular Substances. Svazek, Vol. 50, p. 145, 1956.
23. Rybnikar, F. Measurement of the Transition Temperature of Polymers by Penetrometer Technique. Chem. Listy, Vol. 52, p. 896, 1958.
24. Rybnikar, F. Glass Transition of Nylon 6 and Nylon 66. Jour. Polymer Sci., Vol. 28, p. 633, 1958.
25. Sakanoue, S. Viscoelastic Properties of Asphalts. Nippon Kagaku Zasshi, Vol. 84, p. 384, 1963.
26. Schweyer, H. E., and Bransford, T. L. Viscosity Measurements With the Sliding Plate Microviscometer. Proc. Assoc. Asphalt Paving Technologists, Vol. 30, p. 422, 1962.
27. Scott, N. D. The Detection of Transition Phenomena in Polymers by Differential Thermal Analysis. Polymer, Vol. 1, p. 114, 1960.
28. Sisko, A. W. Determination and Treatment of Asphalt Viscosity Data. Highway Research Record 67, p. 27, 1965.
29. Strella, S. Differential Thermal Analysis of Polymers. I: The Glass Transition. Jour. Appl. Polymer Sci., Vol. 7, p. 569, 1963.
30. Tobolsky, A. V., and Eyring, H. Mechanical Properties of Polymeric Materials. Jour. Chem. Phys., Vol. 11, p. 125, 1943.
31. Ueberreiter, K., and Orthmann, H. J. The Viscosity of Vitreous Selenium From 0° to 100°C. Kolloid Z., Vol. 123, p. 84, 1951.
32. Van Wazer, J. R., Lyons, J. W., Kim, K. Y., and Colwell, R. E. Viscosity and Flow Measurements—A Laboratory Handbook of Rheology. Interscience Publishers, 1963.
33. Wada, Y., and Hirose, H. J. Glass Transition Phenomenon and Rheological Properties of Petroleum Asphalt. Jour. Phys. Soc., Japan, Vol. 15, p. 1885, 1960.
34. Williams, M. L., Landel, R. F., and Ferry, J. D. The Temperature Dependence of Relaxation Mechanisms in Amorphous Polymers and Other Glass Forming Liquids. Jour. Am. Chem. Soc., Vol. 77, p. 3701, 1955.
35. Williams, M. L. The Temperature Dependence of Mechanical and Electrical Relaxation in Polymers. Jour. Phys. Chem., Vol. 59, p. 95, 1955.

Asphalt Durability and Its Relation to Pavement Performance—Rheology, I

A. W. SISKO and L. C. BRUNSTRUM, American Oil Company

ABRIDGMENT

•ASPHALT roads are two-phase systems—stones of various sizes and shapes held together by a viscoelastic binder. Road durability depends on, among other things, how well the binder resists changes in strength properties. Because roads are loaded dynamically under traffic, the dynamic mechanical properties of the binder were evaluated.

The four asphalts studied were selected from the current cooperative survey being conducted by the Bureau of Public Roads and The Asphalt Institute. They represented viscosity grades, AC-5, AC-10, AC-20, and AC-40. Routine tests and special tests for composition, wax, molecular weight, and glass transition temperature were run. Asphalts were aged in the thin film oven test (TFOT) for 5 and 24 hours and by weathering Marshall specimens. Instrument requirements were met by modifying a Farol rheogoniometer to permit accurate measurements of stress and strain and their phase relationship at low service temperatures (0 to 40 F).

Viscoelastic properties (storage modulus, loss modulus, and dynamic viscosity) of aged and unaged asphalts were measured at 0, 20, 40, 60, and 80 F over a 1000-fold range of stress frequencies. The data were combined into master curves for comparison of properties at 20 F. Storage and loss moduli increase with frequency and level off at high frequencies to ultimate values of about 5×10^9 and 8×10^8 dynes/cm^2, respectively. Dynamic viscosity depends on frequency in a manner similar to the dependence of steady shear viscosity on shear rate with limiting values at low frequencies and limiting slopes at high frequencies.

Comparison of unaged asphalts shows that the more viscous asphalts also have higher elastic moduli. Differences between grades are large at low frequencies but all have about the same modulus at high frequencies. Dynamic viscosities behave similarly.

Aging increases the elastic and loss moduli and the dynamic viscosity at low frequencies; however, the properties at high frequencies are the same as for the unaged asphalts. The moduli curves are shifted so that the ultimate values are reached at lower frequencies. In addition, relaxation times increase with age. These changes suggest that asphalts become more like solids and less like liquids and that the failure mechanism changes from ductile to brittle fracture. The viscoelastic properties of asphalts extracted from Marshall specimens are very similar to those of the 5-hr TFOT residues. Rheological properties do not appear to change significantly at the glass transition temperature.

Measurements of durability by relative changes in relaxation time with age showed that the four asphalts are equal in durability.

Paper sponsored by Committee on Characteristics of Bituminous Materials and presented at the 45th Annual Meeting.

Note: The complete paper is available from the Highway Research Board at $1.00 per copy (Supplement XS-8).